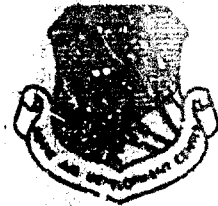


UNCLASSIFIED

AD NUMBER
AD851363
NEW LIMITATION CHANGE
TO Approved for public release, distribution unlimited
FROM Distribution authorized to U.S. Gov't. agencies and their contractors; Administrative/Operational Use; MAR 1969. Other requests shall be referred to Rome Air Development Center, Attn: EMCRS, Griffiss AFB, NY 13440.
AUTHORITY
Rome Air Development Center ltr dtd 17 Sep 1971

THIS PAGE IS UNCLASSIFIED

EMDC-TR-69-27  
Final Technical Report  
March 1969



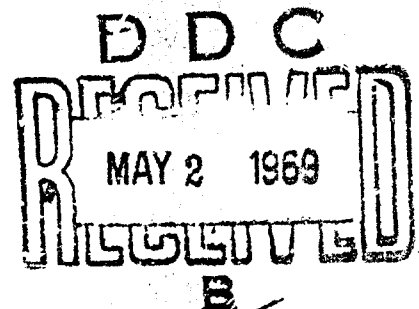
AD851363

## DIGITAL FILTERING TECHNIQUES

Ira M. Langenthal

This document is subject to special export controls and each transmittal to foreign governments, foreign nationals or representatives thereto may be made only with prior approval of RADC (EMCRS), GAFB, N.Y. 13440.

Home Air Development Center  
Air Force Systems Command  
Griffiss Air Force Base, New York



## DIGITAL FILTERING TECHNIQUES

Ira M. Longenthal

This document is subject to special export controls and each transmittal to foreign governments, foreign nationals or representatives thereto may be made only with prior approval of RADC (EMCRS), GAFB, NY 13440.

## FOREWORD


This final report was prepared by Mr. Ira M. Langenthal of Signal Analysis Industries Corporation, sub-contractor to The Marquardt Corporation, under Contract F30602-67-C-0160, System 760C, Project 4519, Task 451902. Mr. Charles N. Meyer (EMCRS) was the RADC Project Engineer.

The author would like to express his appreciation to Mr. Myron Kaufman and other members of the staff at Signal Analysis Industries Corporation (SAICOR) for their efforts on this program; also to Mr. Meyer for his suggestions.

The distribution of this document is limited because the information is embargoed under the Department of State ITIARs.

This technical report has been reviewed and is approved.

Approved:

  
CHARLES N. MEYER  
Project Engineer

Approved:

  
RICHARD M. COSEL  
Colonel, USAF  
Chief, Communications Division

FOR THE COMMANDER:

  
IRVING J. GABELMAN  
Chief, Advanced Studies Group

## ABSTRACT

This investigation was concerned with various digital filtering techniques and associated constraints. The synthesis procedures discussed in this report emphasize the interplay of the various critical design parameters. Generalized design procedures for lowpass, bandpass and band stop filters are developed using a tabular procedure which enables one to obtain the digital filter coefficients by inspection. This approach allows for a simpler evaluation and interpretation of such problems as coefficient truncation, stability and error constraints as well as illustrating the importance and significance of the concept of normalization in digital filters. The inter-relations among the foregoing are discussed in detail leading to performance curves for various implementations. A bandpass and band stop synthesis technique which is accomplished through a simple conversion of the lowpass coefficients is also developed. Bandpass filters having arithmetic symmetry are then synthesized using a frequency shift technique as well as a lowpass to bandpass transformation. The validation of these approaches for various ratios of sampling rate to carrier frequency is discussed. An analysis of synthesis errors is then accomplished. Under the assumption that tabular data is available, design procedures which minimize the sum-squared error are developed for design of non-recursive digital filters. A second approach to the design of these filters was accomplished under the assumption that a satisfactory recursive digital filter design using the bilinear transform was available.

## TABLE OF CONTENTS

	<u>Page</u>
I. INTRODUCTION	1
A. Summary of Results	2
II. GENERAL DESIGN PROCEDURES	7
A. Bilinear Transformation - Lowpass Applications	7
B. Bandpass Digital Filters - LP-BP Transformation	18
C. Bandpass Digital Filters - A Shifting Technique	25
D. Bandstop Digital Filters - A Feedback Technique	28
III. ARITHMETICALLY SYMMETRICAL BANDPASS FILTERS	34
A. Design Procedure for Elliptic Analog Filters	34
B. Digitized Lowpass Elliptic Filters	37
C. Application of the Shifting Technique	44
D. Symmetry Errors and Choice of Center Frequency	47
E. Application of the LP-BP Transformation	53
IV. NONRECURSIVE DIGITAL FILTERS	60
A. Nonrecursive Design From Tabulated Data	62
B. A Digital Impulse Invariant Technique	65
C. Zero Removal and Relocation	71
V. ERROR CONSIDERATIONS	78
A. Stability and Coefficient Accuracy	78
B. Cascade vs. Direct Synthesis	84
C. Computational Quantization	93
D. An Auxiliary Storage Technique	98
VI. RECOMMENDATIONS	108

APPENDIX A	A BANDPASS SAMPLING TECHNIQUE	110
APPENDIX B	DIGITAL OSCILLATORS	115
APPENDIX C	REFERENCES	123
APPENDIX D	BIBLIOGRAPHY	124

## EVALUATION

The increasing speed, as well as the decreasing size and cost associated with digital circuitry, that have been and still are resulting from the advances in the field of microelectronics, brings within view the likelihood that digital filters will perform within real time devices, almost all the functions now performed with analog components. The advantage of these digital filters in terms of the increased accuracies attainable, the ability to change filter shapes, the time sharing capabilities, the simplicity of the components needed (multipliers, adders and storage devices) and the variety of attainable filter shapes, among many other advantages, all serve to illustrate the importance and widespread application of this discipline.

Apart from "The Advanced Digital Processing" Contract now under way (Contract No. F30602-69-C-0199) it is strongly recommended that further work exploit the rich opportunities of this fruitful area. In particular the error reduction technique discussed in Section V-D has shown sufficient merit to warrant experimental breadboarding. Furthermore an experimental investigation should be initiated concerning the digital oscillator implementation technique discussed in Appendix B. A further area in this program looks highly rewarding at this time, and that is the question of direct digital design in complement to the presently developing family of digital equivalence procedures.

This approach (direct digital synthesis) warrants detailed investigation in that it will allow for more flexibility in the designs that can be achieved.

*Charles N. Meyer*  
CHARLES N. MEYER  
Project Engineer



## I. INTRODUCTION

The field of digital filters is based essentially on the mathematics of difference equations. In addition, the work accomplished in the fields of sampling, quantizing and related transformation techniques, have helped in both the reinterpretation and furthering of this discipline.

The increasing speed, as well as the decreasing size and cost associated with digital circuitry, that have been and still are resulting from the advances in the field of microelectronics, brings within view the likelihood that digital filters will perform within real-time devices, almost all the functions now performed with analog components. The advantages of these digital filters in terms of the increased accuracies attainable, the ability to change filter shapes, the time sharing capabilities, the simplicity of the components needed (multipliers, adders and storage devices) and the variety of attainable filter shapes, among many other advantages, all serve to illustrate the importance and widespread application of this discipline.

Thus, it is important that design procedures for digital filters be developed so that filters can be practically and economically synthesized, and that engineering designs can be accomplished.

This investigation was concerned with various digital filtering techniques and associated constraints. Section II through Section V develop in detail the foregoing. Recommendations for further study and development are discussed in Section VI. The essential results of this investigation are summarized below.

## A. SUMMARY OF RESULTS

### Section II - General Design Procedures

Design procedures for lowpass, bandpass and bandstop digital filters, are discussed. The bilinear transformation is applied to the design of lowpass filters in such a way that the relationships among the required sampling rate, upper cutoff frequency and order of the filter are brought out. The approach illustrates the importance of the ratio of sampling to cutoff frequency. The concept of normalization and its significance is also discussed. A tabular procedure is developed where these digital coefficients can be written down by inspection. Furthermore, this approach allows for a simpler evaluation and interpretation of coefficient truncation, stability and errors, as discussed in detail in Section V.

A lowpass to bandpass transformation is used in conjunction with the bilinear transformation. This combined transformation is then structured in such a form that a bandpass design can be accomplished by specifying the ratio of sampling frequency to bandwidth and sampling frequency to carrier frequency. Thus, once again, normalized frequency parameters are shown to be significant. An example illustrates how the foregoing are related to the factor  $Q$ , an often used parameter in analog filters. By an adjustment of the sampling-to-carrier frequency ratio a technique is described which allows a lowpass filter to be converted to a bandpass design without changing any of the coefficients.

A second bandpass design procedure which utilizes a frequency shifting technique is described. This approach shows considerable promise in the design of arithmetically symmetrical filters as discussed in Section III. This shifting procedure also suggests a technique for generating the coefficients "on line" from a lowpass design.

Lastly, a feedback technique is described which offers a simple

procedure for designing bandstop or notch filters. Once again, the procedure is accomplished through a simple conversion of the lowpass coefficients and shows clearly the relationship between the depth of the notch and value of the resulting coefficients.

### Section III - Arithmetically Symmetrical Bandpass Filters

A formalized, step-by-step procedure is outlined for the design of elliptic analog filters with examples illustrating the technique. These filters are then digitized as lowpass filters using the approach discussed in Section II. To convert these digital lowpass filters to bandpass, the frequency shifting technique of Section II is applied and the mechanism of the coefficient changes described. The examples chosen indicated that it was possible to reduce the symmetry errors to zero. Thus, a mathematical analysis of symmetry errors utilizing this shifting technique was accomplished. It was shown that there are two types of errors. A symmetry error about the carrier frequency and the error resulting from the shift from lowpass to bandpass. It is shown that the former error can be reduced to zero and the latter error to a negligible amount by appropriately choosing the relationship between carrier frequency and sampling rate.

It is then shown that for a particular ratio of sampling to carrier frequency, the LP-BP transformation yielded an arithmetically symmetrical design with zero symmetry error. This technique is then compared with the shifting technique at the same ratio. Although in general the shifting technique is excellently suited for the design of symmetrical filters, (and the LP-BP technique is not) the LP-BP transformation at this one sampling-to-carrier frequency ratio proves to be a simpler technique to apply if one already has the digital lowpass filter implementation.

#### Section IV - Nonrecursive Digital Filters

Under the assumption that tabular data is available in terms of the desired frequency characteristics, (both amplitude and phase), a design procedure for nonrecursive digital filters is developed which minimizes the sum squared error between the desired and actual response characteristics. These design equations are then related to an equivalent procedure which can be used when the desired response characteristics are available as a continuous function of frequency.

A second approach to the design of nonrecursive filters was accomplished under the assumption that a satisfactory recursive digital filter design was available.

Thus the procedure consists essentially of developing a finite Fourier series approximation to the recursive filter. It was assumed that the recursive filter was designed using the bilinear transform and that the nonrecursive approximation was to be a minimum mean square approximation to the recursive form. A simple technique (referred to as a digital impulse invariant technique) for converting the recursive coefficients to the required nonrecursive coefficients is developed. This approach yields zero error in the impulse responses of the two filters up to the number of terms retained in the nonrecursive form.

It was noted that there are essentially two types of errors in nonrecursive filter design. The first was due to a transformation procedure, the second due to truncation. The process of zero removal and relocation is discussed in the context of removing this second source of error. The interpretation of raised cosine pulses is accomplished using this technique as well as the relationships among several other nonrecursive design procedures. Ideally, this procedure offers the possibility of a complete characterization of finite pulses.

## Section V - Error Considerations

It is noted that there are three types of errors which occur in digital filter processing. The first of these is related to the process of sampling and quantizing the input signal. The second occurs as a result of truncating the representation of the filter coefficients. The third error is referred to as computational quantization. That is, the errors that occur as a result of quantizing the weighted multiplications and additions that occur within the digital filter's arithmetic unit. In recursive filters the results of these computations are fed back and utilized in later computations. This section discusses the latter two types of errors.

The relationship between coefficient accuracy and filter stability is determined using the tabular approach discussed in Section II. Simple relationships are derived which clearly show the interplay between the order of the filter, the ratio of sampling rate to critical filter parameters and the bit requirements for the filter's coefficients. Using this tabular approach, the filter degradation and onset of instability is interpreted as a function of the bit truncation of the coefficients. It is noted that when the ratio of sampling rate to filter cutoff frequency (in conjunction with the order of the filter) go beyond a specified value relative to the number of bits retained, the direct approach should not be used.

The foregoing constraints are illustrated through the design of a high order lowpass filter synthesized using the bilinear transformation. The superiority of the cascade approach (and the conditions under which it is superior) is then illustrated by synthesizing a filter utilizing the same number of bits per coefficient as in the direct form. This is accomplished twice. The first time the critical parameter are adjusted so that the direct and cascade approach yield similar results. Then this same is parameter adjusted so that the direct form does not yield useful results whereas the cascade approach does.

The relationship between the direct and canonical recursion implementations are discussed as to their performance when computational quantization occurs.

Illustrative examples indicate that a crossover point exists at which one implementation is more preferable than the other. It is noted once again that the determining factor is the normalized sampling rate.

Lastly, an auxiliary storage technique is discussed which offers the possibility of reducing the errors due to computational quantization. An example illustrates the approach.

#### Appendix A - A Bandpass Sampling Technique

Allowable sampling rates are discussed for bandpass signals so that no overlap distortion occurs. A curve is obtained relating the allowable sampling rate to the bandwidth and carrier frequency. As noted in the previous sections, these relationships are of extreme importance for bandpass filter design.

#### Appendix B - Digital Oscillators

Various implementations for a digital oscillator are discussed. An implementation utilizing the canonical form representation yields the smallest errors (due to computational quantization) and also requires the least amount of hardware. This device is exceedingly useful both as a frequency synthesizer and as a device to be used in conjunction with tracking filters, frequency translators and bandpass filtering.

## II. GENERAL DESIGN PROCEDURES

### A. BILINEAR TRANSFORMATION - LOWPASS APPLICATIONS

The basic form of a linear-time-invariant recursive digital filter is given by

$$y_n = \sum_{j=0}^N \frac{a_j}{b_0} x_{n-j} - \sum_{j=1}^M \frac{b_j}{b_0} y_{n-j} \quad \text{II-1}^*$$

or equivalently in terms of its transfer function as

$$H(Z) = \frac{\sum_{j=0}^N a_j Z^{-j}}{\sum_{j=0}^M b_j Z^{-j}} \quad \text{II-2}$$

where  $Z^{-1} = e^{-j\bar{\omega}T}$  is the unit delay operator,  $T$  is the time between successive samples (equal spacing assumed),  $\bar{\omega}$  is the digital frequency variable,\*\*  $H(Z)$  the transfer function,  $x_n$  and  $y_n$  the input and output samples, and  $a_j$  and  $b_j$  the digital filter coefficients. Thus the digital filter is an arithmetic unit which performs the operations of weighted multiplications and additions on past and present input and output data samples. The inclusion of non-zero  $b_j$  coefficients gives rise to the terminology recursive or feedback type filter in which prior output samples are utilized.

---

\* Alternate equivalent realizations will be discussed in Section V.

\*\* It is to be noted that the digital frequency variable,  $\bar{\omega}$ , appears only as a product  $\bar{\omega}T = 2\pi T/f_s$  where  $f_s$  is the sampling rate. The significance of the foregoing will be discussed on the following pages relative to the important concept of normalization for digital filters.

The general problem of recursive digital filter design is the determination of the coefficients  $a_j$  and  $b_j$  so that a desired filter characteristic is obtained. A basic approach to this problem has been to utilize existing continuous (analog) filter theory to "find" a suitable response and then apply a transformation technique which digitizes the continuous filter in such a way that the response is transformed without any appreciable distortion.\* This is referred to as a digital equivalence technique.

A transformation which has been used with considerable success is the so-called bilinear <sup>(1)</sup> or Tustin <sup>(2)</sup> transformation given by the mapping between the variables  $S$  and  $Z^{-1}$  given by

$$S \rightarrow \frac{2}{T} \frac{(1 - Z^{-1})}{(1 + Z^{-1})} \quad \text{II-3}$$

or

$$Z^{-1} \rightarrow \frac{1 - (ST/2)}{1 + (ST/2)} \quad \text{II-4}$$

The advantageous properties of this transformation in terms of preservation of stability (the left of the  $s$  plane is mapped into the interior of the unit circle of the  $Z$  plane), the maintenance of the cascading property (as well as dc gain) and the simplicity of its application in that it is purely algebraic in nature, has been discussed by several authors. <sup>(3)</sup> A disadvantage of this technique is that the transformation given in II-3 causes a distortion in the frequency domain. That is, with  $s = j\omega$  and  $Z^{-1} = e^{-j\bar{\omega}T}$ , II-3 becomes

$$\frac{\omega T}{2} \rightarrow \tan \bar{\omega} T/2 \quad \text{II-5}$$

---

\* The approach for the design of nonrecursive filters often uses a more direct approach without resorting to transformation techniques. These filters ( $b_j = 0, 1 \leq j \leq M$ ) will be discussed in Section IV.



Thus, the relationship between the analog and digital frequency variables is not linear. The deviation from linearity given by II-5 is dependent on the product ( $\omega T/2$ ). Since  $T$  is the reciprocal of the sampling rate, this distortion or so-called warping of the frequency scale is reduced when the ratio of sampling rate to critical frequency points is made larger. There are however, other constraints on this ratio which will be discussed. Furthermore, compensation of this distortion will also be discussed.

In that the bilinear transformation properly occupies a central position in the design of digital filters, it has been utilized extensively in this investigation. In order to illustrate the design approach and discuss the interrelationships among the various critical parameters, consider a normalized (unity cutoff frequency, in rad/sec) low pass (LP) analog (or continuous) filter of the form

$$G(S) = \frac{\sum_{n=0}^N A_n S^n}{\sum_{n=0}^N B_n S^n} \quad \text{II-6}^*$$

The concept of a normalized frequency response characteristic is widely accepted in the synthesis of continuous filters as a procedure which allows for a universal design. In order to convert this normalized response to a low-pass filter with an upper cutoff frequency of  $\omega_u$ , if one applies the conventional LP to LP transformation

$$S \rightarrow \frac{S}{\omega_u} \quad \text{II-7}$$

---

\* Although the numerator and denominator are usually of different order, they can always be written as shown, by adding the required zeros.

in conjunction with the bilinear transformation from  $S$  to  $Z$ , it can be shown that the synthesized digital filter  $H(Z)$  becomes

$$H(Z) = G\left(\frac{S}{\omega_u}\right) \bigg|_{S = \frac{2}{T} \frac{1 - Z^{-1}}{1 + Z^{-1}}} \quad \text{II-8}$$

or

$$H(Z) = \frac{\sum_{n=0}^N A_n \left(\frac{\omega_u T}{2}\right)^{N-n} (1 - Z^{-1})^n (1 + Z^{-1})^{N-n}}{\sum_{n=0}^N B_n \left(\frac{\omega_u T}{2}\right)^{N-n} (1 - Z^{-1})^n (1 + Z^{-1})^{N-n}} \quad \text{II-9}$$

In the determination of II-9, fractions were cleared by multiplying the numerator and denominator by  $(\omega_u T/2)^N$  and  $(1 + Z^{-1})^N$ . Now, suppose  $\bar{\omega}_u$  is the desired digital upper cutoff frequency of the digital filter.

Using the transformation of II-5, the analog cutoff frequency variable  $\omega_u$  is replaced by its equivalence in terms of  $\bar{\omega}_u$  and then II-9 becomes

$$H(Z) = \frac{\sum_{n=0}^N A_n K_{\bar{\omega}_u}^{N-n} (1 - Z^{-1})^n (1 + Z^{-1})^{N-n}}{\sum_{n=0}^N B_n K_{\bar{\omega}_u}^{N-n} (1 - Z^{-1})^n (1 + Z^{-1})^{N-n}} = \frac{\sum_{n=0}^N a_n Z^{-n}}{\sum_{n=0}^N b_n Z^{-n}} \quad \text{II-10}$$

where the  $a_n$  and  $b_n$  are the coefficients of  $Z^{-n}$  obtained by expanding the summations in II-10 and

$$K_{\bar{\omega}_u} = \tan\left(\bar{\omega}_u \frac{T}{2}\right) \quad \text{II-11}$$

Thus, the frequency response of a digital filter is a function of the normalized (with respect to the sampling rate) digital cutoff frequency. Furthermore, since

$Z^{-1} = e^{-j\bar{\omega} T}$  and the  $A_n$  and  $B_n$  are the constants obtained from the normalized lowpass analog filter, the entire digital frequency characteristic ( $H(Z)$ ) is such that the digital frequency variable  $\bar{\omega}$  appears only as the product  $\bar{\omega} T$ . Thus if this characteristic is plotted as a function of  $\bar{\omega} T$  and not  $\bar{\omega}$ , one obtains a normalized digital frequency characteristic which provides a universal curve in the same sense as normalization with respect to  $\omega = 1$  rad/sec did in the analog case.

This is exceedingly important to note in that

the coefficients ( $a_n, b_n$ ) for this digital lowpass filter remain fixed as long as the product  $\bar{\omega}_u T = 2\pi f_u / f_s$  remains fixed.

Therefore, the coefficients for a digital lowpass filter with a cutoff at  $f_u = 10$  KHz operating on data sampled at  $f_s = 100$  KHz are exactly the same as those obtained for any other  $f_u$  and  $f_s$  as long as the ratio  $f_u / f_s = .1$ . Hence, by plotting the characteristic as a function of  $\bar{\omega} T$  (i.e. in radians or degrees) one has a "universal" digital filter characteristic (the digital coefficients remain fixed) for that particular ratio of  $f_u$  to  $f_s$  (or equivalently a fixed  $K_{\bar{\omega}_u}$ ). To convert this angular abscissa to actual frequencies, one merely utilizes the actual sampling rates used on the input data. These rates are of course dictated by the bandwidth of the input data and the constraints of the sampling theorem. For the foregoing reasons all digital filter characteristics in this report are plotted as a function of angle. The above results are of course applicable to bandpass, bandstop and all other digital filter forms. The critical ratio and parameters in these cases will be discussed in II-B.

In order to obtain the a's and b's of the digital filter in terms of  $K_{\bar{\omega}_u}$  and the A's and B's of the analog filter, II-10 must be expanded. It is also to be noted that the form of the numerator and denominator of II-10 is similar to one another. Thus the expansion equations will likewise be similar. During this investigation it has been shown that these digital coefficients for any order filter

are given by the following table.

TABLE I

Coefficients	$P_0 K \frac{N}{\omega_u}$	$P_1 K \frac{N-1}{\omega_u}$	$P_2 K \frac{N-2}{\omega_u}$	....	$P_N K \frac{0}{\omega_u}$
$z^0(a_0, b_0)$	1	1	1	....	1
$z^{-1}(a_1, b_1)$	$C_1^N$	( )	( )		( )
$z^{-2}$	$C_2^N$	( )	( )		( )
.	.	.	$d_{i,j}$		.
..	.	.			.
..	.	.			.
$z^{-N}(a_N, b_N)$	$C_N^N$	( )	...		( )

where

$$C_r^N = \frac{N!}{r! (N-r)!}$$

The entry  $d_{i,j}$  in row  $i$  and column  $j$  is given by

$$d_{i,j} = d_{i,j-1} - [d_{i-1,j-1} + d_{i-1,j}] \quad \text{II-12}$$

The interpretation of this table to obtain the digital filter coefficients is as follows: To obtain the numerator coefficients  $a_k$ , substitute for  $P_j$  the appropriately subscripted numerator coefficient of the analog filter and sum all the products of the table entries and column headings. The same procedure is used for the denominator coefficients except that the analog denominator coefficients are now substituted for the  $P_j$ .

As noted from this Table, the first row consists of all "ones" and the first column consists of the binomial coefficients. It can also be shown that

the last row is identical to the first row except with alternating signs and the last column identical to the first column except for alternating signs. Utilizing II-12, it can also be shown that the sum of the table entries over any column except the first is equal to zero. The above relationships will be found to be useful in the discussion of coefficient accuracy and stability considerations discussed in Section V.

As an example of the above, Table II lists the digital filter coefficients for a sixth order digital filter. The coefficients in this table are obtained utilizing II-12.

TABLE II  
Sixth Order Digital Filter Coefficients

$(a_0 \text{ or } b_0) =$	$P_0 K_{\omega_u}^6 + P_1 K_{\omega_u}^5 + P_2 K_{\omega_u}^4 + P_3 K_{\omega_u}^3 + P_4 K_{\omega_u}^2 + P_5 K_{\omega_u} + P_6$
$(a_1 \text{ or } b_1) =$	$6 P_0 K_{\omega_u}^6 + 4 P_1 K_{\omega_u}^5 - 2 P_2 K_{\omega_u}^4 - 2 P_4 K_{\omega_u}^2 - 4 P_5 K_{\omega_u} - 6 P_6$
$(a_2 \text{ or } b_2) =$	$15 P_0 K_{\omega_u}^6 + 5 P_1 K_{\omega_u}^5 - P_2 K_{\omega_u}^4 - 3 P_3 K_{\omega_u}^3 - P_4 K_{\omega_u}^2 + 5 P_5 K_{\omega_u} + 15 P_6$
$(a_3 \text{ or } b_3) =$	$20 P_0 K_{\omega_u}^6 - 4 P_2 K_{\omega_u}^4 + 4 P_4 K_{\omega_u}^2 - 20 P_6$
$(a_4 \text{ or } b_4) =$	$15 P_0 K_{\omega_u}^6 - 5 P_1 K_{\omega_u}^5 - P_2 K_{\omega_u}^4 - 3 P_3 K_{\omega_u}^3 - P_4 K_{\omega_u}^2 - 5 P_5 K_{\omega_u} + 15 P_6$
$(a_5 \text{ or } b_5) =$	$6 P_0 K_{\omega_u}^6 - 4 P_1 K_{\omega_u}^5 + 2 P_2 K_{\omega_u}^4 - 2 P_4 K_{\omega_u}^2 + 4 P_5 K_{\omega_u} - 6 P_6$
$(a_6 \text{ or } b_6) =$	$P_0 K_{\omega_u}^6 - P_1 K_{\omega_u}^5 + P_2 K_{\omega_u}^4 - P_3 K_{\omega_u}^3 + P_4 K_{\omega_u}^2 - P_5 K_{\omega_u} + P_6$

Although error considerations will be discussed in detail in Section V, Table II illustrates some of the constraints among the various parameters and how they affect the required number of bits to be retained for the coefficients. As can be seen from this Table (and Table I),  $K_{\omega_u}$  appears in the equations

raised to powers up to the order of the filter. This factor (given by II-11) is proportional to the ratio of upper cutoff frequency to sampling frequency. Thus, when this ratio is small and the order of the filter high,  $K \frac{N}{\omega_u}$  is a small number. Qualitatively from these tables it can be seen that to include the effect of  $P_0$  a sufficient number of bits must be retained. For example, if the ratio of sampling to cutoff frequency is 30:1 then  $K \frac{6}{\omega_u} \approx 10^{-6}$  and as many as six decimal digits might be required in the synthesis. It should be recalled that the sampling rate is dictated by the signal bandwidth and aliasing considerations and therefore cannot be made arbitrarily smaller. Thus, if it is required to design a filter with a 3 db point at 30 KHz to filter a signal with a bandwidth of .3 MHz, then with a sampling rate of 3 times maximum the ratio discussed above becomes  $30:1 = f_s:T_u$ .

As an illustrative example of the use of the foregoing tables, consider the design of a normalized lowpass elliptic filter\* designed to meet the following specifications.

Passband Spec. .01 db ripple  $0 \leq \omega \leq 1$

Stopband Spec. 40 db attenuation  $1.38 \leq \omega \leq \omega^{**}$

The above specifications can be shown to yield a sixth order analog filter of the form

$$G(S) = \frac{S^4 + A_2 S^2 + A_0}{S^6 + B_5 S^5 + B_4 S^4 + B_3 S^3 + B_2 S^2 + B_1 S + B_0} \quad \text{II-13}$$

\* These filters will be discussed at length in Section III.

\*\* Note the normalizations on the analog filter. That is the stopband begins 38% beyond the passband.

where the coefficients are given as\*

TABLE III

$A_0 = 6.79609$	$B_2 = 5.71737$
$A_2 = 5.40108$	$B_3 = 6.29689$
$B_0 = 1.26743$	$B_4 = 5.06663$
$B_1 = 3.44569$	$B_5 = 2.62193$
$B_6 = 1$	

Solving for the roots of the numerator and denominator yield the pole-zero configuration for this filter given by

TABLE IV

$z_0 = \pm j 1.84538$	(zeros)
$z_1 = \pm j 1.41268$	
$p_1 = -.10102 \pm j 1.12369$	(poles)
$p_2 = -.39699 \pm .99211$	
$p_3 = -.81294 \pm .45946$	

It was decided to digitize this filter for a ratio of sampling rate to cut-off frequency of 18:1. This could correspond to the problem of filtering sampled data in the band from 0 to 1 KHz from a signal with a bandwidth of 6 KHz that has been sampled at three times its bandwidth or  $f_s = 18$  KHz, thus yielding  $f_s/f_u = 18$ .

---

\*The procedure to obtain these coefficients will be discussed in Section III, where additional references on analog filter coefficient determination will be given.

For this ratio, the product  $\bar{\omega}_u T$  becomes

$$\bar{\omega}_u T = 2\pi \frac{f_u}{f_s} = \frac{2\pi}{18} \text{ (rad)} = 20^\circ \quad \text{II-14}$$

Thus  $K_{\bar{\omega}_u}$  becomes

$$K_{\bar{\omega}_u} = \tan\left(\frac{\bar{\omega}_u T}{2}\right) = \tan(10^\circ) = .17633 \quad \text{II-15}$$

Using the analog coefficients given in Table III, the factor  $K_{\bar{\omega}_u}$  given above, and the transformation equations of Table II, the digital filter coefficients obtained by summing each row of this table are given as

TABLE V

$a_0 = .0365179$	$b_0 = 1.6605333$
$a_1 = -.0505161$	$b_1 = -8.1507334$
$a_2 = -.0332495$	$b_2 = 17.0485046$
$a_3 = .1075630$	$b_3 = -19.3912146$
$a_4 = -.0332495$	$b_4 = 12.6265180$
$a_5 = -.0505161$	$b_5 = -4.4568329$
$a_6 = .0365179$	$b_6 = .6656633$
(numerator)	(denominator)

A plot of the resulting magnitude characteristic is shown in Figure II-1.

Two significant items are to be noted from the above. First, the digital filter obtained is valid (without changing any coefficient) at any frequency as long as the 18:1 ratio is maintained. Second, the plotting of the magnitude characteristic is shown as a function of angle -- not frequency. Thus, the cut-offs are adjusted to the desired frequency by a selection of the sampling rate.



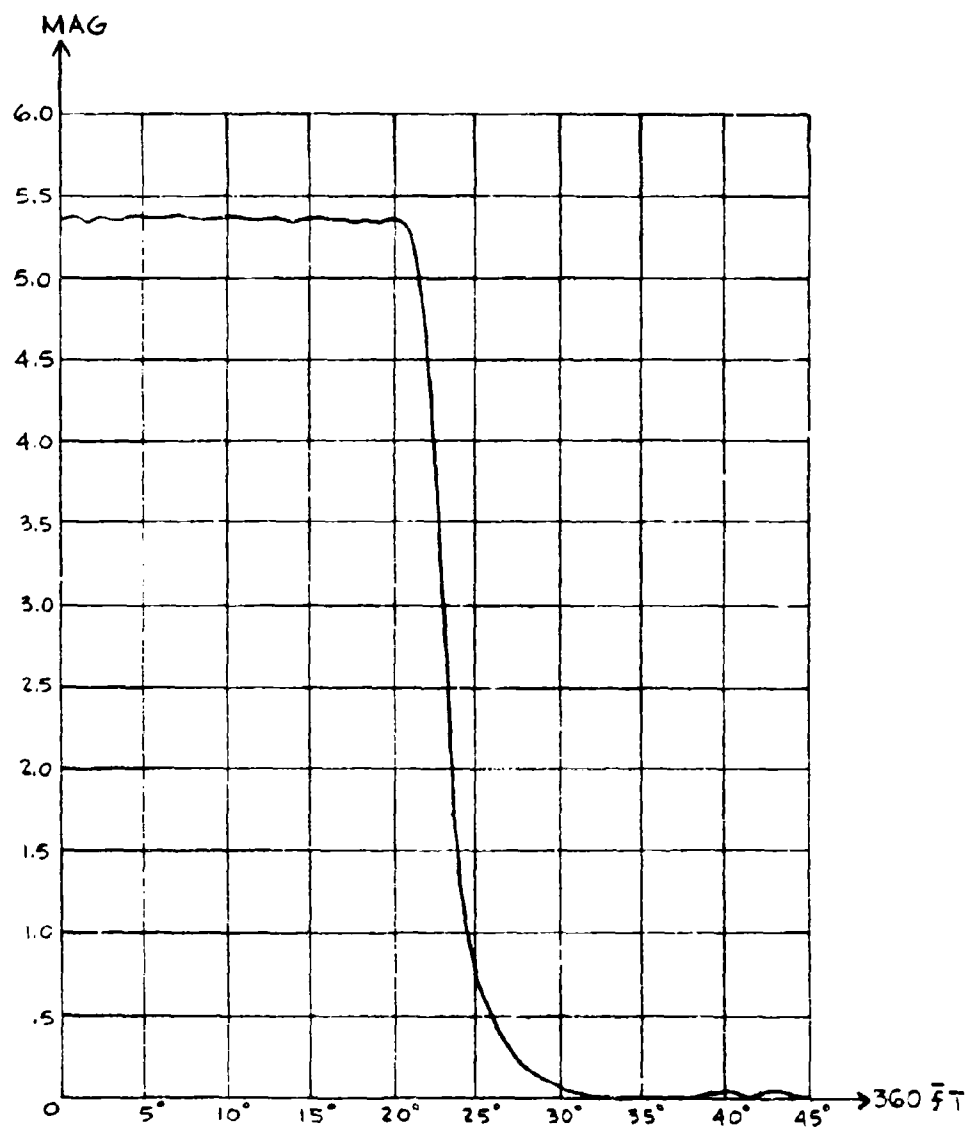


FIGURE II-1: ELLIPTIC FILTER WITH 20° CUTOFF

The foregoing illustrated a design procedure for lowpass filters which is simple to apply and which yields accurate results. Consideration on coefficient bit lengths, errors and implementation procedures, will be discussed in Section V.

## B. BANDPASS DIGITAL FILTERS - LP-BP TRANSFORMATION

As noted in the previous section, digital filter normalization can be accomplished for all filter forms. A transformation from low pass to bandpass will now be discussed which illustrates the manner in which the critical parameters affect the design.

The conventional lowpass to bandpass transformation (LP-BP) used in analog filter design is given as

$$\begin{array}{l} \text{LP-BP (analog)} \\ S \rightarrow \frac{S^2 + \omega_o^2}{BS} \end{array} \quad \text{II-16}$$

where  $B = \omega_2 - \omega_1$  (bandwidth);  $\omega_o^2 = \omega_1 \omega_2$  (center frequency squared) and  $\omega_1$  and  $\omega_2$  are respectively the lower and upper cutoff analog frequencies. If II-16 is combined with the bilinear transformation given in II-3, then II-16 becomes

$$S \rightarrow \frac{1 + \omega_o^2 T^2 / 4}{\frac{BT}{2}} \left[ \frac{1 - 2 \left[ \left( 1 - \frac{\omega_o^2 T^2}{4} \right) / \left( 1 + \frac{\omega_o^2 T^2}{4} \right) \right] Z^{-1} + Z^{-2}}{1 - Z^{-2}} \right] \quad \text{II-17}$$

Now, the bilinear transformation transforms analog frequencies to digital frequencies as

$$\frac{\omega T}{2} \rightarrow \tan \frac{\bar{\omega} T}{2} \quad \text{II-18}$$

Thus, utilizing the above and the relationships between  $\omega_o$ ,  $\omega_1$  and  $\omega_2$  the factors

in II-17 become

$$\frac{1 + \frac{\omega_o^2 T^2}{4}}{\frac{BT}{2}} = \frac{1 + \tan\left(\frac{\bar{\omega}_1 T}{2}\right) \tan\left(\frac{\bar{\omega}_2 T}{2}\right)}{\tan\left(\frac{\bar{\omega}_2 T}{2}\right) - \tan\left(\frac{\bar{\omega}_1 T}{2}\right)} = \frac{1}{\tan\left[\left(\frac{\bar{\omega}_2 - \bar{\omega}_1}{2}\right) T\right]} = \frac{1}{K_B} \quad \text{II-19}$$

$$\frac{1 - \frac{\omega_o^2 T^2}{4}}{1 + \frac{\omega_o^2 T^2}{4}} = \frac{1 - \tan^2\left(\frac{\bar{\omega}_o T}{2}\right)}{1 + \tan^2\left(\frac{\bar{\omega}_o T}{2}\right)} = \cos \bar{\omega}_o T$$

where

$$\frac{\omega_o T}{2} \rightarrow \tan\left(\frac{\bar{\omega}_o T}{2}\right)$$

$$\frac{\omega_1 T}{2} \rightarrow \tan\left(\frac{\bar{\omega}_1 T}{2}\right)$$

II-20

$$\frac{\omega_2 T}{2} \rightarrow \tan\left(\frac{\bar{\omega}_2 T}{2}\right)$$

Thus II-17 becomes

LP-BP (digital)

$$S \rightarrow \frac{1 - 2(\cos \bar{\omega}_o T) Z^{-1} + Z^{-2}}{K_B (1 - Z^{-2})} \quad \text{II-21}$$

The transformation from S to Z is now given in terms of the digital parameters of (1) digital carrier frequency  $\bar{\omega}_o$  and (2) digital bandwidth  $(\bar{\omega}_2 - \bar{\omega}_1)$ . Once again, the parameters are normalized with respect to the sampling rate.

Similarly, the lowpass to bandstop transformation is merely the inverse of II-21 or

$$S \rightarrow \frac{K_{\bar{B}}(1 - Z^{-2})}{1 - 2(\cos \bar{\omega}_0 T)Z^{-1} + Z^{-2}} \quad \text{II-22}$$

Thus, one now has two simple transformations to convert a normalized lowpass analog filter to either a bandpass or bandstop digital filter by specifying the normalized digital center frequency and normalized digital bandwidth. Qualitatively, this equation can be related to the lowpass transformation by noting that the factor  $K_{\bar{B}}$  has replaced the lowpass factor  $K_{\bar{\omega}_u}$  and the numerator of II-21 can be interpreted by noting that

$$1 - 2(\cos \bar{\omega}_0 T)Z^{-1} + Z^{-2} = (Z^{-1} - e^{-j\bar{\omega}_0 T})(Z^{-1} - e^{+j\bar{\omega}_0 T}) \quad \text{II-23}$$

Thus since  $Z^{-1} = e^{-j\bar{\omega}_0 T}$ , the roots have been shifted to  $\bar{\omega} = \pm \bar{\omega}_0$ , the digital carrier frequency.

As a simple example of the application of the LP-BS transformation, consider the lowpass R-C filter

$$G_{LP}(S) = \frac{1}{S + 1} \quad \text{II-24}$$

substituting II-22 in the above yields

$$H(Z) = \frac{1 - 2(\cos \bar{\omega}_0 T)Z^{-1} + Z^{-2}}{(1 + K_{\bar{B}}) - 2(\cos \bar{\omega}_0 T)Z^{-1} + (1 - K_{\bar{B}})Z^{-2}} \quad \text{II-25}$$

Thus II-25 represents a digitized R-C bandstop filter for any normalized digital center frequency and normalized digital bandwidth (or notch or rejection band). The resulting digital filter is of the same form as would result from applying the bilinear transform directly to the familiar analog notch filter given by

$$\frac{s^2 + \lambda^2}{s^2 + 2\xi\lambda s + \lambda^2} \quad \text{II-26}$$

where  $\lambda$  is the analog notch frequency and  $\xi$  is the analog damping ratio. This is so because the R-C filter is converted to the above by the LP-BS (analog) transformation.

A further interpretation of the factor  $K_{\overline{B}}$  or terms of the  $Q$  of the filter is as follows

$$K_{\overline{B}} = \tan \left[ (\overline{\omega}_2 - \overline{\omega}_1) T / 2 \right] = \tan \pi \overline{B}_f T \quad \text{II-27}$$

$$\overline{B}_f = \text{dig}, 1 \text{ bW} \quad \text{II-28}$$

Now  $(1/T) = f_s = \text{sampling rate}$ . However, if one assumes that

$$f_s = r T_o \quad \text{II-29}$$

and

$$Q = \frac{T_o}{\overline{B}_f} = \frac{\text{carrier frequency}}{\text{Bandwidth}} \quad \text{II-30}$$

then  $K_{\overline{B}}$  becomes

$$K_{\overline{B}} = \tan \frac{\pi}{kQ} \quad \text{II-31}$$

Thus, for high  $Q$  filters ( $Q > 10$ ) this can be approximated by

$$K_{\overline{B}} \approx \frac{\pi}{kQ} \quad \text{II-32}$$

As expected, the higher the  $Q$  of the filter, the narrower the bandwidth. If, for example,  $k$  is chosen to be equal to four -- signifying that the sampling rate is four times the desired carrier frequency and  $Q \approx \pi \times 100/2$  (for example), then the digitized R-C of II-25 becomes

$$H(Z) = \frac{1 + Z^{-2}}{1.005 + .995 Z^{-2}}$$

A plot of this filter within the rejection band is shown in Figure II-2.

Note, once again that this filter has been plotted as a function of angle. Since it was assumed that  $f_s/\bar{f}_0 = 4$ , then  $\bar{\omega}_0 T = \pi/4$  or  $90^\circ$ . Thus the normalized center frequency of this bandpass filter is  $90^\circ$ .

The digital LP-BP and LP-BS transformations given in II-21 and II-22 have interesting properties when compared with the LP-LP transformation of

$$S \rightarrow \frac{(1 - Z^{-1})}{K_{\omega_u} (1 + Z^{-1})} \quad \text{II-34}$$

obtained by combining the bilinear transformation with  $S \rightarrow S/\omega_u$ .

Consider II-21 when the ratio of sampling rate to carrier frequency  $f_s/\bar{f}_0$  is 4:1. In this case  $\cos \bar{\omega}_0 T = 0$  and II-21 becomes

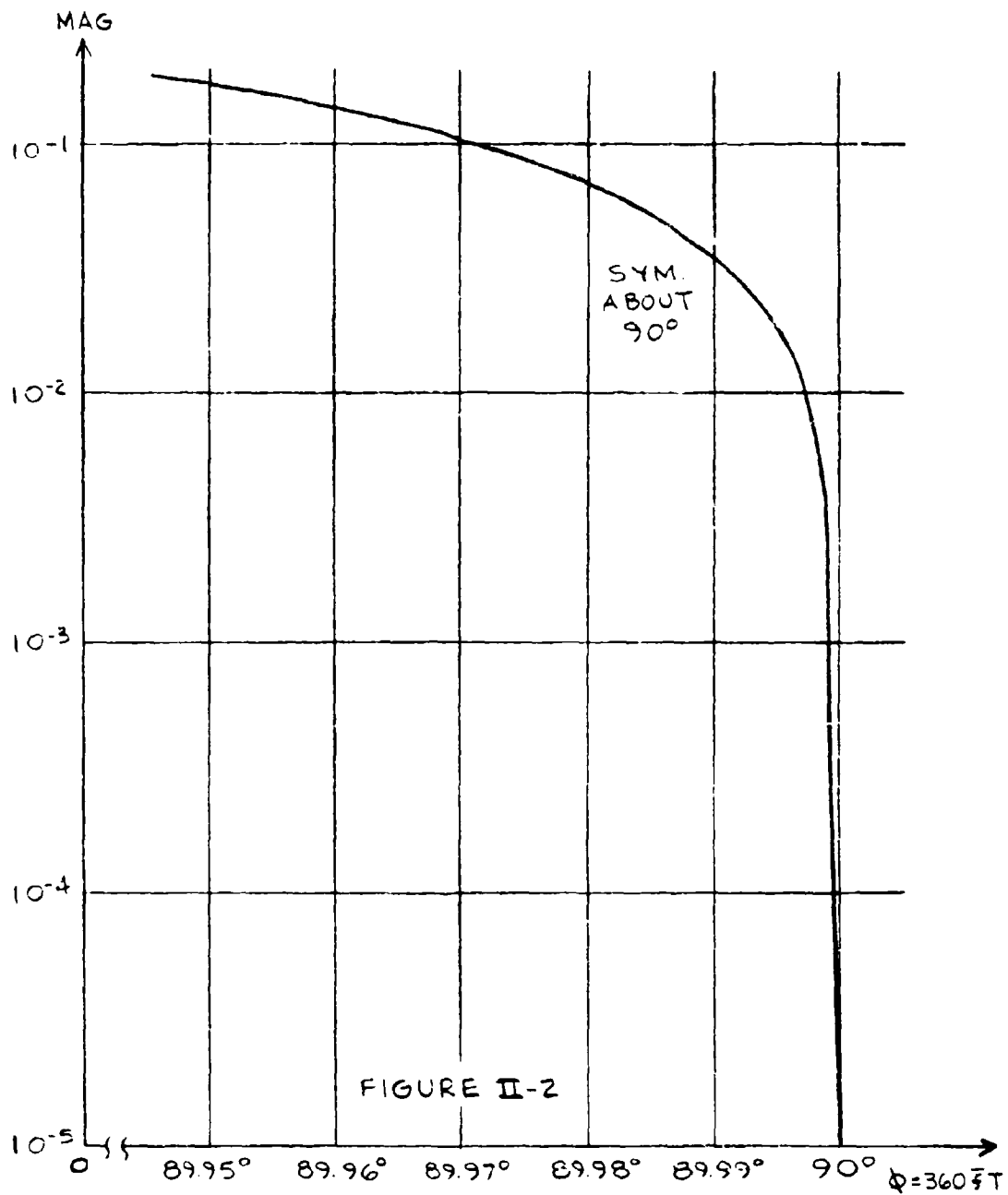
$$S \rightarrow \frac{1}{K_B} \frac{(1 + Z^{-2})}{(1 - Z^{-2})} \quad \text{II-35}$$

Similarly the LP-BS transformation becomes

$$S \rightarrow K_B \frac{(1 - Z^{-2})}{(1 + Z^{-2})} \quad \text{II-36}$$

Comparing II-34 and II-35, one notes that if  $K_{\omega_u}$  is replaced by  $K_B$  and  $Z^{-1}$  is replaced by  $-Z^{-2}$  then II-34 is converted to II-35. Thus, one has a procedure to convert a lowpass digital filter to a bandpass digital filter without changing the magnitude of any of the coefficients. The constraints are that the upper frequency cutoff of the lowpass filter is made to coincide with the digital bandwidth and the 4:1 ratio be maintained. Thus a digital lowpass filter of the form

$$H(z) = \frac{1+z^{-2}}{1.005 + .995z^{-2}}$$



$$H_{LP}(Z) = \frac{\sum_{n=0}^N a_n Z^{-n}}{\sum_{n=0}^M b_n Z^{-n}} \quad \text{II-37}$$

is converted to a digital bandpass filter of the form

$$H_{BP}(Z) = \frac{\sum_{n=0}^N a_n (-1)^n Z^{-2n}}{\sum_{n=0}^M b_n (-1)^n Z^{-2n}} \quad \text{II-38}$$

Similarly, the LP-BS transformation is obtained by replacing  $Z^{-1}$  by  $Z^{-2}$  and  $K_{\omega_u}$  by  $1/K_B$ . As an example of the latter, consider applying II-34 to the analog R-C filter of II-24. Making the substitution yields

$$H_{LP}(Z) = \frac{1 + Z^{-1}}{(\frac{1}{K_{\omega_u}})(1 - Z^{-1}) + (1 + Z^{-1})} \quad \text{II-39}$$

Making the substitution noted above yields

$$H_{BS}(Z) = \frac{1 + Z^{-2}}{K_B(1 - Z^{-2}) + (1 + Z^{-2})} \quad \text{II-40}$$

$$H_{BS}(Z) = \frac{1 + Z^{-2}}{(1 + K_B) + (1 - K_B) Z^{-2}} \quad \text{II-41}$$

Equation II-41 reduces to the notch of II-33 when  $K_B = .005$  which is in the example.

The above procedures illustrate the use of a digitized LP-BP and BS



transformations. As noted above, when the ratio of sampling to carrier frequency is 4:1, bandpass filters can be obtained without changing the magnitude of the coefficients. It is to be noted that the highest negative power of Z is twice what it was in the lowpass case, implying twice the number of delay elements.

### C. BANDPASS DIGITAL FILTERS - A SHIFTING TECHNIQUE

The bandpass design procedure discussed in the foregoing utilized the LP-BP transformation in conjunction with the bilinear transformation. The analog LP-BP transformation is of a form which yields a realizable (in terms of R's, L's and C's) analog filter. One need not be constrained in this manner in the design of digital filters. A technique will now be described which parallels that of a heterodyning procedure in analog signal theory.

If one has the Fourier transform pair

$$f(t) \longleftrightarrow F(\omega) \quad \text{II-42}$$

Then

$$g(t) = f(t) \cos \omega_0 t \longleftrightarrow \frac{F(\omega - \omega_0) + F(\omega + \omega_0)}{2} \quad \text{II-43}$$

Thus if  $f(t)$  were a lowpass signal, then  $g(t)$  is a bandpass signal centered at  $\omega_0$ .

Consider the application of the above to the lowpass digital filter

$$H_{LP}(Z) = \frac{\sum_{n=0}^N a_n Z^{-n}}{\sum_{n=0}^M b_n Z^{-n}} \quad \text{II-44}$$

By dividing out the denominator, II-44 can be written as

$$H_{LP}(Z) = \sum_{n=0}^{\infty} h_n Z^{-n} \quad \text{II-45}$$

or, the input-output equation becomes

$$y_n = \sum_{k=0}^{\infty} h_k x_{n-k} \quad \text{II-46}$$

Multiplying the  $h_n$  coefficients by  $\cos n\bar{\omega}_0 T$  and taking the Z transform of II-45 yields

$$H_{BP}(Z) = \frac{H_{LP}(Ze^{j\bar{\omega}_0 T}) + H_{LP}(Ze^{-j\bar{\omega}_0 T})}{2} \quad \text{II-47}$$

Combining Eqs. II-44 and II-47 yields

$$H_{BP}(Z) = \frac{\sum_{k=0}^N \sum_{n=0}^M a_k b_n Z^{-(k+n)} \cos \bar{\omega}_0 T (n-k)}{\sum_{k=0}^N \sum_{n=0}^M b_k b_n Z^{-(k+n)} \cos \bar{\omega}_0 T (n-k)} \quad \text{II-48}$$

which is of the form discussed by Broome.<sup>(4)</sup>

It can be shown that II-48 can be rewritten as

$$H_{BP}(Z) = \frac{\sum_{n=0}^{N+M} A_n Z^{-n}}{\sum_{n=0}^{N+M} B_n Z^{-n}} \quad \text{II-49}$$

where

$$A_n = \sum_{r=0}^M a_{n-r} b_r \cos \bar{\omega}_0 T (n-2r) \quad \text{II-50}$$

and

$$B_n = \sum_{r=0}^M b_{n-r} b_r \cos \bar{\omega}_0 T (n-2r) \quad \text{II-51}$$

Thus, the numerator coefficients of the BP filter are a function of both the numerator and denominator coefficients of the lowpass filter. It should also be noted that the bandpass coefficients are once again a function of the normalized carrier frequency and that II-48 and II-49 are in the form of a convolution sum suggesting a synthesis procedure, which will be discussed in the following sections.

Perhaps the greatest application for this technique lies in the design of symmetrical bandpass filters -- an application which will be discussed at length in the next section. The above application is due to the fact that the design procedure was accomplished through a translation of the frequency characteristic to the left and right by  $\bar{\omega}_0$ . The LP-BP transformation discussed previously had properties of geometric symmetry ( $\omega_0^2 = \omega_1 \omega_2$ ).

As in the case of the LP-BP transformation, a simplification is obtained for a 4:1 ratio of sampling frequency to center frequency. For this case, II-50 and II-51 become

$$A_n = (-1)^n \sum_{r=0}^M (-1)^r b_r a_{n-r} \quad n \text{ even} \quad \text{II-52}$$

$$B_n = (-1)^n \sum_{r=0}^M (-1)^r b_r b_{n-r} \quad \text{II-53}$$

$$A_n = B_n = 0 \quad n \text{ odd}$$

Illustrative examples comparing the above and the LP-BP transformation will be discussed in the next section. The two approaches presented provide for convenient synthesis of bandpass (and bandstop) digital filters in terms of their critical parameters.

#### D. BANDSTOP DIGITAL FILTERS - A FEEDBACK TECHNIQUE

Consider a bandpass digital filter given as  $H_{BP}(Z)$ . Then form a new digital filter- given by

$$H_{BS}(Z) = \frac{1}{1 + K H_{BP}(Z)} \quad \text{II-54}$$

where  $K$  is a constant adjusted to be much greater than the maximum gain of  $H_{BP}(Z)$ . Now, assuming that the gain of  $H_{BP}(Z)$  is unity in the passband then  $H_{BS}(Z)$  is given by

$$H_{BS}(Z) = \frac{1}{1 + K} \approx \frac{1}{K} \quad \left( \begin{array}{l} \text{In the passband} \\ \text{of } H_{BP}(Z) \end{array} \right) \quad \text{II-55}$$

In the region where  $H_{BP}(Z)$  is small ( $K H_{BP}(Z) \ll 1$ ),  $H_{BS}$  is

$$H_{BS}(Z) \approx 1 \quad \left( \begin{array}{l} \text{In stopband} \\ \text{of } H_{BP}(Z) \end{array} \right) \quad \text{II-56}$$

Thus, the attenuation in the stopband is controlled by  $K$  and the passband gain is unity.

Consider the digital filter coefficients generated by this technique. Let

$$H_{BP}(Z) = \frac{N(Z)}{D(Z)} \quad \text{II-57}$$

Then II-54 becomes

$$H_{BS}(Z) = \frac{D(Z)}{D(Z) + K N(Z)} \quad \text{II-58}$$

Thus, the numerator and denominator coefficients are given respectively by

$$\begin{aligned} a'_n &= b_n \\ b'_n &= b_n + K a_n \end{aligned} \quad \text{II-59}$$

The primed coefficients are those of the resulting bandstop filter. The unprimed coefficients are those of the bandpass filter. If this technique is combined

with the lowpass to bandpass technique discussed in section B, then II-59 becomes

$$\begin{aligned} a'_{2n} &= (-1)^n b_n \\ b'_{2n} &= (-1)^n b_n + K(-1)^n a_n \\ a'_q &= b'_q = 0; \quad q \text{ odd} \end{aligned} \quad \text{II-60}$$

The unprimed coefficients are now those of the lowpass filter.

As an example of this technique, consider a normalized fourth order low-pass Chebycheff filter with a 1/2 db ripple. The coefficients for this analog filter are tabulated in many analog filter design handbooks and are given as

TABLE VI  
Analog Fourth Order Chebycheff LP Filter  
(1/2 db ripple)

$A_0 = 1$	$B_0 = .379$
$A_1 = 0$	$B_1 = 1.025$
$A_2 = 0$	$B_2 = 1.717$
$A_3 = 0$	$B_3 = 1.197$
$A_4 = 0$	$B_4 = 1$

The coefficients for the lowpass digital filter with a  $20^\circ$  cutoff frequency (18:1 ratio of sampling rate to cutoff frequency) become (using the expansion procedure associated with Table I)

TABLE VII

Digital Lowpass Chebycheff Filter  
(20° cutoff)

$a_0 = 9.667 \times 10^{-4}$	$b_0 = 1.271$
$a_1 = 3.867 \times 10^{-3}$	$b_1 = -4.410$
$a_2 = 5.800 \times 10^{-3}$	$b_2 = 5.896$
$a_3 = 3.867 \times 10^{-3}$	$b_3 = -3.588$
$a_4 = 0.667 \times 10^{-4}$	$b_4 = .837$

Utilizing II-60, the bandstop filter coefficients are generated with K chosen as  $K = 10^4$  (an 80 db attenuation). These digital filter coefficients are then given as

TABLE VIII

Bandstop Chebycheff Filter  
(carrier frequency = 90°)  
Bandwidth = 20°

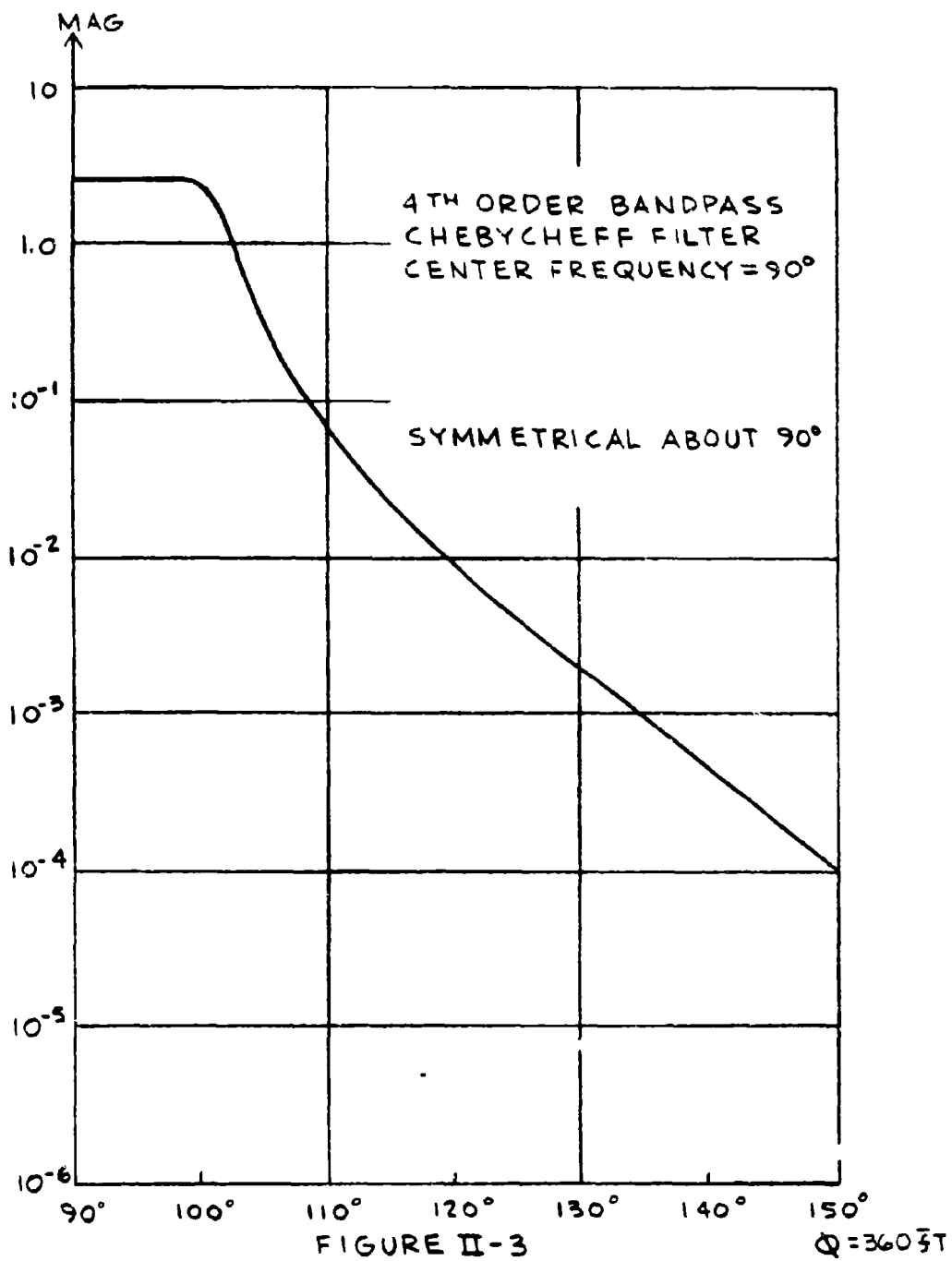
$a'_0 = 1.271$	$b'_0 = 10.938$
$a'_2 = 4.410$	$b'_2 = 34.260$
$a'_4 = 5.896$	$b'_4 = 63.899$
$a'_6 = 2.588$	$b'_6 = 35.082$
$a'_8 = .837$	$b'_8 = 10.504$

An interesting feature of this technique is that the resulting "a" and "b" coefficients (Table VIII) are approximately the same order of magnitude, although the lowpass filter's numerator coefficients (Table VII) are approximately  $10^{-4}$  of the denominator coefficients. In fact, it can be shown that as the lowpass filter's bandwidth is made smaller, the "a" coefficients also get smaller. Thus, one

can design a notch or band rejection filter with increasing notch depth as the notch width gets narrower and still maintain a small dynamic range for the filter coefficients. The bandpass and bandstop filter coefficients of Tables VII and VIII are plotted in Figures II-3 and II-4.

The technique utilized here is analogous to placing the bandpass filter in the feedback portion of a loop which has a forward loop gain of  $K$ . If a bandstop filter were placed in the feedback loop, the resulting filter would be a bandpass filter.

Various transformation techniques have been discussed for use in the generalized design of lowpass, bandpass and bandstop filters. The concept of normalization, common to all of the above, was noted to be of extreme importance in the design of digital filters. Techniques satisfying particular constraints as well as various error considerations will be discussed in the following sections.





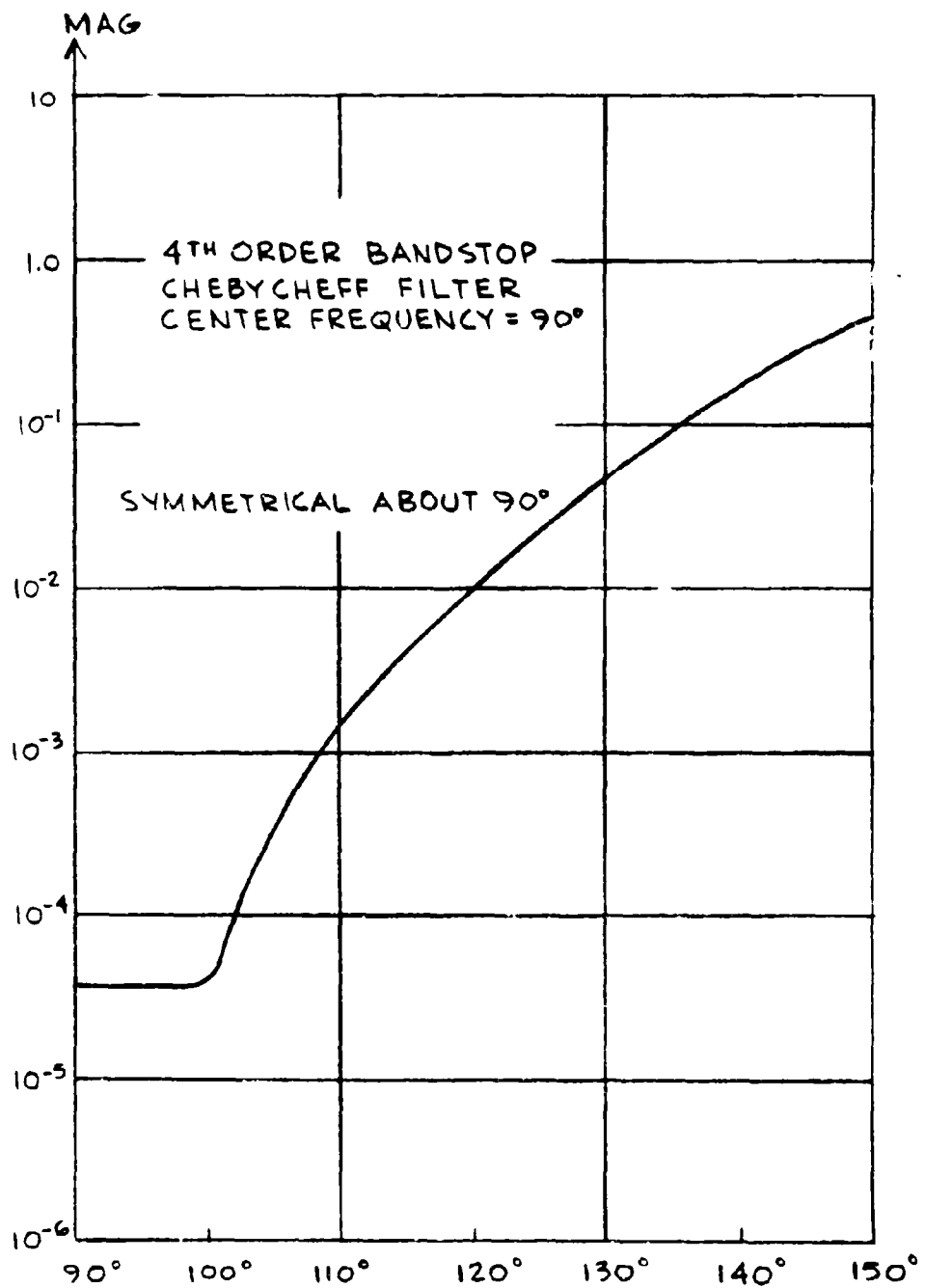


FIGURE II-4

$Q=360\sqrt{1}$

### III. ARITHMETICALLY SYMMETRICAL BANDPASS FILTERS

A design technique was investigated which yielded bandpass digital filters with equal ripple amplitude characteristics in the passband and stopband, having arithmetically symmetrical cutoff characteristics. Filters having arithmetic symmetry have application in many AM and FM problems. Conventional analog filters which have been transformed to bandpass have geometric symmetry properties. The approach taken was to design an equiripple or elliptic analog filter at lowpass and then convert this filter to a lowpass digital filter through the use of the bilinear transformation. Finally, these filters were converted to a bandpass digital filter while preserving the desired properties. Errors and constraining relations among the parameters are discussed. The foregoing procedures will now be detailed.

#### A. DESIGN PROCEDURE FOR ELLIPTIC ANALOG FILTERS

It was desired to formalize a design procedure to be used for elliptic analog filters. As discussed by Calahan,<sup>(5)</sup> this procedure can be formalized as follows:

Consider the lowpass characteristic as shown below

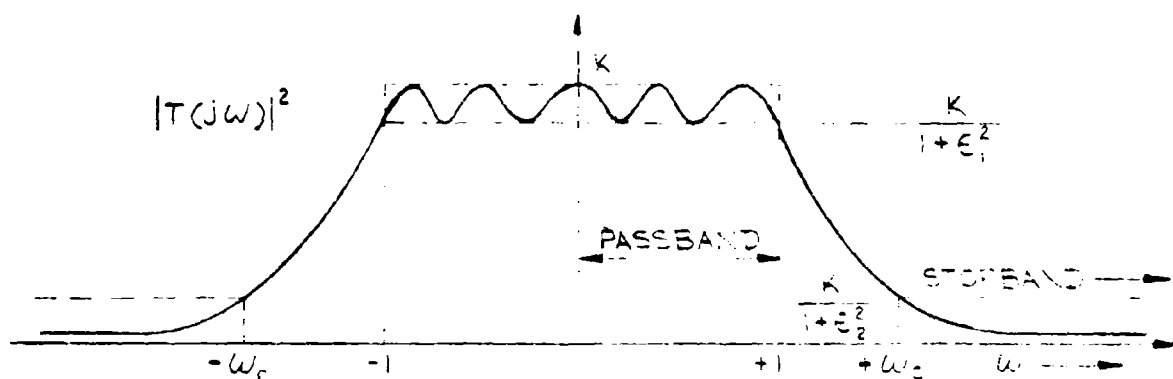


Figure III-1

The equiripple characteristic is such that

$$a. \text{ at } \omega = 0 \quad |T(\omega)|^2 = K$$

$$b. \text{ at } \omega = 1 \quad |T(\omega)|^2 = \frac{K}{1 + \epsilon_1^2}$$

$$c. \text{ at } \omega = \omega_c \quad |T(\omega)|^2 = \frac{K}{1 + \epsilon_2^2}$$

( $\omega \geq \omega_c$  defines the stopband;  $\omega \leq 1$  defines the passband.)

With the above definitions, the following procedure is used

1. Calculate  $m = 1/\omega_c^2$      $m' = (\epsilon_1/\epsilon_2)^2$
2. Determine the order of the filter,  $N$ , by choosing  $N$  as the smallest integer satisfying

$$N \geq \frac{K(m'_1) K(m)}{K(m_1) K(m')}$$

where  $m_1 = 1 - m$ ,  $m'_1 = 1 - m'$  and

$$K(m) = \int_0^{\pi/2} \frac{dx}{(1 - m \sin^2 x)^{1/2}}$$

which is the real quarter period of the elliptic integral of the first kind.

$N$  can be approximated for values of  $m$  near 1 and  $m'$  near zero by

$$N \geq (2/\pi^2) \ln(4\epsilon_2/\epsilon_1) \ln 8/(\omega_c - 1)$$

3. Determine the zeros and poles of the transfer function from the formulas

$$\begin{aligned} Z_r &= \frac{\pm j}{m^{1/2} \operatorname{sn}(\frac{r}{N} K(m); m)} \\ &= j \operatorname{sn}(\pm \frac{r}{N} K(m) + j r_o; m) \end{aligned}$$

where  $r = 2, 4, \dots, N-1$      $N$  odd

$r = 1, 3, \dots, N-1$      $N$  even

$$r_o = \frac{K(m) \operatorname{sc}^{-1} \left( \frac{1}{\epsilon_1} j m' \right)}{N K(m')} \approx \frac{K(m)}{K(m')} \sinh^{-1} \left( \frac{1}{\epsilon_1} \right)$$

for  $m'$  near zero.

The term  $\operatorname{sn}(\cdot)$  is the elliptic sine and the term  $\operatorname{sc}^{-1}(\phi; m)$  is the elliptic arc tangent.

As an example of this procedure, consider the following filter specifications

Passband - 2 db ripple     $0 \leq \omega \leq 1$

Stopband - 25 db min.     $1.33 \leq \omega \leq \infty$

For this example, the above parameters become

$$m = .566 \quad K(m) = 1.909$$

$$\epsilon_1 = .765 \quad v_o = .438$$

$$\epsilon_2 = 161 \quad N = 2.98 \text{ (choose } N=3)$$

$$z_1 = \pm j 1.47 \quad p_1 = -.463 \quad p_2 = -.129 \pm j .962$$

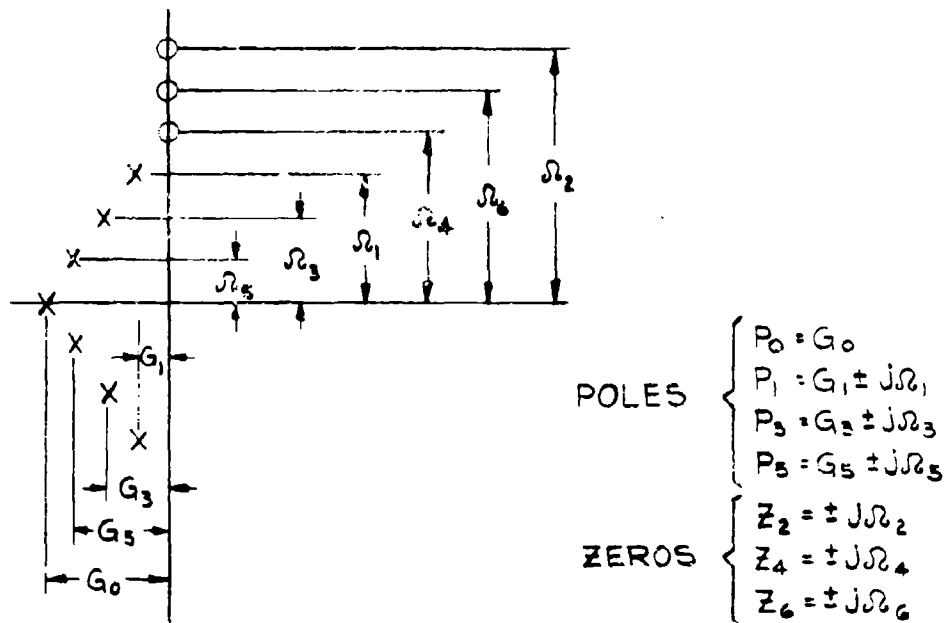
With the above pole zero configuration, the resulting transfer function becomes

$$G(S) = \frac{S^2 + 2.16}{S^3 + .721 S^2 + 1.061 S + .437} \quad \text{III-1}$$

Using the above approach, several lowpass elliptic filters will be synthesized and then digitized using the bilinear transformation.

## B. DIGITIZED LOWPASS ELLIPTIC FILTERS

The general pole-zero configuration for a lowpass elliptic filter is shown below.



The pattern shown is for a seven pole, or seventh order elliptic filter. The pole positions for these filters lie on an elliptical contour. The values for these poles and zeros were determined so that they would satisfy the following specifications:

$$\text{Passband Spec.} \quad < .5 \text{ db ripple} \quad 0 \leq \omega \leq 1$$

$$\text{Stopband Spec.} \quad 60 \text{ db min.} \quad 1.25 \leq \omega \leq \infty$$

A seventh order filter with the following characteristic was found to satisfy these requirements.

TABLE I

$p_0 = .3889$	$z_2 = \pm j 2.391$
$p_1 = .0377 \pm j 1.0120$	$z_4 = \pm j 1.2711$
$p_3 = .1399 \pm j .8939$	$z_6 = \pm j 1.4709$
$p_5 = .2932 \pm j .5731$	

Applying the bilinear transformation to this filter with a sampling rate equal to 4 times the cutoff frequency -- or a normalized cutoff at  $\bar{\omega}_u T = 90^\circ$  ( $K_{\bar{\omega}_u} = \tan(45^\circ) = 1$ ) yields

$$H(Z) = \frac{\sum_{n=0}^7 a_n Z^{-n}}{\sum_{n=0}^7 b_n Z^{-n}}$$

III-2

where

TABLE II

$a_0 = .556$	$b_0 = 12.252$
$a_1 = 2.007$	$b_1 = -14.381$
$a_2 = 4.254$	$b_2 = 30.397$
$a_3 = 5.976$	$b_3 = -26.018$
$a_4 = 5.976$	$b_4 = 24.095$
$a_5 = 4.254$	$b_5 = -13.421$
$a_6 = 2.007$	$b_6 = 5.917$
$a_7 = .556$	$b_7 = -1.519$

A plot of this filter is shown in Figure III-2.

A second design was carried out for a filter with greater attenuation in the stopband but a larger transition region. The specifications on this filter were

$$\text{Passband Spec.} \quad < .5 \text{ db ripple} \quad 0 \leq \omega \leq 1$$

$$\text{Stopband Spec.} \quad 90 \text{ db min.} \quad 2 \leq \omega \leq 1$$

A seventh order filter with the following pole zero pattern was found to satisfy these requirements.

TABLE III

$$\begin{array}{ll} p_0 = .323 & z_2 = \pm j 4.354 \\ p_1 = .057 \pm j 1.016 & z_4 = \pm j 2.044 \\ p_3 = .17 \pm j .841 & z_6 = \pm j 2.490 \\ p_5 = .278 \pm j .486 & \end{array}$$

Applying the bilinear transformation to this filter with a normalized cutoff at  $\bar{\omega}_u T = 90^\circ$  yields

$$H(Z) = \frac{\sum_{n=0}^7 a_n Z^{-n}}{\sum_{n=0}^7 b_n Z^{-n}} \quad \text{III-3}$$

where the coefficients  $a_n$  and  $b_n$  are as given in Table IV.

TABLE IV

$a_0 = .744$	$b_0 = 11.077$
$a_1 = 4.075$	$b_1 = -16.234$
$a_2 = 10.465$	$b_2 = 28.883$
$a_3 = 16.172$	$b_3 = -27.885$
$a_4 = 16.172$	$b_4 = 23.559$
$a_5 = 10.465$	$b_5 = -13.562$
$a_6 = 4.075$	$b_6 = 5.630$
$a_7 = .744$	$b_7 = -1.371$

A plot of this filter is shown in Figure III-3.

A third elliptic filter synthesized was that discussed in Section A with the normalized cutoff frequency at  $\bar{\omega}_u T = 20^\circ$ . The characteristic for this filter is

$$H(Z) = \frac{\sum_{n=0}^3 a_n Z^{-n}}{\sum_{n=0}^3 b_n Z^{-n}} \quad \text{III-4}$$

where

TABLE V

$a_0 = .188$	$b_0 = 1.162$
$a_1 = -.141$	$b_1 = -3.087$
$a_2 = -.141$	$b_2 = 2.847$
$a_3 = .188$	$b_3 = -.903$



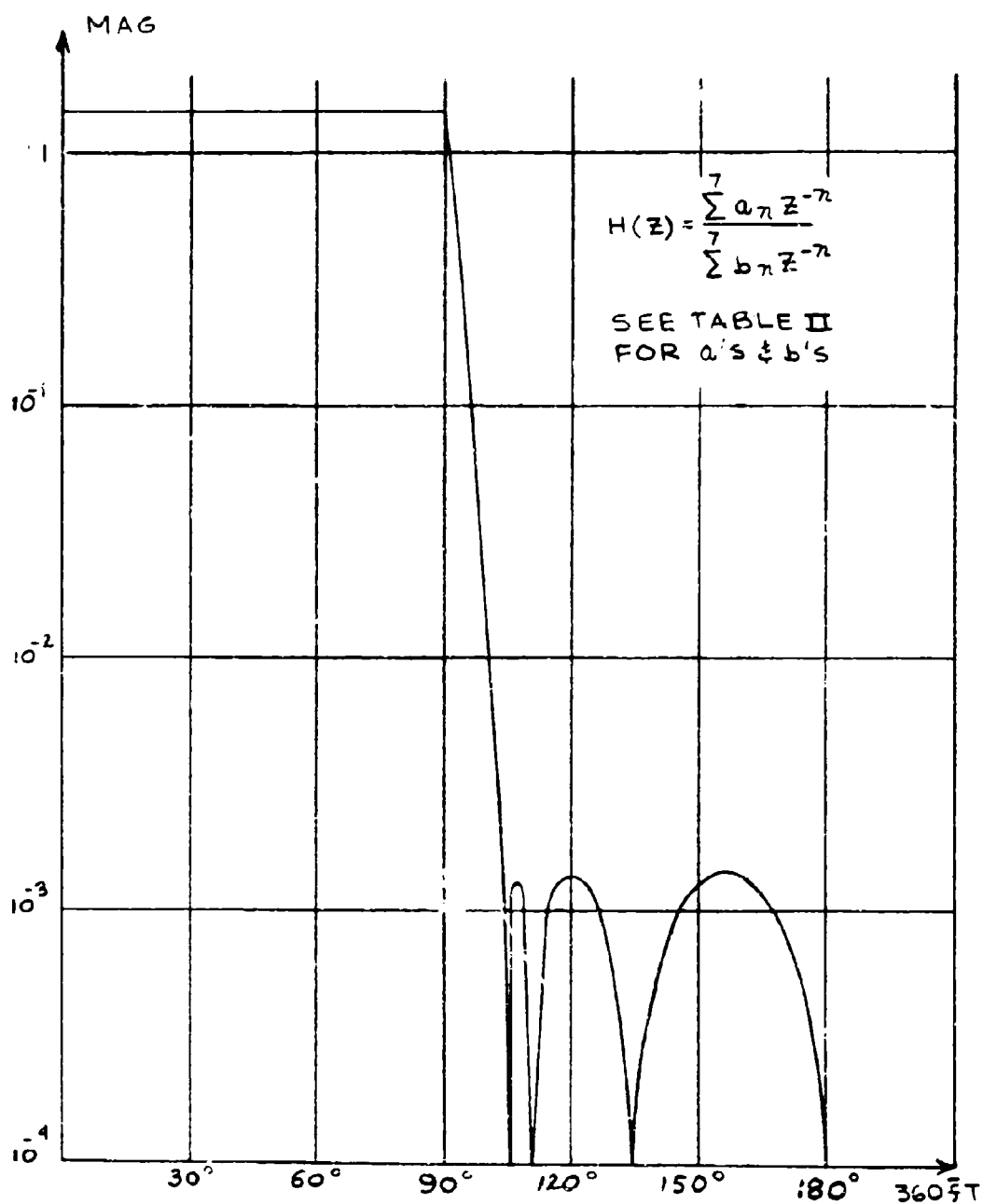
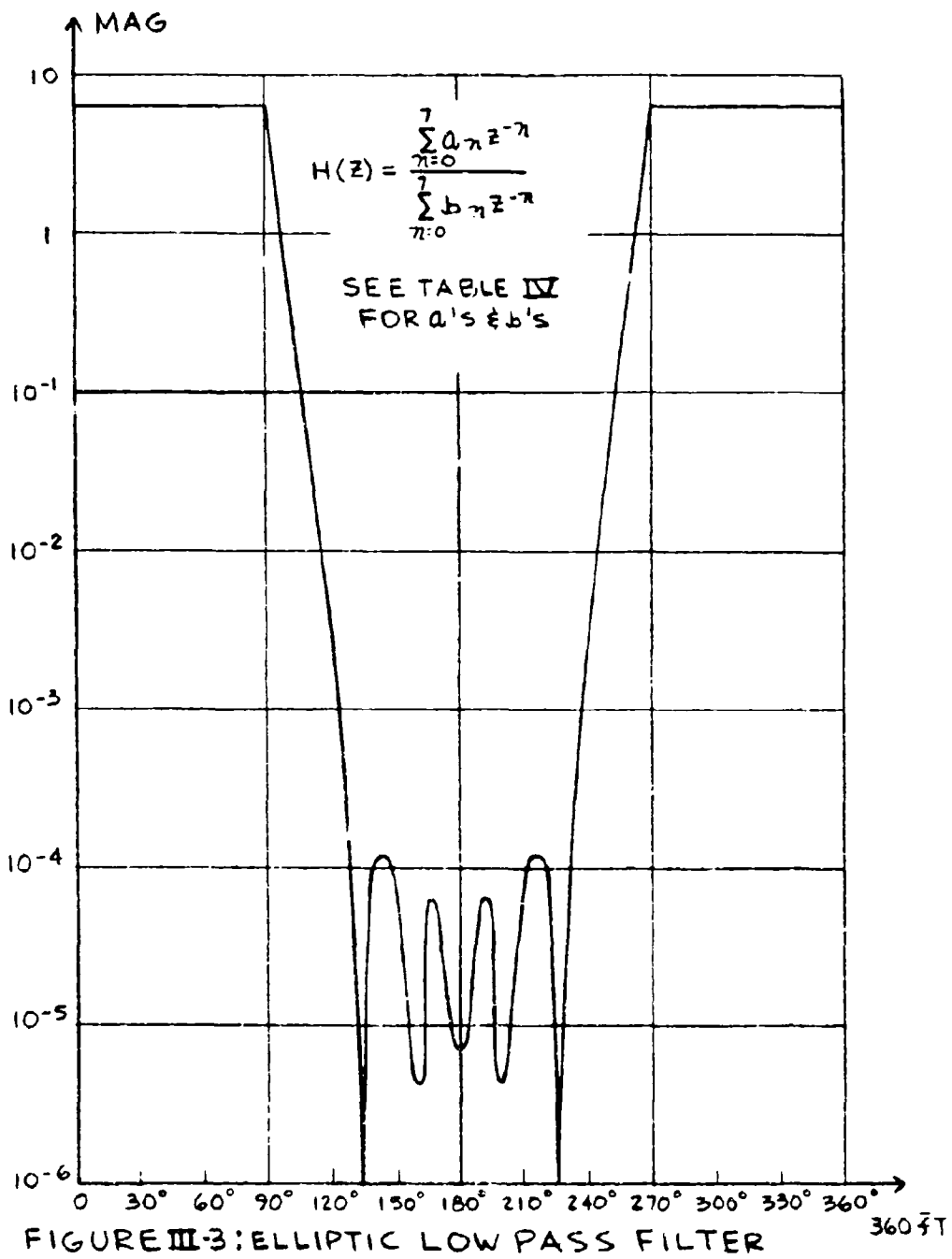


FIGURE III-2: ELLIPTIC LOW PASS FILTER



$$H(z) = \frac{.188 - .141z^{-1} - .141z^{-2} + .188z^{-3}}{1.162 - 3.087z^{-1} + 2.847z^{-2} - .903z^{-3}}$$

CUTOFF @ 360 Hz = 20°

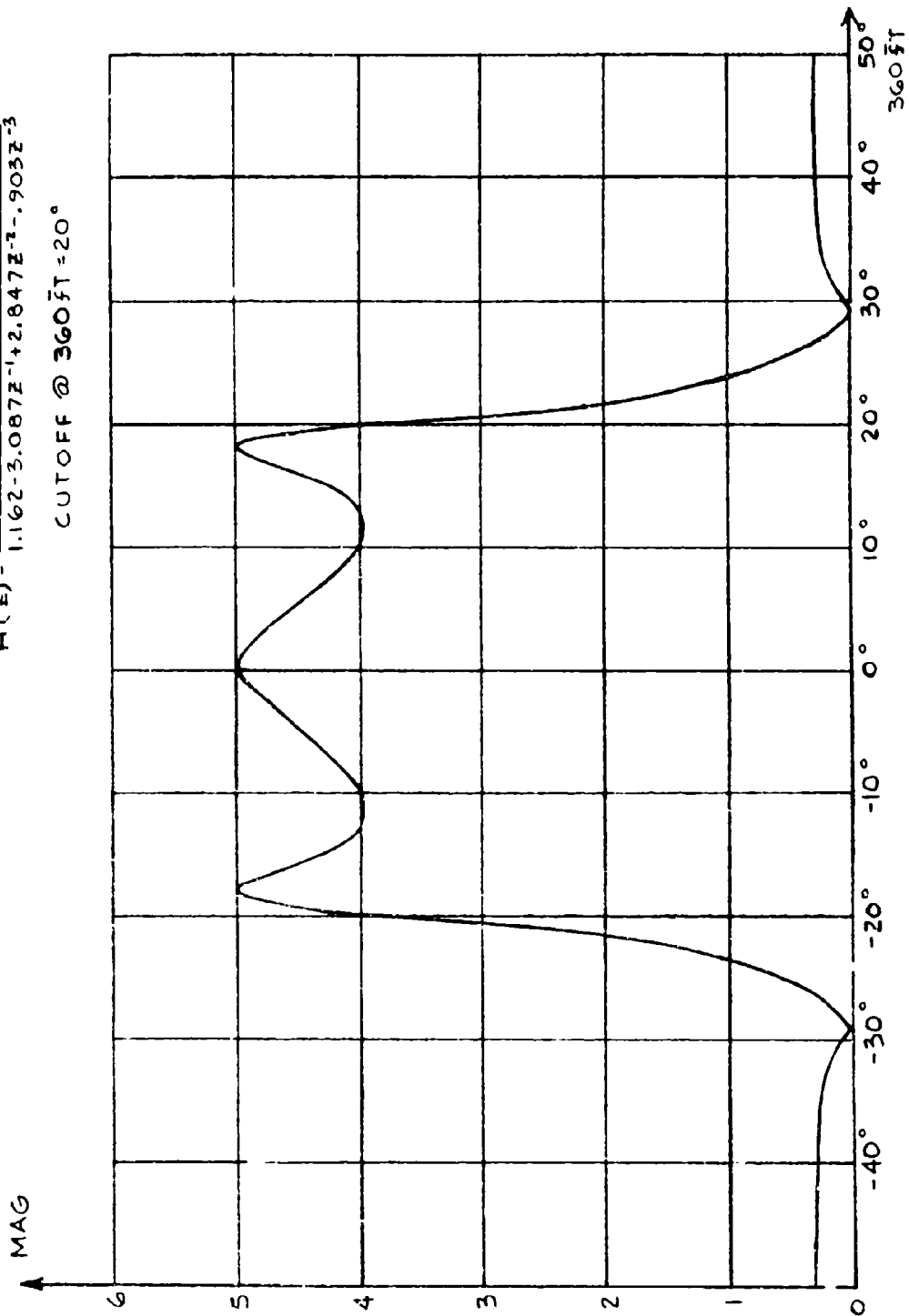


FIGURE III-4: LOW PASS ELLIPTIC FILTER

A plot of this filter is shown in Figure III-4.

A technique which converts these lowpass digital filters to bandpass filters will now be discussed.

### C. APPLICATION OF THE SHIFTING TECHNIQUE

It was initially decided to utilize the filter of Figure III-4 for the synthesis of an arithmetically symmetrical bandpass filter. The technique used is the shifting technique described in Section II and qualitatively consists of shifting the lowpass characteristic to the left and to the right by an amount (in degrees) equal to the normalized center frequency. As discussed, this is simply the digital counterpart of multiplying a time waveform by  $\cos \omega_0 t$  and observing the resulting spectral plot.

The required equations for this transformation are given in Section II as

$$A_n = \sum_{r=0}^M a_{n-r} b_r \cos \omega_0 T (n - 2r)$$

$$B_n = \sum_{r=0}^M b_{n-r} b_r \cos \omega_0 T (n - 2r)$$

III-5

where the "small" a's and b's are the numerator and denominator coefficients of the lowpass filter and the "capital" A's and B's are the corresponding bandpass coefficients. From this equation it can be seen that the bandpass coefficients are obtained by a weighted convolution (or correlation) of lowpass coefficients, where the weighting function depends on the desired carrier frequency.

Utilizing these equations with a normalized center frequency of  $\bar{\omega}_0 T = 90^\circ$  yields

$$H(Z) = \frac{\sum_{n=0}^3 A_{2n} Z^{-2n}}{\sum_{n=0}^3 B_{2n} Z^{-2n}} \quad \text{III-6}$$

where

TABLE VI

$A_0 = .219$	$B_0 = 1.351$
$A_2 = .063$	$B_2 = 2.910$
$A_4 = .053$	$B_4 = 2.528$
$A_6 = -.170$	$B_6 = .816$

A plot of this filter is shown in Figure III-5.

A detailed computer analysis of the magnitude characteristic of this filter shows that this filter is arithmetically symmetrical about  $90^\circ$  with no symmetry error. A detailed comparison of the lowpass elliptic filter in Figure III-4 and the bandpass filter in Figure III-5 shows that the passband error between these two filters is less than  $1/2\%$ . These errors are due to the tails of the shifted characteristic extending back into the passband of the filter.\*

Based on the above results, it was conjectured that the symmetry error can be reduced to zero. The following derivation will show this to be so for particular values of the normalized (with respect to the sampling rate) carrier frequency.

---

\* In comparing Figures III-4 and III-5, the factor of 2 from Eq. II-47 must be included.

$$H(z) = \frac{.219 + .063z^{-2} + .053z^{-4} + .170z^{-6}}{1.351 + 2.910z^{-2} + 2.528z^{-4} + .816z^{-6}}$$

CENTER FREQUENCY =  $\omega_0 T = 90^\circ$   
 BAND PASS  $70^\circ \leq 360^\circ T \leq 110^\circ$

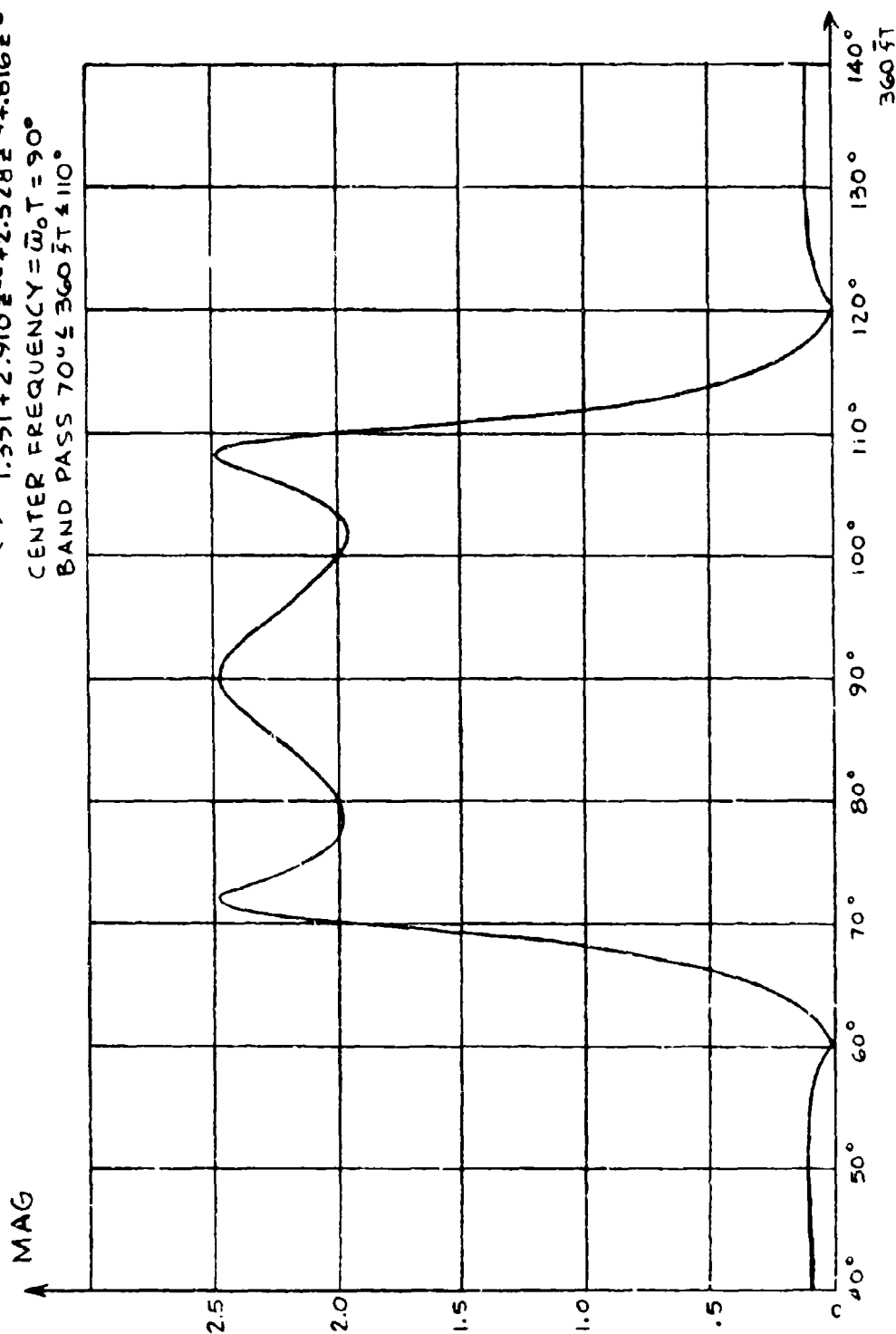


FIGURE III-5: BAND PASS ELLIPTIC FILTER

#### D. SYMMETRY ERROR AND CHOICE OF CENTER FREQUENCY

Consider the lowpass filter to be expressed as a function of angle, that is  $F_{LP}(\theta)$ , where  $\theta = \bar{\omega}T$  and  $\bar{\omega}$  is the digital frequency and  $1/T = f_s$ , the sampling rate. Now due to the periodicity of digital filters one has

$$F_{LP}(\theta) = F_{LP}(\theta + 2\pi) \quad \text{III-7}$$

Because of symmetry requirements

$$|F_{LP}(\theta)| = |F_{LP}(-\theta)| \quad \text{III-8}$$

Therefore

$$|F_{LP}(-\pi + \theta)| = |F_{LP}(\pi - \theta)| \quad \text{III-9}$$

Now

$$F_{LP}(-\pi + \theta) = F_{LP}(-\pi + \theta + 2\pi) = F_{LP}(\pi + \theta) \quad \text{III-10}$$

or

$$|F_{LP}(\pi + \theta)| = |F_{LP}(\pi - \theta)| \quad \text{III-11}$$

From the discussion in Section II, it can be shown that the bandpass filter resulting from utilizing this shifting technique yields a bandpass filter  $F_{BP}(\theta)$  given as (neglecting a scale factor of 2):

$$F_{BP}(\theta) = F_{LP}(\theta + \theta_o) + F_{LP}(\theta - \theta_o) \quad \text{III-12}$$

where  $\theta_o = \bar{\omega}_o T$  and  $\bar{\omega}_o$  is the desired center frequency.

Now consider the response of the bandpass filter at a distance  $\phi$  (in angle) away from  $\theta_o$ . Thus,

$$F_{BP}(\theta_o + \phi) = F_{LP}(2\theta_o + \phi) + F_{LP}(\phi) \quad \text{III-13}$$

$$F_{BP}(\theta_o - \phi) = F_{LP}(2\theta_o - \phi) + F_{LP}(-\phi)$$

In order for symmetry to exist at bandpass, Eqs. III-13 would have to be such

that

$$|F_{BP}(\theta_o + \phi)| = |F_{BP}(\theta_o - \phi)| \quad \text{III-14}$$

Moreover, in order for there to be no shifting error from lowpass to bandpass, one requires that

$$\begin{aligned} F_{BP}(\theta_o + \phi) &= F_{LP}(\phi) \\ F_{BP}(\theta_o - \phi) &= F_{LP}(-\phi) \end{aligned} \quad \text{III-15}$$

(or, the above modified by a scale factor).

As can be seen by comparing Eqs. III-15 and III-13, this latter error is

$$\text{LP-BP SYM. ERROR} = F_{LP}(2\theta_o + \phi) \quad \text{III-16}$$

or

$$F_{LP}(2\theta_o - \phi)$$

Consider the case where  $\theta_o = \pi/2$ . This choice of center frequency is equivalent to a sampling rate of four times the center frequency. That is

$$\theta_o = \omega_o T = \frac{2\pi f_o}{f_s} = \frac{\pi}{2} ; \frac{f_o}{f_s} = \frac{1}{4} \quad \text{III-17}$$

For the above choice of  $\theta_o$ , Eqs. III-13 become

$$\begin{aligned} F_{BP}(\theta_o + \phi) &= F_{LP}(\pi + \phi) + F_{LP}(\phi) \\ F_{BP}(\theta_o - \phi) &= F_{LP}(\pi - \phi) + F_{LP}(-\phi) \end{aligned} \quad \text{III-18}$$

From Eqs. III-9 and III-11, Eq. III-18 becomes

$$F_{BP}(\theta_o + \phi) = M_1 < \Delta_1 + M_2 < \Delta_2 = K < a \quad \text{III-19}$$

$$F_{BP}(\theta_o - \phi) = M_1 < -\Delta_1 + M_2 < -\Delta_2 = F_{BP}^*(\theta_o + \phi)$$

Thus for a 4 to 1 ratio of sampling rate to carrier frequency there is no symmetry error at bandpass. The error between the lowpass filter and the



bandpass filter is given by

$$F_{LP}(\pi + \phi) = M_1 < \Delta_1 \quad \text{III-20}$$

or

$$F_{LP}(\pi - \phi) = M_1 < -\Delta_1$$

However, since the filter passband extends for  $\pm 20^\circ$  (see Figures III-4 and III-5),  $M_1$  is extremely small within the filter passband. It can be shown that for the example under discussion, the maximum passband value of  $M_1 = .03$  yielding an error of approximately 1/2%.

Consider now the interesting choice of  $\theta_0 = \pi$ . This corresponds to a two-to-one ratio of sampling frequency to carrier frequency. With the above choice, Eqs. III-13 become

$$F_{BP}(\theta_0 + \phi) = F_{LP}(2\pi + \phi) + F_{LP}(\phi) = 2F_{LP}(\phi) \quad \text{III-21}$$

$$F_{BP}(\theta_0 - \phi) = F_{LP}(2\pi - \phi) + F_{LP}(-\phi) = 2F_{LP}(-\phi)$$

since

$$F_{LP}(2\pi + \phi) = F_{LP}(\phi); F_{LP}(2\pi - \phi) = F_{LP}(-\phi) \quad \text{III-22}$$

Thus for this choice of  $\theta_0$  there is no symmetry error at bandpass and no shifting error from lowpass to bandpass.

The above choice of  $\theta_0$  was applied to the lowpass elliptic filter described in Eq. III-4 and Table V. Utilizing the technique discussed, the bandpass filter is given as

$$H_{BP}(Z) = \frac{\sum_{n=0}^6 A_n Z^{-n}}{\sum_{n=0}^6 B_n Z^{-n}} \quad \text{III-23}$$

where the filter coefficients become

TABLE VII

$A_0 = .21875370$	$B_0 = 1.35144968$
$A_1 = .74456616$	$B_1 = 7.17729147$
$A_2 = .80670596$	$B_2 = 16.1488383$
$A_3 = -.08252552$	$B_3 = 19.6781117$
$A_4 = -.85454586$	$B_4 = 13.6836573$
$A_5 = .66294855$	$B_5 = 5.14441316$
$A_6 = -.17000589$	$B_6 = .8162383720$

A plot of this bandpass filter is shown in Figure III-6. A comparison of the computer print-outs for this filter and the equivalent lowpass filter bears out the foregoing analytical conclusions.

It is of interest to note the recursion equations which result from the above choices for  $\theta_0$ . In general these recursion equations are

$$A_n = \sum_{r=0}^M a_{n-r} b_r \cos[\theta_0(n-2r)]$$

III-24

$$B_n = \sum_{r=0}^M b_r a_{n-r} \cos[\theta_0(n-2r)]$$

where  $\theta_0 = \bar{\omega}_0 T$ .

For  $\theta_0 = \pi$  (a two-to-one ratio), these equations become

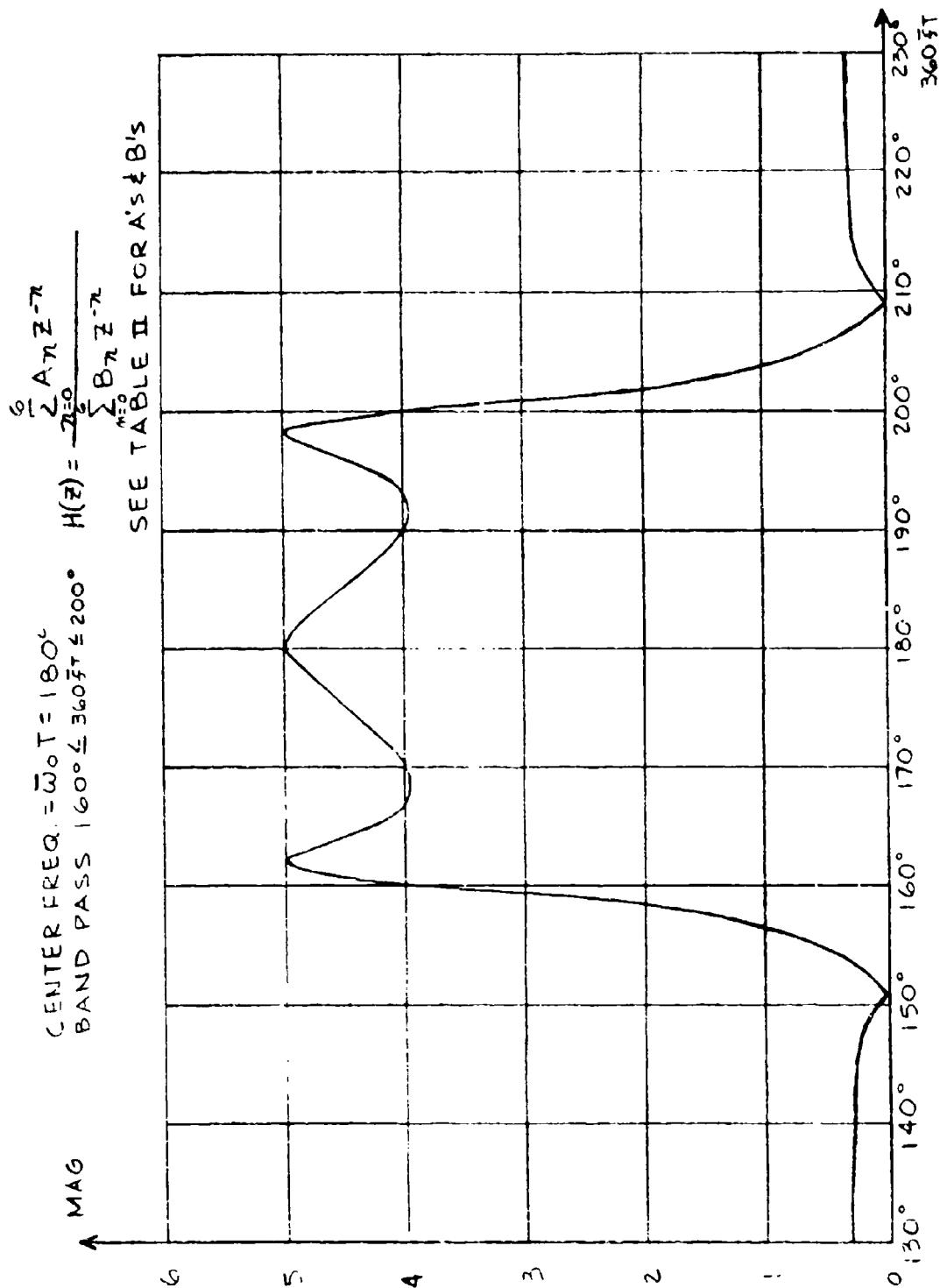


FIGURE III-6: BAND PASS ELLIPTIC FILTER

$$A_n = (-1)^n \sum_{r=0}^M a_{n-r} b_r$$

III-25

$$B_n = (-1)^n \sum_{r=0}^M b_r b_{n-r}$$

Thus, the bandpass filter coefficients ( $A_n$ ,  $B_n$ ) are the result of convolving the appropriate lowpass filter coefficients ( $a_n$ ,  $b_n$ ) with each other. Since a digital filter performs the operation of convolution, this suggests the following automated procedure to generate the bandpass coefficients once the lowpass filter has been implemented. If one assumes that the lowpass filter has been synthesized using the direct form\* and the "x bank" or feed forward section is impulsed, then the outputs are the "a" coefficients. If these outputs are fed into the "y bank" or feedback section, its outputs are the "A" or numerator coefficients of the bandpass filter. The "B" coefficients can be obtained in a similar manner using only the feedback bank. This procedure appears to be of advantage in that the lowpass coefficients can be altered and the lowpass filter itself used to generate the bandpass equivalent.

The equations analogous to III-5 for  $\theta_0 = \pi/2$  (a four-to-one ratio) are

$$A_n = \left(\cos n \frac{\pi}{2}\right) \sum_{r=0}^M (-1)^r a_{n-r} b_r$$

III-26

$$B_n = \left(\cos n \frac{\pi}{2}\right) \sum_{r=0}^M (-1)^r b_{n-r} b_r$$

---

\* This approach is not limited to any one implementation.

A similar implementation can be utilized for the above. It should also be noted that  $A_n$  and  $B_n$  are both zero for  $n$  odd. Thus, although the total delay required for both bandpass filters are the same, only half the multiply-add operations are required when a four-to-one ratio ( $f_s/f_o = 4$ ) is used.

#### E. APPLICATION OF THE LP-BP TRANSFORMATION

In Section II, the lowpass to bandpass transformation

$$S \rightarrow \frac{1 - 2(\cos \bar{\omega}_o T) Z^{-1} + Z^{-2}}{K_{\bar{B}} (1 - Z^{-2})} \quad \text{III-27}$$

was utilized in the design of bandpass digital filters. Mention was also made of the simplification resulting from adjusting the sampling rate to be four times the carrier frequency. This choice causes  $\bar{\omega}_o T = \pi/2$  and Eq. III-27 becomes

$$S \rightarrow \frac{1 + Z^{-2}}{K_{\bar{B}} (1 - Z^{-2})} \quad \text{III-28}$$

It is desired to investigate the application of the LP-BP transformation to the design of arithmetically symmetrical filters for the above choice of normalized digital center frequency. This transformation is recognized as being that of the lowpass bilinear transformation with  $Z^{-1}$  replaced by  $-Z^{-2}$ . Since  $-Z^{-2}$  can be written as

$$-Z^{-2} = e^{\pm j\pi} e^{j2\bar{\omega}T} = e^{2j(\bar{\omega}T \pm \frac{\pi}{2})} \quad \text{III-29}$$

This transformation can be viewed as a shift of  $90^\circ$  accompanied by a scale change by a factor of 2. Thus, with these parameters, a lowpass filter

$$H_{LP}(Z) = \frac{\sum_{n=0}^N a_n Z^{-n}}{\sum_{n=0}^N b_n Z^{-n}} \quad \text{III-30}$$

becomes

$$H_{BP}(Z) = \frac{\sum_{n=0}^N a_n (-1)^n Z^{-2n}}{\sum_{n=0}^N b_n (-1)^n Z^{-2n}} \quad \text{III-31}$$

Now, consider the bandpass filter evaluated at  $(\theta + \pi/2) = \pi/2$ . Equation III-31 becomes

$$H_{BP}(Z) = \frac{\sum_{n=0}^N a_n (-1)^n e^{-j\pi n} e^{-2jn\theta}}{\sum_{n=0}^N b_n (-1)^n e^{-j\pi n} e^{-j2n\theta}} \quad \text{III-32}$$

$$H_{BP}(Z) = \frac{\sum_{n=0}^N a_n e^{-2jn\theta}}{\sum_{n=0}^N b_n e^{-2jn\theta}} \quad \text{III-33}$$

This is recognized as being identical to the lowpass filter evaluated at  $2\theta$ . Similarly,  $H_{BP}(\pi/2 - \theta) = H_{LP}(-2\theta)$ . Thus, this technique yields an arithmetically symmetrical lowpass filter with no symmetry error either at bandpass or in the shift from lowpass to bandpass. Two examples of this technique are a 4th order Chebycheff lowpass filter and a 10th order Butterworth lowpass

filter that have been shifted to bandpass. The coefficients for these filters are

TABLE VIII

10th Order Butterworth

Lowpass Coefficients $\tan(\bar{\omega}_0 T/2) = 1$		Bandpass Coefficients $\bar{\omega}_0 T = \pi/2$	
<u>Numerator</u>	<u>Denominator</u>	<u>Numerator</u>	<u>Denominator</u>
$a_0 = 1$	$b_0 = 345.252$	$A_0 = 1$	$B_0 = 345.252$
$a_1 = 10$	$b_1 = -4 \times 10^{-3}$	$A_2 = -10$	$B_2 = 4 \times 10^{-3}$
$a_2 = 45$	$b_2 = 462.771$	$A_4 = 45$	$B_4 = 462.771$
$a_3 = 120$	$b_3 = 8 \times 10^{-3}$	$A_6 = -120$	$B_6 = -8 \times 10^{-3}$
$a_4 = 210$	$b_4 = 188.270$	$A_8 = 210$	$B_8 = 188.270$
$a_5 = 252$	$b_5 = -8 \times 10^{-5}$	$A_{10} = -252$	$B_{10} = 8 \times 10^{-5}$
$a_6 = 210$	$b_6 = 26.613$	$A_{12} = 210$	$B_{12} = 26.613$
$a_7 = 120$	$b_7 = -9 \times 10^{-3}$	$A_{14} = -120$	$B_{14} = 9 \times 10^{-3}$
$a_8 = 45$	$b_8 = 1.093$	$A_{16} = 45$	$B_{16} = 1.093$
$a_9 = 10$	$b_9 = -4 \times 10^{-3}$	$A_{18} = -10$	$B_{18} = 4 \times 10^{-3}$
$a_{10} = 1$	$b_{10} = .024$	$A_{20} = 1$	$B_{20} = .024$
		$(A_n = 0; n \text{ odd})$	$(B_n = 0; n \text{ odd})$

TABLE IX

## 4th Order Chebycheff

Lowpass Coefficients $\tan(\bar{\omega}T/2) = .17633$ ( $20^\circ$ cutoff)		Bandpass Coefficients $\bar{\omega}_0 T = \pi/2$	
Numerator	Denominator	Numerator	Denominator
$a_0 = 1$	$b_0 = 5.319$	$A_0 = 1$	$B_0 = 5.319$
$a_1 = 4$	$b_1 = -2.828$	$A_2 = -4$	$B_2 = 2.828$
$a_2 = 6$	$b_2 = 4.841$	$A_4 = 6$	$B_4 = 4.140$
$a_3 = 4$	$b_3 = -2.140$	$A_6 = -4$	$B_6 = 2.140$
$a_4 = 1$	$b_4 = .870$	$A_8 = 1$	$B_8 = .870$
		$(A_n = 0; n \text{ odd}) \quad (B_n = 0; n \text{ odd})$	

These filters are plotted in Figures III-7 and III-8.

It is of interest to note that the scale change caused by this transformation yields a bandwidth at bandpass that is one half that of the lowpass filter. Thus, for the 4th order Chebycheff filters the bandwidth is  $\pm 20^\circ$  at lowpass and  $\pm 10^\circ$  at bandpass. Of course, since these bandwidths are normalized to the sampling rate, the actual bandwidth can be controlled by this rate. It should also be noted that the filter coefficients generated are obtained directly from the lowpass design. By contrast, the shifting technique used in the foregoing yields a more complicated structure. For example, the third order elliptic filter of Table V had bandpass coefficients using the shifting technique as given below. The coefficients obtained through the substitution  $Z^{-1} = -Z^{-2}$  are shown in parenthesis in Table X.



10<sup>1</sup> ORDER BANDPASS BUTTERWORTH  
 FILTER - CENTER FREQUENCY = 90°

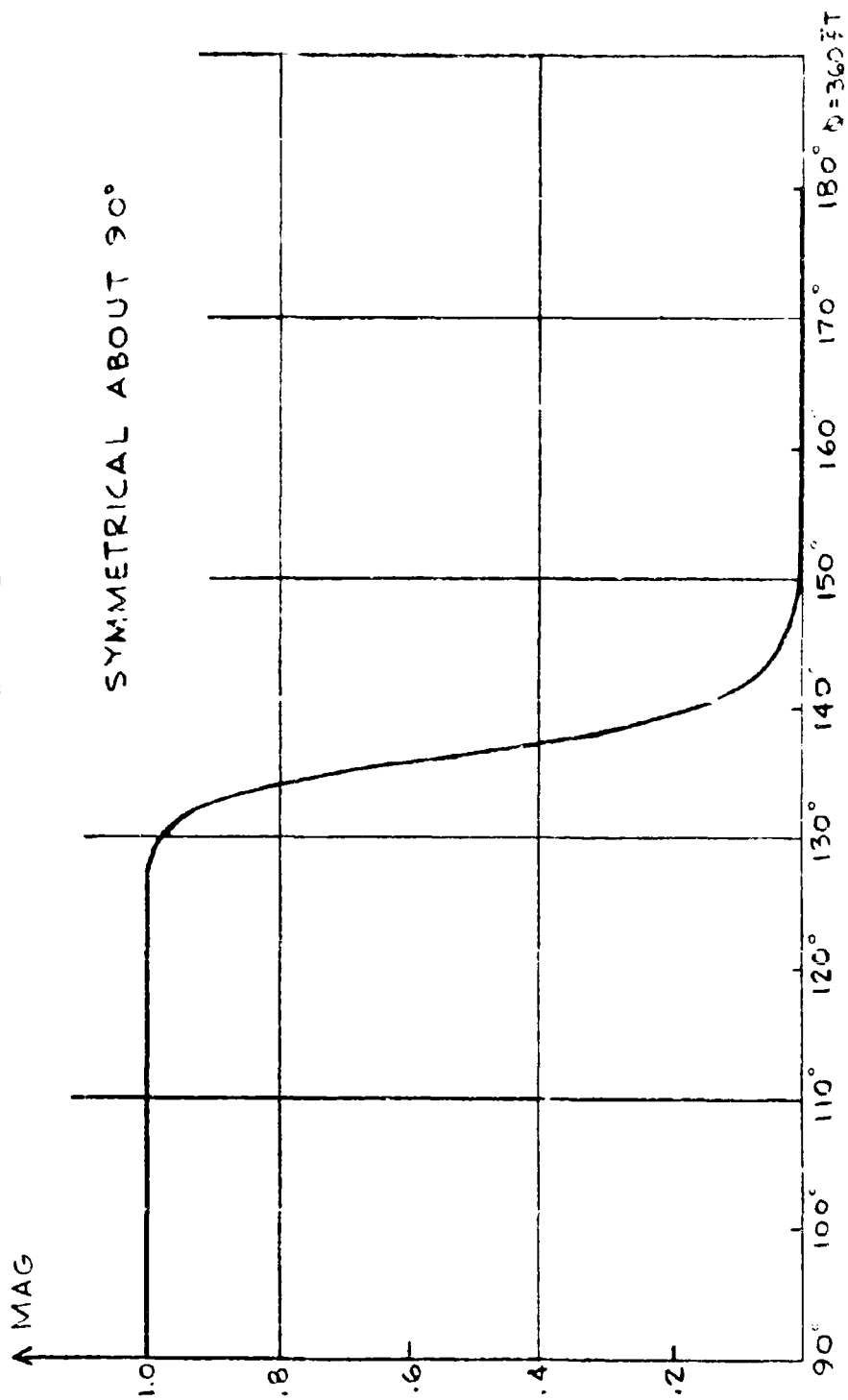


FIGURE III -7

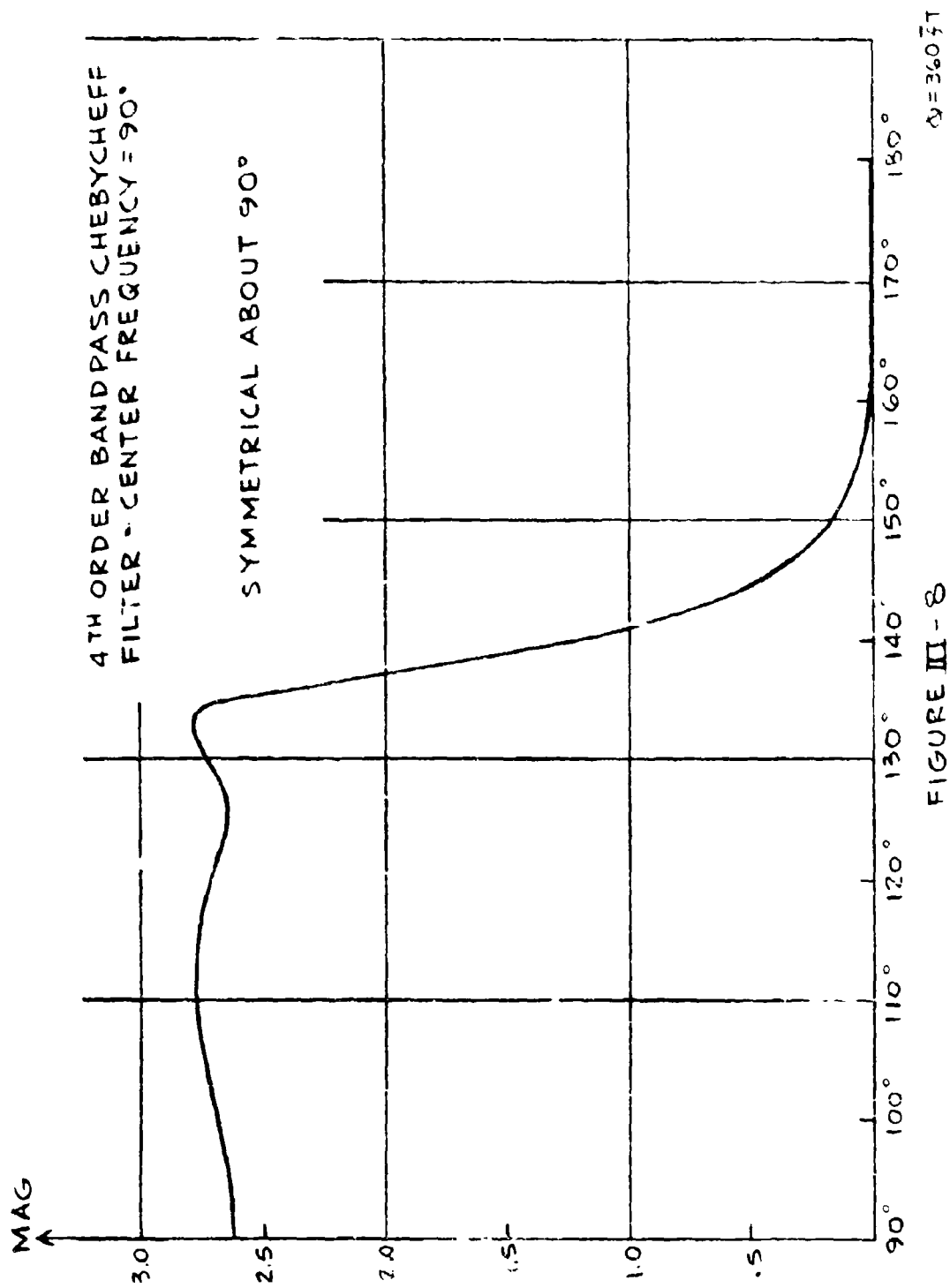


FIGURE III - 8

TABLE X

Elliptic Filter Coefficients

$A_0 = .219 (.188)$	$B_0 = 1.351 (1.162)$
$A_2 = .063 (.141)$	$B_2 = 2.910 (3.087)$
$A_4 = .053 (-.141)$	$B_4 = 2.528 (2.847)$
$A_6 = -.170 (.188)$	$B_6 = .816 (.903)$

Although the coefficients are similar, those of the shifting technique are generated through a convolution formula, whereas those of the present technique, by a simple sign change. Thus, if it is possible to use a 4:1 ratio, the LP-BP procedure is preferable. For other ratios, however, the LP-BP procedure does not yield satisfactory results.

Two approaches to the synthesis of bandpass digital filters having arithmetic symmetry properties have been discussed. The shifting technique was found to be of general applicability and was shown to yield negligible errors under appropriate choices of the ratio of sampling rate to desired carrier frequency. The equations relating the coefficients of the bandpass digital filter to those of the lowpass digital filter were shown to be in a form convenient for "on line" synthesis. Lastly, the LP-BP transformation was shown to be an excellent (and simple) technique if the problem constraints allowed the use of a 4:1 ratio of sampling rate to carrier frequency.

#### IV. NONRECURSIVE DIGITAL FILTERS

The design of a nonrecursive (i.e., finite memory)\* digital filter consists of choosing coefficients  $h_n$  so that a frequency response characteristic of the form

$$H(Z) = \sum_{n=0}^N h_n Z^{-n}; \quad Z^{-1} = e^{-j\bar{\omega}T} \quad \text{IV-1}^{**}$$

has the desired shape. From this equation it is seen that with  $Z^{-1} = e^{-j\bar{\omega}T}$   $H(Z)$  is represented as a finite Fourier series with coefficients  $h_n$ . The overall

\* Since the input-output equation of a nonrecursive filter is given by

$$y_n = \sum_{k=0}^N h_k x_{n-k}$$

it can be seen that the output samples are a function of the present input as well as past inputs up to the upper limit of the summation. Thus,  $N$  is often referred to as the memory of the filter.

\*\* The link between nonrecursive digital filters and analog tapped delay line or so-called transversal filters can be seen by noting that the input-output equation corresponding to IV-1 is given by

$$y_n = \sum_{k=0}^N h_k x_{n-k}$$

whereas that of a transversal filter is given by

$$y(t) = \sum_{k=0}^N A_k x(t - kT)$$

Thus, if the output is sampled at times  $t = NT$  the  $h_k$  and  $A_k$  are equal to one another. The  $A_k$  are the tap weightings.

question is, how does one choose these coefficients in some optimum manner, or, from what time function do these coefficients come? If the nonrecursive filter is viewed as the finite memory counterpart of a recursive digital filter which has been synthesized through a transformation technique applied to an analog filter, the  $h_n$  coefficients can be related to the impulse response of the analog filter. If the standard Z transform were applied to the analog filter, then the  $h_n$  can be shown to be related to the first  $N + 1$  amplitude samples of the impulse response of the analog filter. If the bilinear transform were applied to the analog filter, the  $h_n$  coefficients would be related to the first  $N + 1$  coefficients in the Laguerre expansion of its impulse response. Still another approach is to expand the desired frequency response in an infinite Fourier series and then choose the first  $N + 1$  terms or some modification thereof to be  $h_n$  coefficients.

Inherent in most of the above procedures are two general sources of error between the desired frequency response and that finally obtained. The first error is that generated by the particular transform technique utilized. This error can normally be controlled and contained within tolerable limits. After obtaining a satisfactory design, this set of coefficients is truncated to achieve the finite memory indicated in IV-1. This truncation procedure is equivalent to multiplying the time function represented by the infinite set of coefficients by a pulse of extent  $NT$ . This procedure produces an error equivalent to convolving the infinite memory response with a  $\sin x/x$  (in frequency) form whose central lobe width varies inversely with  $N$ , the memory of the filter. While this is true, it appears desirable to have considerably more control over this type of error.

The nonrecursive design technique to be discussed in the following sections include design procedures from tabulated frequency data, a digital

impulse invariant technique and the process of zero removal and relocation as they apply to nonrecursive filters.

#### A. NONRECURSIVE DESIGN FROM TABULATED DATA

The majority of design procedures are predicated on the existence of a continuous function of frequency. Often, however, the amplitude and phase characteristics of the desired frequency response characteristic are available only at discrete points. Thus, a design procedure was investigated for this application. With the nonrecursive filter of IV-1 rewritten as

$$H(Z) = \sum_{n=0}^N h_n e^{-jn\bar{\omega}T} = \sum_{n=0}^N h_n e^{-j2\pi T/f_s} \quad \text{IV-2}$$

where  $f_s = 1/T$  = sampling rate, and the desired frequency response data (magnitude and phase) given as  $\hat{H}(f_k)$  where

$$f_k = f_1 + \frac{k f_s}{K} \quad k = 0, \dots, R-1 \quad \text{IV-3}$$

the  $h_n$  coefficients were determined so that the sum-squared error is minimized. With the above assumptions this sum squared error can be written as

$$S = \left\{ \sum_{k=0}^{R-1} \left[ \hat{H}(f_k) - \sum_{n=0}^N h_n e^{-j2\pi n f_k / f_s} \right]^2 \right\} \quad \text{IV-4}$$

Taking a partial with respect to the digital filter coefficient  $h_f$ , setting the result equal to zero and utilizing IV-3 yields

$$0 = \sum_{k=0}^{R-1} \hat{H}(f_k) e^{-j2\pi f \frac{f_k}{f_s}} - \sum_{n=0}^N h_n e^{-j2\pi (f+n) \frac{f_1}{f_s}} \times \sum_{k=0}^{R-1} e^{-j2\pi (f+n) \frac{k}{K}} \quad \text{IV-5}$$

With the use of the identity

$$\sum_{k=0}^{\infty} Z^{-k} = \frac{1}{1 - Z^{-1}} \quad \text{IV-6}$$

Equation IV-5 becomes

$$\sum_{k=0}^{R-1} \hat{H}(f_k) e^{-j 2 \pi f \frac{f_k}{f_s}} = \sum_{n=0}^N h_n e^{-j 2 \pi (\ell + n) \frac{f_1}{f_s}} \times \left[ \frac{1 - e^{-j 2 \pi (\ell + n) \frac{R}{K}}}{1 - e^{-j 2 \pi (\ell + n) \frac{1}{K}}} \right] \quad \text{IV-7}$$

If it is desired to synthesize the response over a half-period, then  $f_1 = 0$ ,

$R = K/2$  ( $K$  even) and IV-7 becomes

$$\sum_{k=0}^{\frac{K}{2}-1} \hat{H}(f_k) e^{-j 2 \pi f \frac{k}{K}} = 2 \sum_{n=0}^N h_n \frac{1}{1 - e^{-j \pi (\ell + n)/K}} \quad \text{IV-8}$$

for  $(\ell + n)$  odd and  $k \geq 2N$ , zero for  $(\ell + n)$  even.

Although the above equations can be used to determine the required  $h_n$ , it was noted that a considerable simplification comes about if the desired digital filter can be written in the form

$$H(Z) = \sum_{n=-N}^N h_n Z^{-n} \quad \text{IV-9}$$

For this case, a development paralleling that discussed above leads to

$$\sum_{k=0}^{K-1} \hat{H}(f_k) e^{-j 2 \pi f \frac{f_k}{f_s}} = \sum_{n=-N}^N h_n e^{-j 2 \pi (\ell + n) \frac{f_1}{f_s}} \times \left[ \frac{1 - e^{-j 2 \pi (\ell + n)}}{1 - e^{-j 2 \pi (\ell + n)/K}} \right] \quad \text{IV-10}$$

Assuming that  $(\ell + n)/K$  is not an integer, the term in the square brackets is equal to zero, except for  $n = -\ell$ . In that case, the form of IV-10 reduces to

$$h_{-l} = \frac{1}{K} \sum_{k=0}^{K-1} \hat{H}(f_k) e^{-j 2 \pi l \frac{f_k}{f_s}}; \quad K \geq 2N \quad \text{IV-11}$$

For synthesis over a full period  $f_1 = -f_s/2$  and  $h_l$  becomes

$$h_l = \frac{1}{2K} \hat{H}\left(-\frac{f_s}{2}\right) e^{-j \pi l} + \frac{1}{K} \sum_{k=1}^{K-1} \hat{H}(f_k) e^{+j 2 \pi l \frac{f_k}{f_s}} + \frac{1}{2K} \hat{H}\left(\frac{f_s}{2}\right) e^{j \pi l} \quad \text{IV-12}$$

Equation IV-12 is recognized as being equivalent to a trapezoidal integration of

$$h_l = \frac{1}{f_s} \int_{-f_s/2}^{f_s/2} \hat{H}(f) e^{j 2 \pi l \frac{f}{f_s}} df \quad \text{IV-13}$$

where  $H(f)$  is defined on  $K$  points over  $f_s$ .

To obtain an expression in terms of magnitude and phase characteristics one notes that

$$\hat{H}(-f) = \hat{H}^*(f) = A(f) e^{-j \theta(f)} \quad \text{IV-14}$$

where  $A(f)$  is even and  $\theta(f)$  is odd, then  $h_l$  becomes

$$h_l = \frac{2}{f_s} \int_0^{f_s/2} A(f) \cos \left[ \theta(f) - 2 \pi f \frac{l}{f_s} \right] df \quad \text{IV-15}$$

or

$$h_l = \frac{1}{N} \left[ A(0) + \sum_{k=1}^{N-1} A(f_k) \cos \left[ \theta(f_k) - 2 \pi f_k \frac{l}{f_s} \right] + (-1)^N A\left(\frac{f_s}{2}\right) \cos \theta\left(\frac{f_s}{2}\right) \right] \quad \text{IV-16}$$

Thus, relationships have been derived (IV-12 and IV-16) which can be utilized to design nonrecursive digital filters from tabulated data.



## B. A DIGITAL IMPULSE INVARIANT TECHNIQUE

It is often of interest to synthesize a nonrecursive digital filter which approximates (in some sense) a recursive digital filter. Thus, it is assumed that the recursive digital design satisfies the filter requirements. However, it is desirable to eliminate the feedback terms ( $b_j$  coefficients) and obtain a nonrecursive form which requires the same amount of processing. Thus, the restriction might be such that the synthesis is to be carried out so that the total number of coefficients are the same for both recursive and nonrecursive designs.

Consider the transfer function of a recursive digital filter given as

$$H_R(Z) = \frac{\sum_{n=0}^N a_n Z^{-n}}{\sum_{n=0}^M b_n Z^{-n}} \quad \text{IV-17}$$

By dividing the denominator into the numerator IV-17 can be rewritten as

$$H_R(Z) = \sum_{n=0}^{\infty} C_n Z^{-n} \quad \text{IV-18}$$

where the  $C_n$  are related to the  $a_n$  and  $b_n$  by

$$\begin{aligned} C_0 &= \frac{a_0}{b_0} \\ C_1 &= \frac{(a_1 - b_1 C_0)}{b_0} \\ &\vdots \end{aligned} \quad \text{IV-19}$$

or, in general by

$$C_k = \frac{a_k}{b_0} - \sum_{j=1}^{\min[k, M]} \frac{b_j}{b_0} C_{k-j} \quad \text{IV-20}$$

where  $M+1$  is the number of denominator coefficients and the summation runs from  $j=1$  to the smaller of the two values  $k$  and  $M$ .

The nonrecursive digital filter is then of the form

$$H_{NR}(Z) = \sum_{n=0}^N h_n Z^{-n} \quad \text{IV-21}$$

The question is -- how should the  $h$ 's be chosen? Or, what is the relationship between the  $h$ 's and the  $C$ 's? If the  $h$ 's are to be chosen to yield a minimum mean square approximation to  $H_R(Z)$ , then the  $h_n$  should be equal to the  $C_n$  up to  $n=N$ . The justification for this is that IV-18 is in the form of an infinite Fourier series and IV-21 is in the form of a truncated Fourier series. Furthermore, if  $H_{NR}(Z)$  is to approximate a recursive filter synthesis through the use of the bilinear transformation, then the desired shape should first be synthesized with a bilinear transformation and then the  $C$ 's of Eq. IV-21 obtained through the use of Eq. IV-20. The conventional approach is to approximate the desired shape directly with a Fourier series and then truncate after a given number of terms (equal to  $N+1$  in the example).

A comparison of the various approaches is shown in Figure IV-1. The ideal filter to be approximated is a rectangular filter whose bandwidth (cut-off frequency) is equal to  $(1/4)$  of the sampling rate (i.e.,  $\bar{\omega}_c T = 90^\circ$ ). The bilinear approximation illustrated (curve 1) is a digitized 4th order

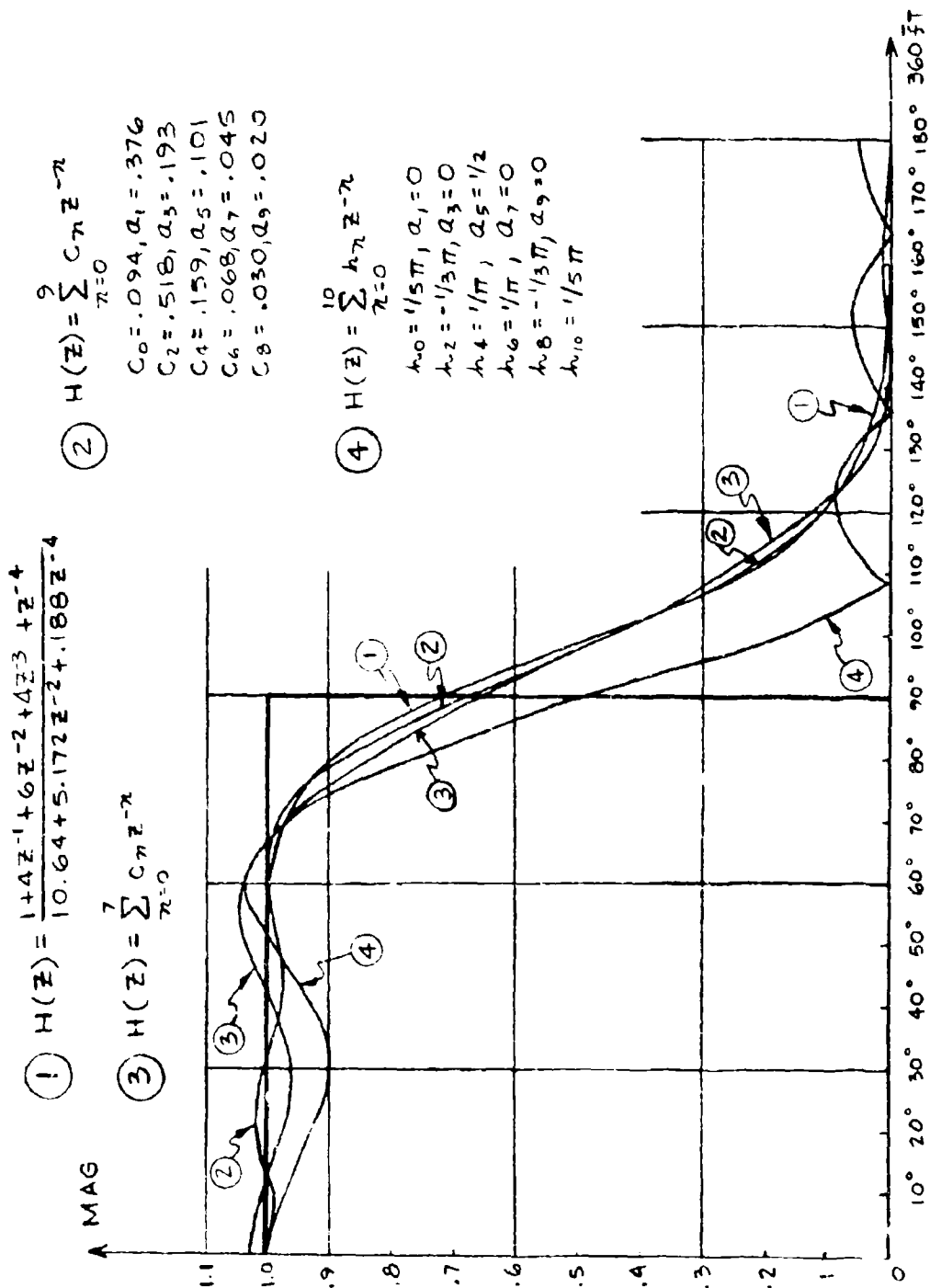


FIGURE IV-1: NON-RECURSIVE FILTERS

Butterworth filter with a resulting transfer function

$$H_R(Z) = \frac{1 + 4Z^{-1} + 6Z^{-2} + 4Z^{-3} + Z^{-4}}{10.64 + 5.17Z^{-2} + .188Z^{-4}} \quad \text{IV-22}$$

The above equation was obtained utilizing the transformation technique discussed in Section II. Curves 2 and 3 are obtained by applying Eq. IV-20 to Eq. IV-22 yielding a set of nonrecursive coefficients given as

TABLE 1

$C_0 = .094$	$C_1 = .376$
$C_2 = .518$	$C_3 = .193$
$C_4 = .159$	$C_5 = .101$
$C_6 = .068$	$C_7 = .045$
$C_8 = .030$	$C_9 = .020$

The nonrecursive filter given as curve 2 utilizes  $C_0$  through  $C_9$ . The filter of curve 3 utilizes  $h_0$  through  $h_7$ .

Curve 4 is obtained utilizing a conventional Fourier series expansion of the ideal rectangular filter. Thus the coefficients can be shown to be

$$h_0 = \frac{1}{2} \quad \text{IV-23}$$

$$h_n = h_{-n} = \frac{\sin n \pi / 2}{n \pi}$$

where

$$H_4(Z) = \sum_{u=0}^{10} h_{u-5} Z^{-u} \quad \text{IV-24}$$

As can be seen from Figure IV-1, curves 2 and 3 represent significantly better approximations to the bilinear recursive form than the conventional Fourier approximation. The ripple characteristics in both the pass and stopbands have been reduced. Another comparison of these various filter forms is shown in Figure IV 2. Here each of the four filters accepted a step at its input and the filter outputs computed. Table II summarizes the results.

TABLE II  
Filter Outputs (for Step Input)

Outputs	Bilinear (Curve 1)	10 term Approx. (Curve 2)	8 term Approx. (Curve 3)	Fourier Approximation (Curve 4)
$y_0$	.094	.094	.094	.064
$y_1$	.47	.47	.47	.064
$y_2$	.988	.988	.988	- .042
$y_3$	1.181	1.181	1.181	- .042
$y_4$	1.022	1.022	1.022	.276
$y_5$	.921	.921	.921	.776
$y_6$	.989	.989	.989	1.094
$y_7$	1.035	1.034	1.034	1.094
$y_8$	1.005	1.004		.988
$y_9$	.984	.984		.988
$y_{10}$	.998			1.053
$\vdots$	$\vdots$			
$y_{\infty}$	To 1.000			

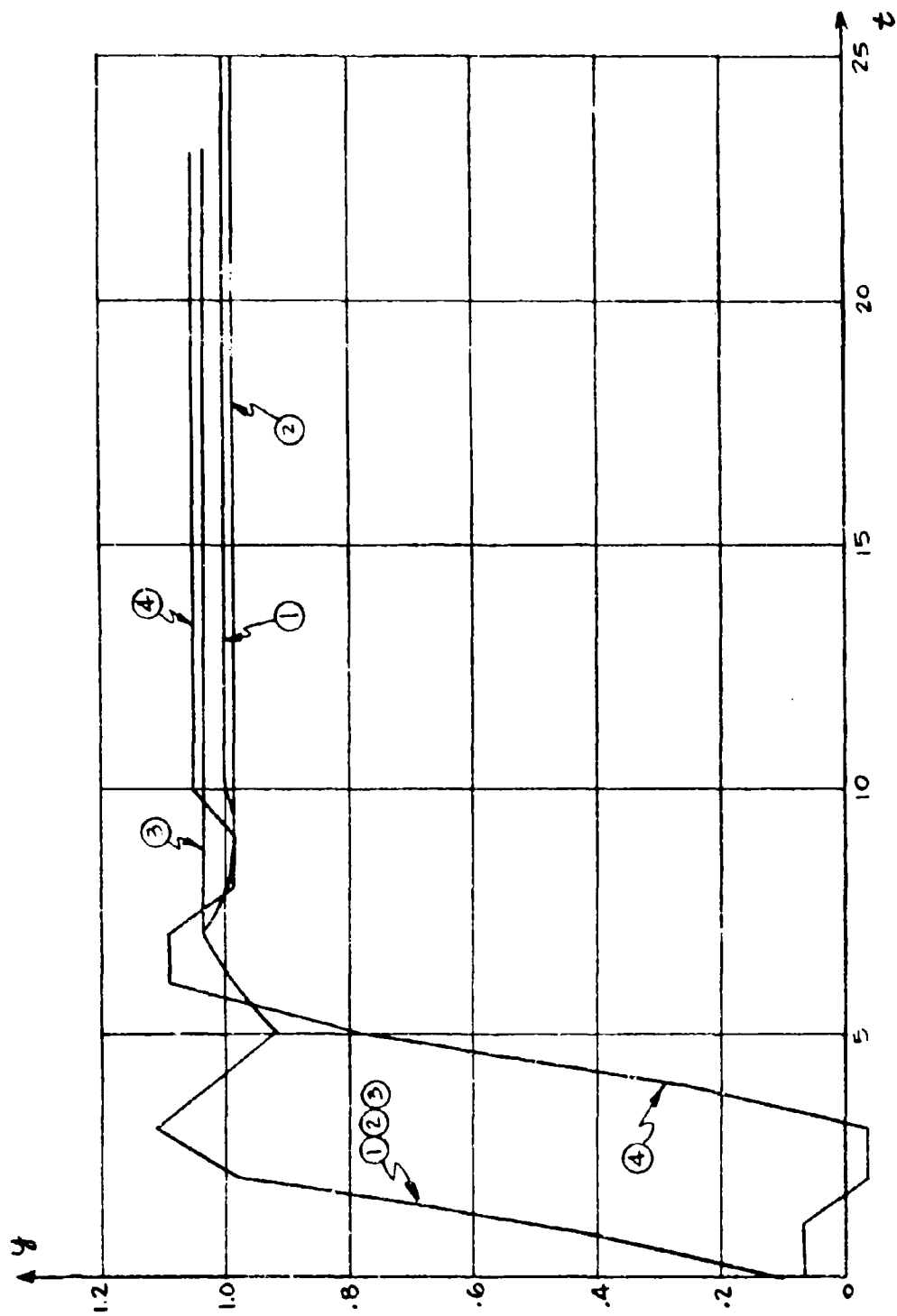


FIGURE 2: STEP RESPONSE NON-RECURSIVE FILTERS

From this figure, the improvement in curves 2 and 3 as an approximation to 1 (over that of the Fourier approximation, curve 4) is evident.

The approximation technique used to obtain curves 2 and 3 can be termed a "Digital Impulse Invariant" technique in that it yields an approximation to the impulse response of the recursive (bilinear in this case) filter which is exact up to the truncation point -- that is, up to the last coefficient retained. This procedure is the digital counterpart to the conversion of an analog filter to a digital filter through the use of standard Z-transforms. This approach yielded a point for point match with the analog filter's impulse response. Still another interpretation of this technique is that the bilinear transformation 'rounded' the corner of the ideal filter of Figure IV-1 and therefore this impulse invariant technique provides a simple procedure for smoothing or modifying the Fourier coefficients. Lastly, this procedure is simple to implement.

#### C. ZERO REMOVAL AND RELOCATION

As noted previously, there are often two sources of error inherent in the design of nonrecursive filters. The second of these errors was due to the truncation procedure used to yield a finite memory filter. A possible approach to nonrecursive filter design is to view the problem in such a way that the second source of error appears to be absent. This is accomplished as follows: From Eq. IV-1, one can view the  $N+1$  unknown coefficients as amplitude samples of some time waveform. Thus, this time waveform is finite in extent (all other samples are actually equal to zero) by definition and not due to truncation. Viewed in this manner, the frequency response characteristics achievable are those whose transforms are finite pulses. Ideally, it would be desirable to have the complete mapping of all finite pulses

and the variety of frequency responses they yield. Then one would choose the response "closest" to the one desired and then sample the finite pulse at an appropriate rate. Although the above mapping was not accomplished, the following will illustrate the procedure and will serve to tie together the various approaches to nonrecursive design.

Initially a characterization of finite pulses was desired. As noted by Campbell, et.al,<sup>(6)</sup> a pulse (in time) of finite extent is completely characterized by the fact that its transform (complex Fourier) has an infinite set of zeros. This is most easily seen by noting a rectangular pulse and its  $\sin x/x$  transform which consists of an infinite number of zeros uniformly distributed over the real frequency axis. Subject to certain constraints<sup>(7)</sup> these zeros can be removed and/or relocated to alter the frequency characteristic while still retaining the finite pulse structure of the time waveform.

Perhaps the simplest illustration of the process of zero removal is to consider a rectangular pulse existing for  $|t| \leq 1/2$ . If the first zero pair is removed, it can be shown that the resulting pulse is of the form

$$(1 + \cos 2\pi t) p(t) \quad \text{IV-25}$$

where  $p(t)$  is the rectangular pulse existing over  $|t| < 1/2$ .

Thus, the familiar  $\cos^2 x$  weighting function can be viewed in the frequency domain as a multiplication of the  $\sin x/x$  form by a factor  $(1/1 - f^2)$ . Similarly, the form of the pulse, as a result of removing  $N$  zeros from a rectangular pulse whose extent is from  $-\pi \leq t \leq \pi$  can be shown to be

$$g(t) = \frac{1}{2\pi} \left[ 1 - \sum_{n=1}^N A_n \cos \mu_n r_1 (t + \pi) \right]; \quad \mu_n = \frac{r_n}{r_1} \quad \text{IV-26}$$

where



$$A_n = \prod_{k=1}^N r_k^2 \left| r_n^2 \prod_{\substack{k=1 \\ k \neq n}}^N \left[ \frac{r_k^2}{r_k^2 - r_n^2} \right] \right| \quad \text{IV-27}$$

and the zeros of the rectangular pulse are at  $\pm r_1, \pm r_2, \dots; \mu_n = r_n/r_1$ .

From IV-26, it can be shown that  $G(\omega)$  the Fourier transform of  $g(t)$  is

$$G(\omega) = 2\pi \left[ \frac{\sin \pi \omega}{\pi \omega} + \sum_{i=1}^N \frac{A_i}{2} \left( e^{j\pi k_i} \frac{\sin \pi (\omega - k_i)}{\pi (\omega - k_i)} + e^{-j\pi k_i} \frac{\sin \pi (\omega + k_i)}{\pi (\omega + k_i)} \right) \right]$$

$$G(\omega) = 2\pi \left[ \frac{\sin \pi \omega}{\pi \omega} + \sum_{i=1}^N A_i \cos \pi k_i \frac{\sin \pi (\omega - k_i)}{\pi (\omega - k_i)} \right] \quad \text{IV-28}$$

Thus, the shape of the pulse in the frequency domain is determined by a weighted summation of delayed  $\sin x/x$  waveforms.

For a pulse of finite extent, it can also be shown that its Fourier transform can be written as

$$G(\omega) = \sum_{n=-\infty}^{\infty} G(n) \frac{\sin \pi (\omega - n)}{\pi (\omega - n)} \quad \text{IV-29}$$

Thus, there is a link between the amplitude samples of the frequency response and the  $A_i$  coefficients which are determined by the zeros.

In a similar manner, a finite  $\cos x$  pulse can be obtained through the process of zero relocation in the following manner. Assume a rectangular pulse over the interval  $|t| \leq \pi$ . Its transform can be shown to be of the form

$$G(\omega) = 2\pi \frac{\sin \pi \omega}{\pi \omega} \quad \text{IV-30}$$

with zeros occurring at  $\pm 1, \pm 2, \dots$ .

Now, if the  $k^{\text{th}}$  zero-pair is moved to the location of the  $r^{\text{th}}$  pair, then  $G(\omega)$  becomes

$$G_1(\omega) = \frac{2\pi \sin \pi \omega \left( \frac{1-\omega^2}{2} \right)^{\frac{r}{2}}}{\pi \omega \left( \frac{1-\omega^2}{2} \right)^{\frac{k}{2}}} \quad \text{IV-31}$$

The corresponding time function becomes

$$g_1(t) = 1 - \left( \frac{\mu^2 - 1}{\mu^2} \right) \cos k(t + \pi) \quad |t| < \pi \quad \text{IV-32}$$

where  $\mu = r/k$ . Thus, one now has independent control over the amplitude and frequency of this time function.

Since the family of raised cosine pulses are used frequently as weighting functions, the transforms of these pulses were obtained to note their relationship to the process of zero removal.

If one assumes a family of raised cosine pulses of the form

$$g(t) = \cos^n \frac{\pi t}{T} \quad |t| \leq \frac{T}{2} \quad \text{IV-33}$$

$$= 0 \quad \text{otherwise}$$

Then  $G(f)$ , the Fourier transform of  $g(t)$  can be shown to be

$$G(f) = \frac{2T}{\pi} \frac{n! \cos \pi f T}{(n-1)/2} \prod_{k=0}^{(n-1)/2} \left[ \frac{\pi}{(2k+1)^2 - 4T^2 f^2} \right] ; \quad n \text{ odd} \quad \text{IV-34}$$

or

$$G(f) = \frac{T n!}{\pi \prod_{k=1}^{n/2} \left[ 4k^2 \left( 1 - T^2 \frac{f^2}{k^2} \right) \right]} \left[ \frac{\sin \pi f T}{\pi f T} \right]; \quad n \text{ even} \quad \text{IV-35}$$

Note, the form of IV-35 is such that a cosine pulse raised to an even power of  $n$  is equivalent to removing the first  $n/2$  zeros of  $\sin(\pi f T)/\pi f T$ . These zeros occur at  $f = k/T$  for  $k = 1, 2, \dots, n/2$  and are those removed by the factor  $(1 - T^2 f^2/k^2)$ .

From Eq. IV-35, a link can be shown to exist between the process of zero removal, modified or weighted Fourier series, and the technique proposed by Blackman.<sup>(8)</sup> This link is illustrated as follows: Consider the synthesis of an arbitrary pulse given by

$$f(t) = \sum_{n=0}^{N-1} A_n \cos^n \left( \frac{\pi t}{T} \right) \quad |t| \leq \frac{T}{2} \quad \text{IV-36}$$

This synthesis can be viewed in two sections. First over even  $n$  and then over odd  $n$ . Those raised cosine pulses over even  $n$  are equivalent to a weighted addition of zero removed  $\sin x/x$  pulses. A cosine pulse raised to an odd power of  $n$  can be viewed as the product of an even power  $(n-1)$  multiplied by  $\cos(\pi t/T)$ . Thus its transform can be written in the form of Eq. IV-35 with a shift to the left and right (in frequency) of  $(1/2 T)$ . Equation IV-36 is therefore a weighted summation of zero removed  $\sin(\pi f T)/\pi f T$  pulses.

The relationship between Eq. IV-36 and a Fourier series expansion is obtained by noting the form of Tchebycheff polynomials. These polynomials are defined as

$$V_n(x) = \cos(n \cos^{-1} x) \quad \text{IV-37}$$

and if  $x = \cos \theta$

$$V_n(x) = \cos n \theta \quad \text{IV-38}$$

then a trigonometric polynomial or Fourier series

$$f(\theta) = \sum_{n=0}^{N-1} B_n \cos n \theta \quad \text{IV-39}$$

is equivalent to a polynomial in  $x$  given by

$$f[\cos^{-1} x] = \sum_{n=0}^{N-1} C_n x^n \quad \text{IV-40}$$

The relationship between the  $B_n$  and  $C_n$  coefficients relate the expansion of IV-39. That is, the  $C_n$  are identical to the  $A_n$  for  $x = \cos(\pi t)/T$ . The polynomials given by Eq. IV-37 relate to  $B_n$  and  $A_n$  coefficients. The procedure would be to first expand a function in a Fourier series. Then, through the use of the Tchebycheff polynomials, calculate the  $C_n$  coefficients. Using equation (or expansion) IV-36 expand the function yielding the  $A_n$  coefficients. Then relate the  $A_n$  and  $B_n$  coefficients yielding a weighted Fourier expansion.

Blackman's technique involves the synthesis of a desired characteristic in the frequency domain through a summation of raised cosine pulses of the form

$$|H(\cos \omega T)|^2 = \sum_{n=0}^{N-1} h_n \cos^n \omega T \quad \text{IV-41}$$

where  $\omega$  is the digital frequency function. Thus Blackman's technique is a

synthesis procedure with raised cosine pulses in the frequency domain and, therefore, zero-removed  $\sin x/x$  pulses in the time domain. His procedure attempts to link the  $h_n$  coefficients with those given by

$$H(Z) = \sum_{n=0}^{N-1} a_n Z^{-n} \quad \text{IV-42}$$

Although the process of zero removal and relocation was not extended to yield the complete characterization of finite pulses, it did illustrate the tie-in among the various synthesis techniques. These techniques all center about a finite Fourier series approximation in some form, whether it results from truncation of the infinite Fourier series expansion of the desired function, the truncation of the infinite Fourier expansion of the characteristic obtained through the bilinear transform (as in IV-B) or the discrete version discussed in IV-A.

Two basic procedures which can be used in the design of nonrecursive digital filters have been discussed. The first procedure was based on the assumption that the desired frequency characteristics were available only at discrete points. The second approach proceeded on the assumption that a satisfactory recursive design was available. These recursive coefficients were then converted to a nonrecursive design with illustrative examples indicating the simplicity of the technique as well as improvement that this technique offers over the more conventional Fourier series approach.

## V. ERROR CONSIDERATIONS

As noted by Kaiser,<sup>(9)</sup> Gold<sup>(10)</sup> and others, there are essentially three sources of errors associated with digital or discrete time processing. The first error results from the sampling and quantization of the input signal. The second error is due to the representation of the filtering coefficients with a finite number of bits. The third error is one of computational quantization. That is, the digital filter is an arithmetic unit which performs the operations of weighted multiplication and additions. There are therefore errors caused by roundoff of these results which are often utilized\* in further computations.

In this section, various aspects of the latter two types of errors will be discussed. The relationship between coefficient accuracy, stability and critical filter parameters will be detailed as well as the effect of alternate synthesis or implementation procedures. The relationships between computational quantization, normalized sampling rates and various implementations will be discussed along with an error reducing procedure.

### A. STABILITY AND COEFFICIENT ACCURACY

It can be shown that the evaluation of the denominator of the digital filter transfer function  $H(Z)$  at the point  $Z^{-1} = 1$  gives an indication of the maximum allowed variation of the digital filter coefficients for stability to be maintained.<sup>(11)</sup> For a digital filter of the form

---

\*In recursive or feedback type filters, prior outputs are reprocessed.

$$H(Z) = \frac{\sum_{n=0}^N a_n Z^{-n}}{\sum_{n=0}^N b_n Z^{-n}} \quad V-1$$

this index is of the form

$$I = \sum_{j=1}^N b_j \quad V-2$$

or as it is more conventional to divide through by the  $b_0$  coefficient, this index is given as

$$F_0 = 1 + \sum_{j=1}^N \frac{b_j}{b_0} \quad V-3$$

The tabular approach to digital lowpass filter synthesis utilizing the bilinear transform as discussed in Section II, provides for a simple evaluation and interpretation of the above stability index. Consider the table used to generate the coefficients as shown on the next page.

TABLE I

Coefficients	$P_0 K_{\varepsilon_u}^N$	$P_1 K_{\varepsilon_u}^{N-1}$	$P_2 K_{\varepsilon_u}^{N-2}$	....	$P_N K_{\varepsilon_u}^0$
$z^0(a_0, b_0)$	1	1	1	....	1
$z^{-1}(a_1, b_1)$	$C_1^N$	( )	( )		( )
$z^{-2}$	$C_2^N$	( )	( )		( )
.	.	.	$d_{i,j}$		.
.	.	.			.
.	.	.			.
$z^{-N}(a_N, b_N)$	$C_N^N$	( )	....		( )

where

$$C_r^N = \frac{N!}{r!(N-r)!}$$

In addition, the constraining relationships among the  $d_{ij}$  are given by

$$\sum_{i=1}^N d_{i,j} = 0 \quad 1 \leq j \leq N$$

$$\sum_{i=0}^N d_{i,0} = 2^N \quad V-4$$

To obtain the denominator ( $b_j$ ) coefficients from Table I, one substitutes for  $P_j$  the appropriately subscripted denominator coefficients of the analog filter ( $B_j$ ) and sums all the products of the table entries and column



headings for row  $j$ . If, however, the stability index is formed by summing down each column then, utilizing V-4,  $F_0$  becomes

$$F_0 = \frac{(2K_{\bar{\omega}_u})^N B_0}{\sum_{i=1}^N B_i K_{\bar{\omega}_u}^{N-i}} \quad V-5$$

where

$$K_{\bar{\omega}_u} = \tan(\pi \frac{\bar{f}_u}{f_s}) \quad V-6$$

It can also be shown that stability becomes marginal when  $F_0$  is equal to zero. Thus, the coefficient accuracy problem is most acute when the order of the filter is high and the factor  $K_{\bar{\omega}_u}$  is small. With  $K_{\bar{\omega}_u}$  defined as in V-6, small values of  $K_{\bar{\omega}_u}$  occur when the ratio of sampling rate to cutoff frequency is high. When this is so, V-5 can be approximated by

$$F_0 \approx (2K_{\bar{\omega}_u})^N \quad V-7$$

and the digital filter coefficients approach in magnitude the binomial coefficients and alternate in sign. This result is obtained from Table I in that the coefficients of the last column can be shown to be the above mentioned binomial coefficients.

This equation clearly exhibits the effect of the order of the filter and the ratio of bandwidth to sampling rate on the stability problem. Table I also gives a great deal of insight into the effect of truncating the filter coefficients. Consider row  $i$  of the table, given as

$$R_i = C_i^N B_0 K \frac{N}{\omega_u} + d_{i,2} B_1 K \frac{N-1}{\omega_u} + \dots + d_{i,a} B_{a-1} K \frac{N-a+1}{\omega_u} + \dots + C_i^N B_N$$

V-8

Now the coefficients of the analog filter paired as  $(B_0, B_N)$ ,  $(B_1, B_{N-1})$ ,  $(B_i, B_{N-i})$  are most often of the same order of magnitude. Furthermore, it can be shown that the  $d_{i,j}$  coefficients can also be paired in the same manner. Thus, if the summation is accomplished in the foregoing pair-wise manner, then one is adding terms of the form

$$M K \frac{k}{\omega_u} \left[ K \frac{N-2k}{\omega_u} \pm 1 \right]$$

V-9

When the ratio of sampling rate to bandwidth is high and the order of the filter,  $(N)$  is large, then  $K \frac{N-2k}{\omega_u}$  can be considerably less than 1 -- especially for small  $k$  (towards the outer edges of the table). Therefore, in effect, the truncation problem effects the highest order analog filter coefficient first. That is,  $B_N$  is effectively set equal to zero in both the numerator and denominator. Thus, if the analog filter was originally of the form

$$G(S) = \frac{A_N S^N + A_{N-1} S^{N-1} + \dots + A_0}{B_N S^N + B_{N-1} S^{N-1} + \dots + B_0}$$

V-10\*

It then becomes

$$G(S) = \frac{A_{N-1} S^{N-1} + \dots + A_0}{B_{N-1} S^{N-1} + \dots + B_0}$$

V-11

---

\* Although the numerator and denominator are usually of different order, they can always be written as shown, by adding the required zeros.

Therefore, one is actually synthesizing a lower order filter as one truncates the coefficients. Of course, the more coarse the quantization, the more coefficients (from the high end) become deleted. This reduction of the order of the filter explains the results obtained, in that as the quantization process continues, the filter slopes do decrease, which signifies a lower order filter. The onset of instability is due to the fact that the remaining coefficients are not changed as the order is reduced so that the zeros (or poles) of the polynomial shift in a complicated manner. It should be noted that for values of  $K_{\bar{\omega}_u}$  close to .5,  $F_0$  gets smaller with increasing  $N$  at a very slow rate. This value of  $K_{\bar{\omega}_u}$  corresponds to a sampling to cutoff frequency ratio of approximately 7:1.

A similar result can be obtained for the bandpass case. This is most easily seen if one applies the LP-BP transformation with a 4:1 ratio of sampling to carrier frequency. As noted in Section II, this transformation is obtained by replacing  $Z^{-1}$  by  $-Z^{-2}$  and  $K_{\bar{\omega}_u}$  by  $K_{\bar{B}}$ . Thus, the same table can be used if alternate rows (even numbered) are multiplied by -1 and  $K_{\bar{\omega}_u} \rightarrow K_{\bar{B}}$ . It can also be shown that the sum of the entries in any particular column is equal to zero except for column 1 where the entries sum to  $2^N$ . Since, in the low-pass case stability is determined by evaluating the denominator of the transfer function at  $Z^{-1} = 1$ , then the low-pass case yields  $B_0 2^N K_{\bar{\omega}_u}^N$ . For the bandpass case, the point  $Z^{-1} = e^{+j\bar{\omega}_0 T}$  replaces the point  $Z^{-1} = 1$  in the stability computations. However, for the case under discussion,  $\bar{\omega}_0 T = \pi/2$  and  $Z^{-1} = +j$ . Thus,  $Z^{-2n} = -1$  for  $n$  odd and  $Z^{-2n} = 1$  for  $n$  even. This alternation in sign effectively cancels out the alternation in sign due to the transformation and the stability index for bandpass filters is given by  $B_0 2^N K_{\bar{B}}^N$ . Thus the index becomes

$$I = \frac{B_0 (2K_{\bar{B}})^N}{\sum_{i=0}^N B_i K_{\bar{B}}^{N-i}}$$

V-12

where the  $B_i$  coefficients are the denominator coefficients of the low-pass analog filter.

The foregoing results indicate that synthesis of a high order filter in conjunction with a high ratio of sampling to cutoff (or bandwidth) frequency should be avoided. These conditions on the factor  $K_{\omega_u}$  would, for example, occur whenever it is desired to filter a narrow band segment from a broad bandwidth signal. The narrow band constraint dictates a small  $T_u$  whereas the broad bandwidth dictates (through the use of the sampling theorem) a large  $f_s$ . The foregoing results indicate that rapid degradation occurs when the above ratio exceeds 7:1 ( $K_{\omega_u} \leq .5$ ). Under these conditions, a cascade approach to digital filter synthesis yields a significant improvement. The following will illustrate this improvement.

#### B. CASCADE vs. DIRECT SYNTHESIS

With the foregoing constraints to be illustrated, an elliptic filter was designed with the specifications assumed to be

Passband Spec.      .01 db ripple       $0 \leq \omega \leq 1$

Stopband Spec.      40 db attenuation       $1.38 \leq \omega \leq \infty$

Utilizing the techniques of Section III, the above specifications led to a sixth order analog filter of the form

$$H(S) = \frac{S^4 + A_2 S^2 + A_0}{\sum_{i=0}^6 B_i S^i}$$

V-13

where the coefficients are given as

TABLE II

$A_0 = 6.79609$	$B_2 = 5.71737$
$A_2 = 5.40108$	$B_3 = 6.29689$
$B_0 = 1.26743$	$B_4 = 5.06663$
$B_1 = 3.44569$	$B_5 = 2.62193$
$B_6 = 1$	

Solving the numerator and denominator polynomials of V-13 the pole-zero configuration for this filter can be shown to be

TABLE III

$z_0 = \pm j 1.84538$	(zeros)
$z_1 = \pm j 1.41268$	
$p_1 = - .10102 \pm j 1.12369$	(poles)
$p_2 = - .39699 \pm j .99211$	
$p_3 = - .81294 \pm j .45946$	

Initially, this filter was digitized under the conditions that the signal is sampled at 6 times the cutoff frequency of the filter. Thus,  $K = \tan(\bar{\omega}_0 T/2) = \tan(\pi/6) = .57735$ . Utilizing Table II of Section II, substitution of the above parameters yields the following digital filter coefficients.

TABLE IV

<u>Numerator Coeff.</u>	<u>Denominator Coeff.</u>
$a_0 = 1.1851589$	$b_0 = 6.31772332$
$a_1 = 2.0438115$	$b_1 = -12.9964865$
$a_2 = 2.8421442$	$b_2 = 18.4185255$
$a_3 = 3.9669833$	$b_3 = -14.8467182$
$a_4 = 2.8421442$	$b_4 = 8.34145098$
$a_5 = 2.0438115$	$b_5 = -2.65466173$
$a_6 = 1.1851589$	$b_6 = .424433844$

This filter and the filter obtained by rounding the above coefficients to five significant figures, three to the right and two to the left, are plotted in Figure V-1. As dictated by the 6:1 ratio, the cutoff frequency of this filter is at  $2\pi/6$  rad or  $60^\circ$ . As can be seen, there is essentially no difference in the filter responses.

This filter was then synthesized using the cascade approach. The procedure used was to perform the factorization in the analog domain in the following manner: The filter  $G(S)$  was expressed in cascade form as

$$G(S) = G_1(S) G_2(S) G_3(S) \quad V-14$$

where both  $G_1(S)$  and  $G_2(S)$  are of the form

$$G_1(S) G_2(S) = \frac{S^2 + A_0}{B_0 + B_1 S + S^2} \quad V-15$$

The filter  $G_3(S)$  is of the form

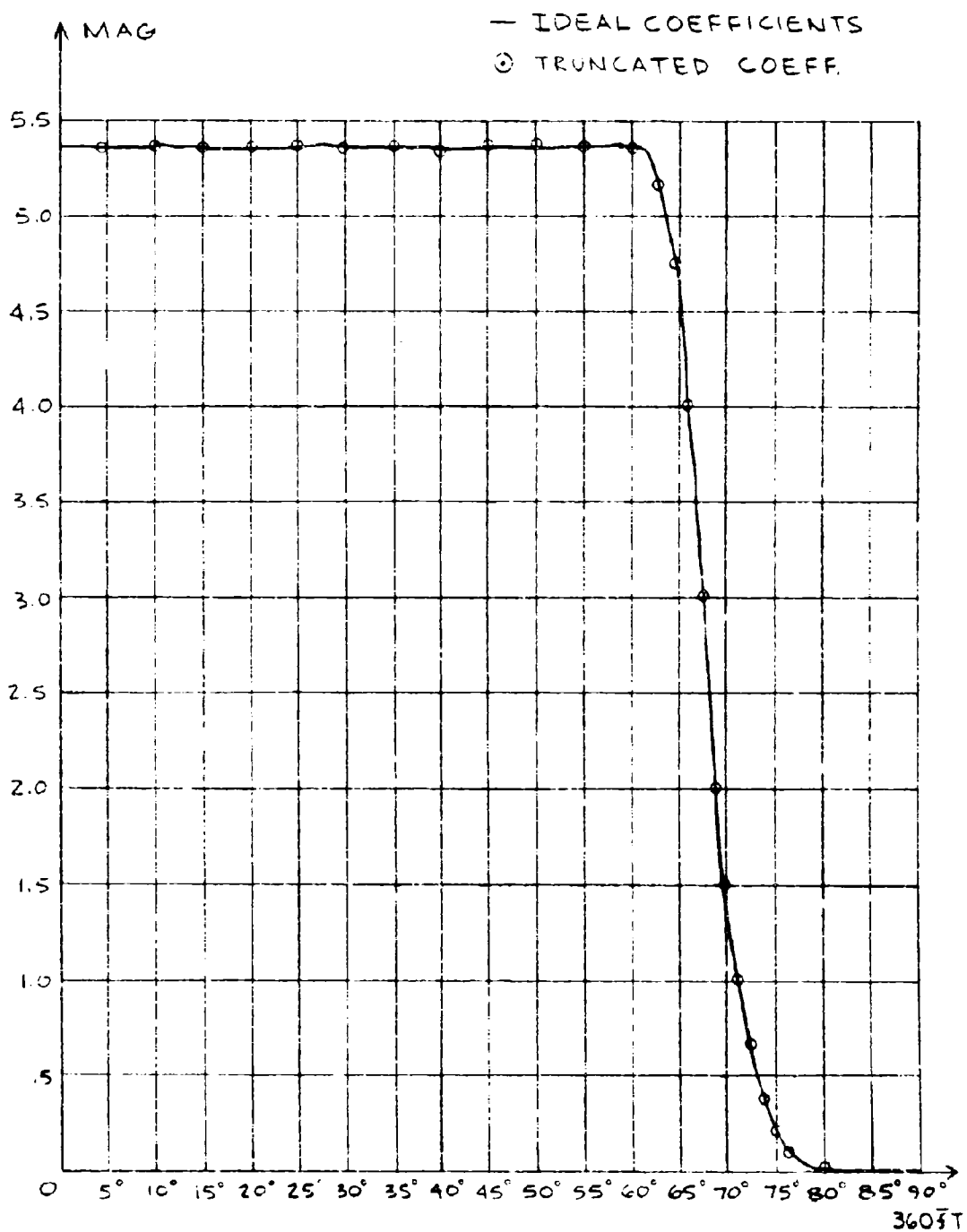


FIGURE V-1 ; ELLIPTIC FILTER WITH 60° CUTOFF

$$G_3(S) = \frac{1}{S^2 + B_1 S + B_0} \quad V-16$$

Using the results of Table III, the foregoing filter characteristics become

$$G_1(S) = \frac{(S + j1.84538)(S - j1.84538)}{(S + .10102 + j1.12369)(S + .10102 - j1.12369)} \quad V-17$$

$$G_2(S) = \frac{(S + j1.41268)(S - j1.41268)}{(S + .39699 + j.99211)(S + .39699 - j.99211)} \quad V-18$$

$$G_3(S) = \frac{1}{(S + .81294 + j.45946)(S + .81294 - j.45946)} \quad V-19$$

If Eqs. V-17 through V-19 are expanded and the bilinear transform applied to these filters utilizing the technique of Section II-A with  $K_{\omega_u} = .57735 = \tan(30^\circ)$  then the three digital filters become

Filter 1 (from  $G_1(S)$ )

$$a_0 = 2.135 \quad b_0 = 1.541$$

$$a_1 = .270 \quad b_1 = -1.151$$

$$a_2 = 2.135 \quad b_2 = 1.308$$

Filter 2 (from  $G_2(S)$ )

$$a_0 = 1.665 \quad b_0 = 1.839$$

$$a_1 = -.670 \quad b_1 = -1.239$$

$$a_2 = 1.665 \quad b_2 = .922$$



Filter 3 (from  $G_3(S)$ )

$$\begin{array}{ll} a_0 = .333 & b_0 = 2.230 \\ a_1 = .667 & b_1 = -1.419 \\ a_2 = .333 & b_2 = .352 \end{array}$$

The product of these responses was obtained and compared with that of Figure II-1, showing no significant difference.

The above procedure was repeated for a higher ratio of sampling to cutoff frequency to illustrate the previously mentioned degradation. Using  $K_{\frac{\omega}{\omega_u}} = .17633 = \tan(10^\circ)$  (i.e., a  $20^\circ$  cutoff) the sixth order digital filter coefficients become

TABLE V

$$\begin{array}{ll} a_0 = .036517931 & b_0 = 1.66053236 \\ a_1 = -.050516111 & b_1 = -8.1507299 \\ a_2 = -.033249521 & b_2 = 17.0485004 \\ a_3 = .107569042 & b_3 = -19.3912146 \\ a_4 = -.033249521 & b_4 = 12.626522 \\ a_5 = -.050516111 & b_5 = -4.4568362 \\ a_6 = .036517931 & b_6 = .665664076 \end{array}$$

This filter and the one obtained by rounding the coefficients as before, (3 decimal digits) are plotted in Figures V-2 and V-3. Note the severe change in filter performance. That is, the curve of V-3 is unrecognizable as a low-pass digital filter. This illustrates the problems involved in a direct synthesis of a high order filter where the ratio of sampling rate to cutoff

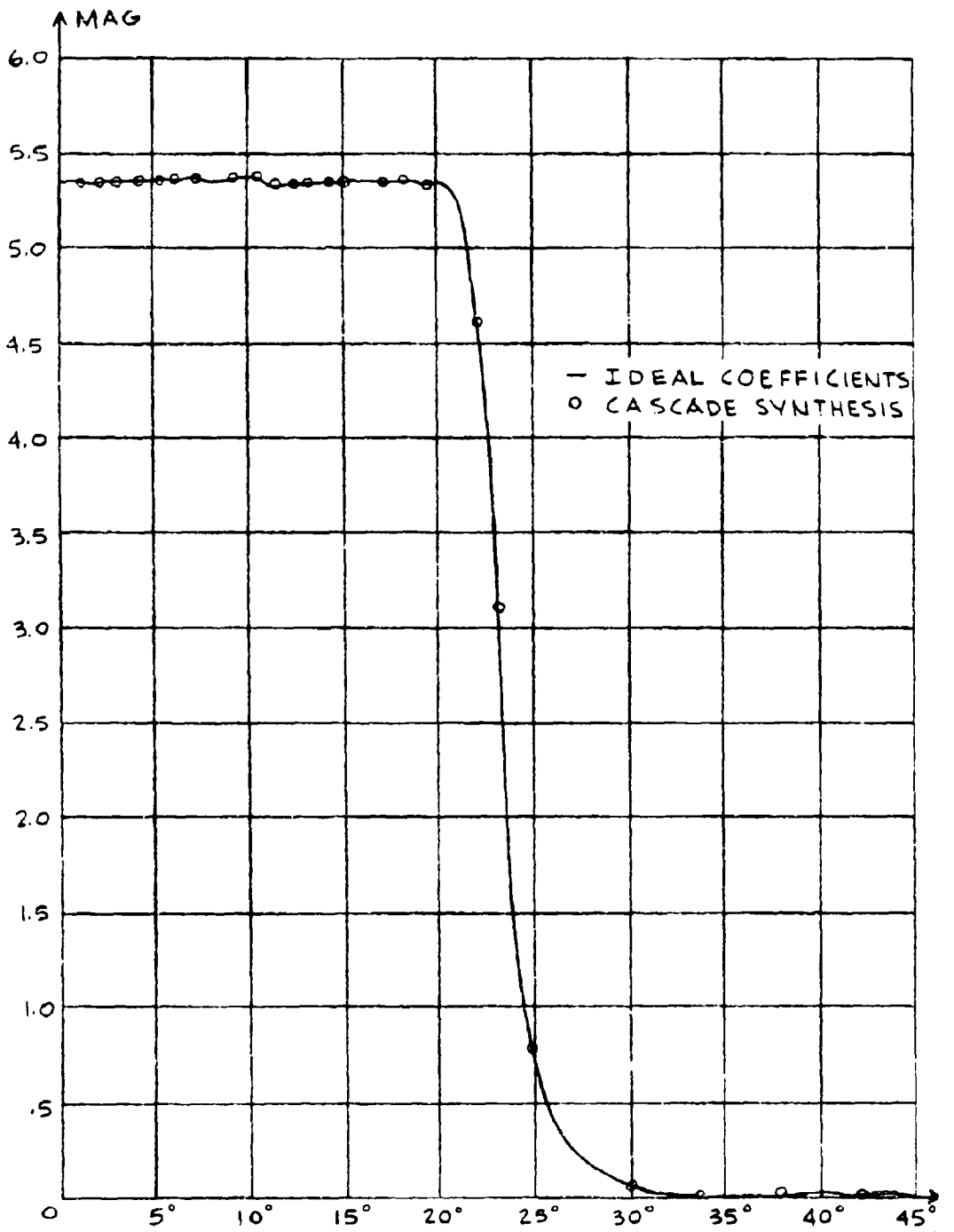


FIGURE X-2: ELLIPTIC FILTER WITH 20° CUTOFF 360°

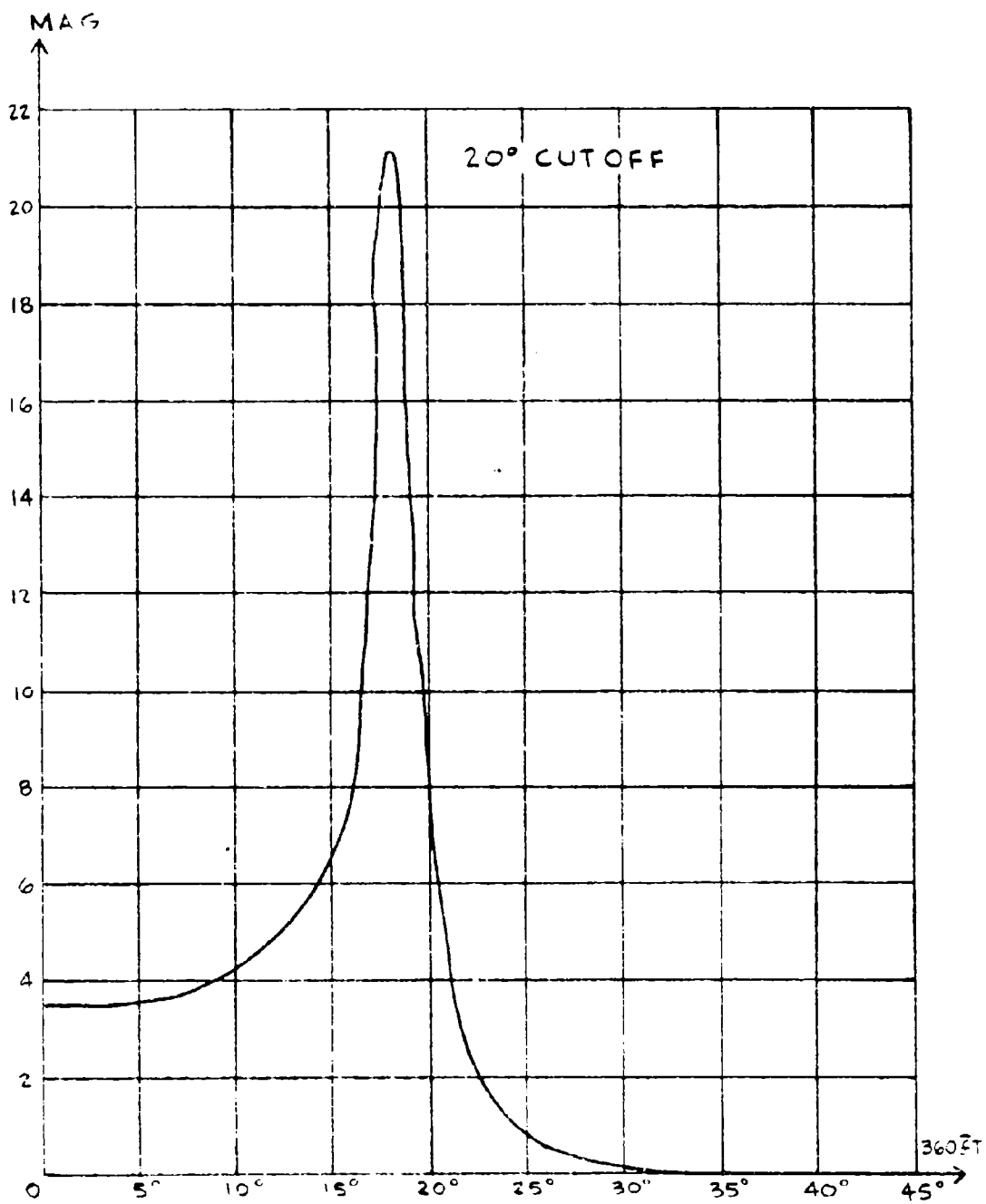


FIGURE V-3: ELLIPTIC FILTER TRUNCATED COEFFICIENTS

frequency is large and coefficient rounding is desired. Once again this filter was synthesized as three cascaded filters with the respective digital coefficients obtained as before as shown below.

Filter 1 (from  $G_1(S)$ )

$$a_0 = 1.106 \quad b_0 = 1.175$$

$$a_1 = -1.788 \quad b_1 = -1.921$$

$$a_2 = 1.106 \quad b_2 = 1.004$$

Filter 2 (from  $G_2(S)$ )

$$a_0 = 1.062 \quad b_0 = 1.175$$

$$a_1 = -1.876 \quad b_1 = -1.929$$

$$a_2 = 1.062 \quad b_2 = .895$$

Filter 3 (from  $G_3(S)$ )

$$a_0 = .031 \quad b_0 = 1.314$$

$$a_1 = .062 \quad b_1 = -1.946$$

$$a_2 = .031 \quad b_2 = .740$$

The product of this response was obtained and plotted in Figure V-2. A comparison of this response and that of the rounded and unrounded direct filter as shows the definite advantage of the cascade approach.\*

---

\* An alternate approach to comparing the cascade vs. direct approach was investigated by Knowles and Olcayto,<sup>(12)</sup> who modeled the coefficient truncation problem as a parallel error filter and used a statistical approach to evaluate performance.

The foregoing results were expected in view of the results on coefficient errors and generalized design procedures which showed that the coefficients are primarily determined by factors  $R_j K_{\omega_u}^{N-j}$  where  $R_j$  is the analog filter coefficient,  $N$  is the order of the filter and  $K_{\omega_u}$  is the normalized cutoff frequency. Thus, as  $K_{\omega_u}$  is reduced the effect of  $R_j$  is lost for large  $N$  as the coefficients are rounded.

### C. COMPUTATIONAL QUANTIZATION

The nature of computational quantization is dependent upon the particular implementation used. A digital filter recursion equation expressed in direct form is given as

$$y_n = \sum_{j=0}^N a_j x_{n-j} - \sum_{j=1}^N b_j y_{n-j} \quad V-20$$

When computational quantization occurs at each operation of V-16, the recursion equation becomes

$$\hat{y}_n = Q_n''' \left\{ \sum_{j=0}^N Q'_{n,j} \left[ a_j x_{n-j} \right] - \sum_{j=1}^N Q''_{n,j} \left[ b_j \hat{y}_{n-j} \right] \right\} \quad V-21$$

where  $Q'[\bullet]$ ,  $Q''[\bullet]$  and  $Q'''[\bullet]$  represent the operation of quantizing the function on which it operates.

If one represents the operation of quantization by an equivalent additive noise source  $n'$  as

$$Q'[a] = n' + a$$

then V-21 becomes

$$\hat{y}_n = Q_n + \sum_{j=0}^N a_j x_{n-j} - \sum_{j=1}^N b_j y_{n-j} \quad V-22$$

where  $Q_n$  is the total quantization noise in the system (i.e.,  $Q_n = n' + n'' + n'''$ ).

Thus, the error becomes

$$\hat{y}_n - y_n = \epsilon_n = Q_n - \sum_{j=1}^N b_j \epsilon_{n-j} \quad V-23$$

If it is assumed that the quantization noise has a white spectral density, the mean square output noise is given by

$$\text{M.S.O.N} = \left( \frac{\sigma_Q^2}{2\pi j} \right) \oint H_1(Z) H_1(Z^{-1}) \frac{dZ}{Z} \quad V-24$$

where

$$H_1(Z) = \frac{1}{1 - \sum_{i=1}^N b_i Z^{-i}} \quad V-25$$

the  $b_i$  are the denominator coefficients of the original filter and  $\sigma_Q^2$  is the mean square input noise which is dependent upon the degree of quantization.

Thus, computational quantization has been expressed by an additive noise source, processed by  $H_1(Z)$  which consists only of the denominator or poles of the original filter.

Consider the input-output equations of a digital filter synthesized using the canonical form. In this case the transfer function corresponding to V-20 given as

$$H(Z) = \frac{Y(Z)}{X(Z)} = \frac{\sum_{n=0}^N a_n Z^{-n}}{\sum_{n=0}^N b_n Z^{-n}} = \frac{N(Z)}{D(Z)} \quad V-26$$

is rewritten as

$$\frac{X(Z)}{D(Z)} = \frac{Y(Z)}{N(Z)} = F(Z) \quad V-27$$

where  $F(Z)$  is some arbitrary function. Inverse transforming the two equations specified in V-27 yields

$$f_n = x_n - \sum_{j=1}^N b_j f_{n-j} \quad V-28$$

$$y_n = \sum_{j=0}^N a_j f_{n-j}$$

where  $f_n$  is an intermediate variable introduced.\* This is the so-called canonical form.

If, as before, one assumes that quantization occurs at each stage and that the operation of quantization is represented by an additive noise source, then it can be shown that the error is given by

$$\epsilon_n = \sum_{j=0}^N a_j Q_{n-j} - \sum_{j=1}^N b_j \epsilon_{n-j} \quad V-29$$

---

\*This pair of equations is related to the state-space concept utilized in optimal control.

Thus, under a white noise assumption, the mean square output noise is given by

$$\text{M.S.O.N.} = \left( \frac{\sigma_Q^2}{2\pi j} \right) \oint H_2(Z) H_2(Z^{-1}) \frac{dZ}{Z} \quad \text{V-30}$$

where

$$H_2(Z) = \frac{\sum_{i=0}^N a_i Z^{-i}}{1 + \sum_{i=1} b_i Z^{-i}} \quad \text{V-31}$$

Thus, for this form, the noise is processed by  $H_2(Z)$  which is identical to the original filter  $H(Z)$ .  $H_1(Z)$  consisted of only the poles of the original filter whereas  $H_2(Z)$  consists of the poles and zeros, that is the entire original filter.

Utilizing the relationships concerning the generalized design procedures for lowpass filters (Table I) it was desired to determine the relationship between the output noise and the ratio of sampling rate to cutoff frequency for lowpass filters synthesized using both of the previous approaches.

The filters investigated were second order lowpass, all pole filters of the form

$$G(S) = \frac{1}{AS^2 + BS + C} \quad \text{V-32}$$

Evaluation of the integrals  $(\text{M.S.O.N.}/\sigma_Q^2)$  and utilization of the generalized synthesis techniques yielded



### Direct Synthesis

$$\frac{\text{M.S.O.N.}}{\sigma_Q^2} = \frac{CK_{\omega_u}^2 + A}{16ABC K_{\omega_u}^3} \quad \text{V-33}$$

### Canonical Synthesis

$$\frac{\text{M.S.O.N.}}{\sigma_Q^2} = \frac{K_{\omega_u} (BK_{\omega_u} + A)}{CK_{\omega_u}^2 + BK_{\omega_u} + A} \quad \text{V-34}$$

where

$$K_{\omega_u} = \tan \frac{\pi f_c}{f_s} \quad \text{V-35}$$

The above results were evaluated for a Butterworth, Chebycheff (1/2 db ripple) and a Maximally Flat Time Delay Filter. The coefficients for these filters are

### Butterworth

$$A = 1 \quad B = \sqrt{2} \quad C = 1$$

$$p_1 = -\frac{\sqrt{2}}{2} \pm j \frac{\sqrt{2}}{2} \quad \text{V-36}$$

### Chebycheff

$$A = 1 \quad B = 1.4256245 \quad C = 1.5162026$$

$$p_1 = -.7128122 \pm j 1.0040425 \quad \text{V-37}$$

### Maximally Flat Time Delay

$$A = 1 \quad B = 3 \quad C = 3$$

$$p_1 = -1.5 \pm j .8660254 \quad \text{V-38}$$

These results are plotted in Figures V-4, 5 and 6.

It is to be noted that at high ratios of sampling rate to cutoff frequency, the canonical form is vastly superior. There are, however, regions where the direct synthesis should be used.

The results obtained indicate the importance of determining the value of the parameters  $K_{\bar{\omega}_u}$ . This parameter not only determines the synthesis technique used, but also determines the required coefficient accuracy.

#### D. AN AUXILIARY STORAGE TECHNIQUE

In the previous section, expressions were derived showing the effect of computational quantization as an error producing equivalent noise source. This discussion will develop the concept of an auxiliary storage to be used to reduce these errors.

If the round-off portion discussed previously is stored in an auxiliary storage and the main computation proceeds as prescribed by the applicable model and some quantization level, the accuracy of the output value,  $y_n$ , may be corrected by appropriately weighting the contents of the storage and adding it to the output.

In order to make a "perfect" correction, all prior round-off-segments have to be stored and multiplied by appropriate coefficients with complete precision. Since this is obviously impractical, in the general case, the technique developed will permit a conservative estimate to be made of the error due to truncation in previously rounded-off samples as well as the quantization present in the round-off arithmetic.

From Eq. V-27, the error,  $E(Z)$ , and the round-off or quantization  $Q(Z)$  are related by

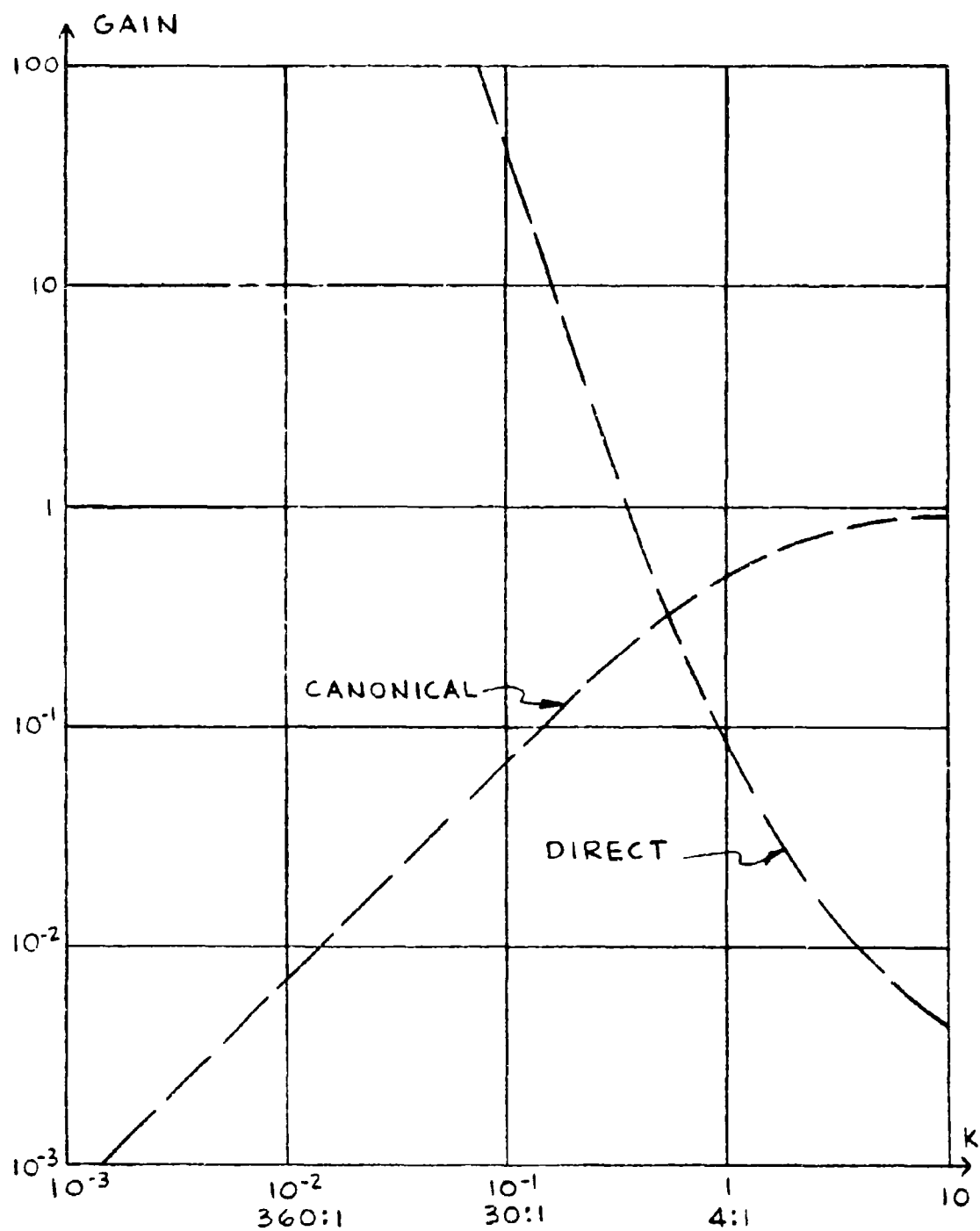


FIGURE V-4: 2<sup>ND</sup> ORDER BUTTERWORTH FILTER

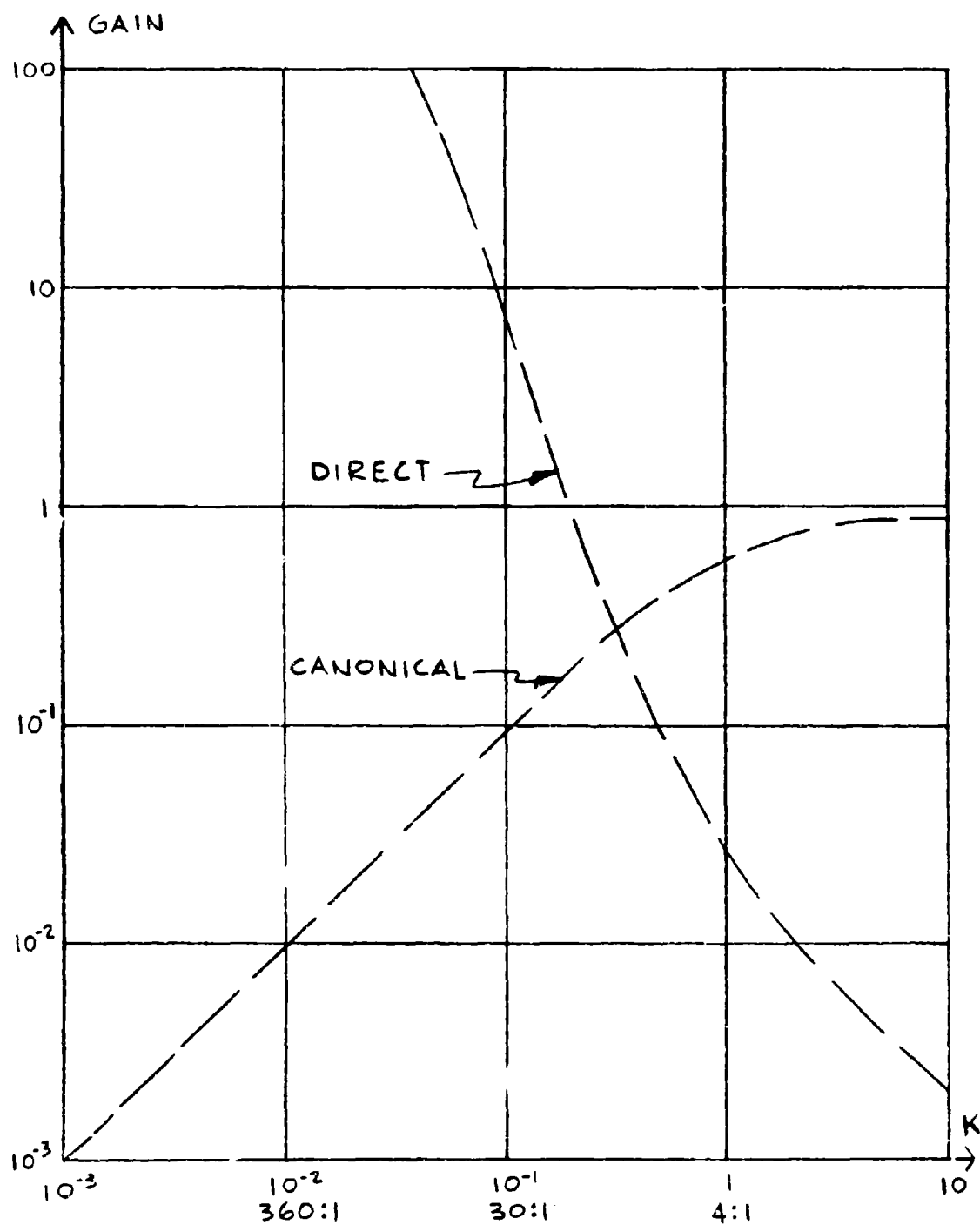


FIGURE V-5: MAXIMALLY FLAT LINE-DELAY

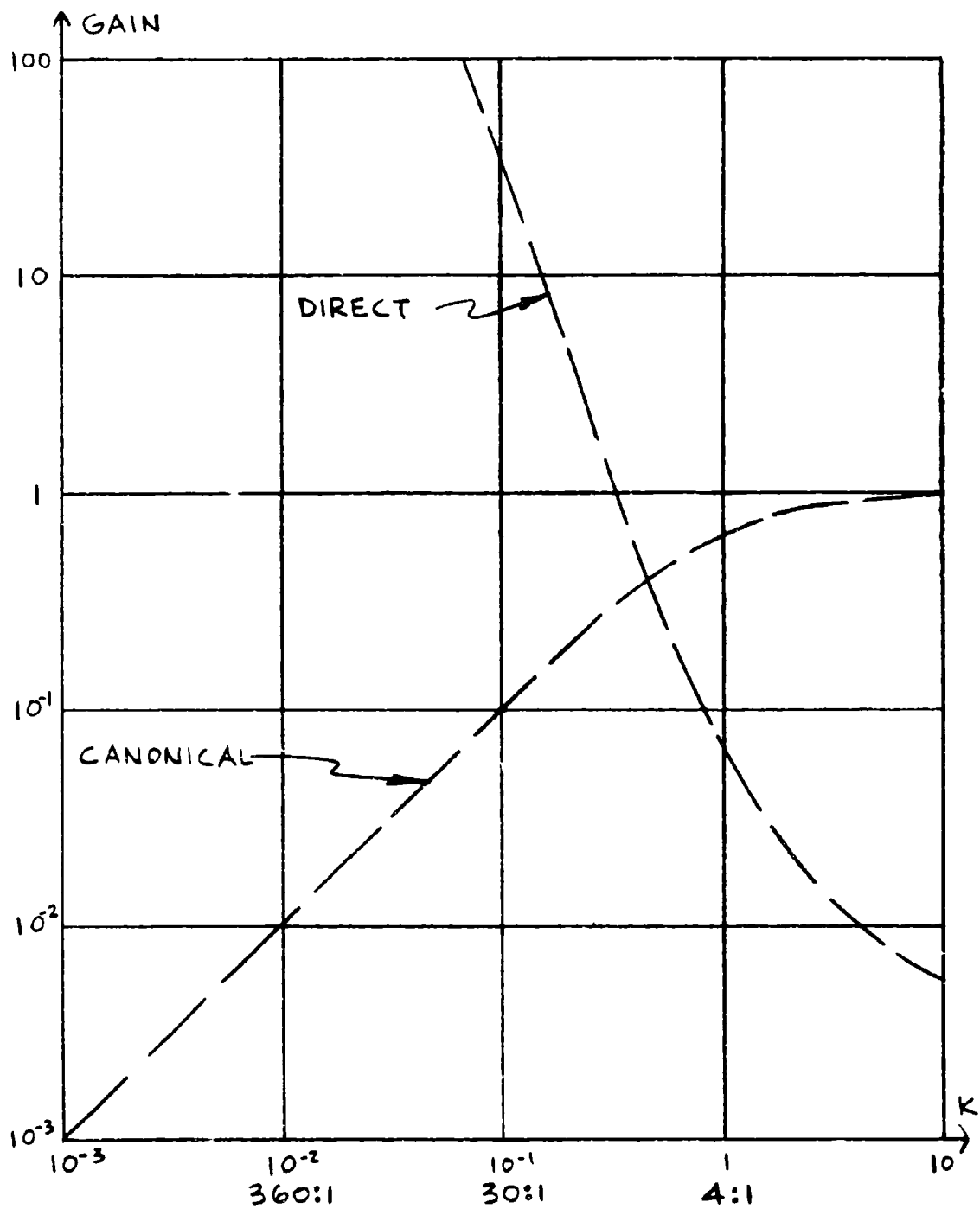


FIGURE V-6: 2<sup>ND</sup> ORDER CHEBYCHEV 1/2 dB RIPPLE

$$E(Z) = \frac{Q(Z)}{N} \quad V-39$$

$$1 + \sum_{j=1} b_j Z^{-j}$$

As noted previously, this recursive equation can be converted to a non-recursive form yielding

$$\epsilon_n = \sum_{k=0}^{\infty} C_k q_{n-k} \quad V-40$$

Thus

$$y_n = \hat{y}_n + \sum_{k=0}^{\infty} C_k q_{n-k} \quad V-41$$

where

$$C_0 = 1$$

$$C_k = - \sum_{j=1}^N b_j C_{k-j} \quad V-42$$

A block diagram of the system utilizing Eq. V-40 and truncating the nonrecursive form after  $k$  terms, is illustrated in Figure V-7.

There are three ways to use this technique to advantage. In the first instance, where only the  $p^{\text{th}}$  filter output is necessary, a relatively gross running arithmetic would be necessary, after which the  $p^{\text{th}}$  output would be refined using some number of current and prior round-off values taken from the piggy-bank. This simplifies the running arithmetic at the expense of increased storage.

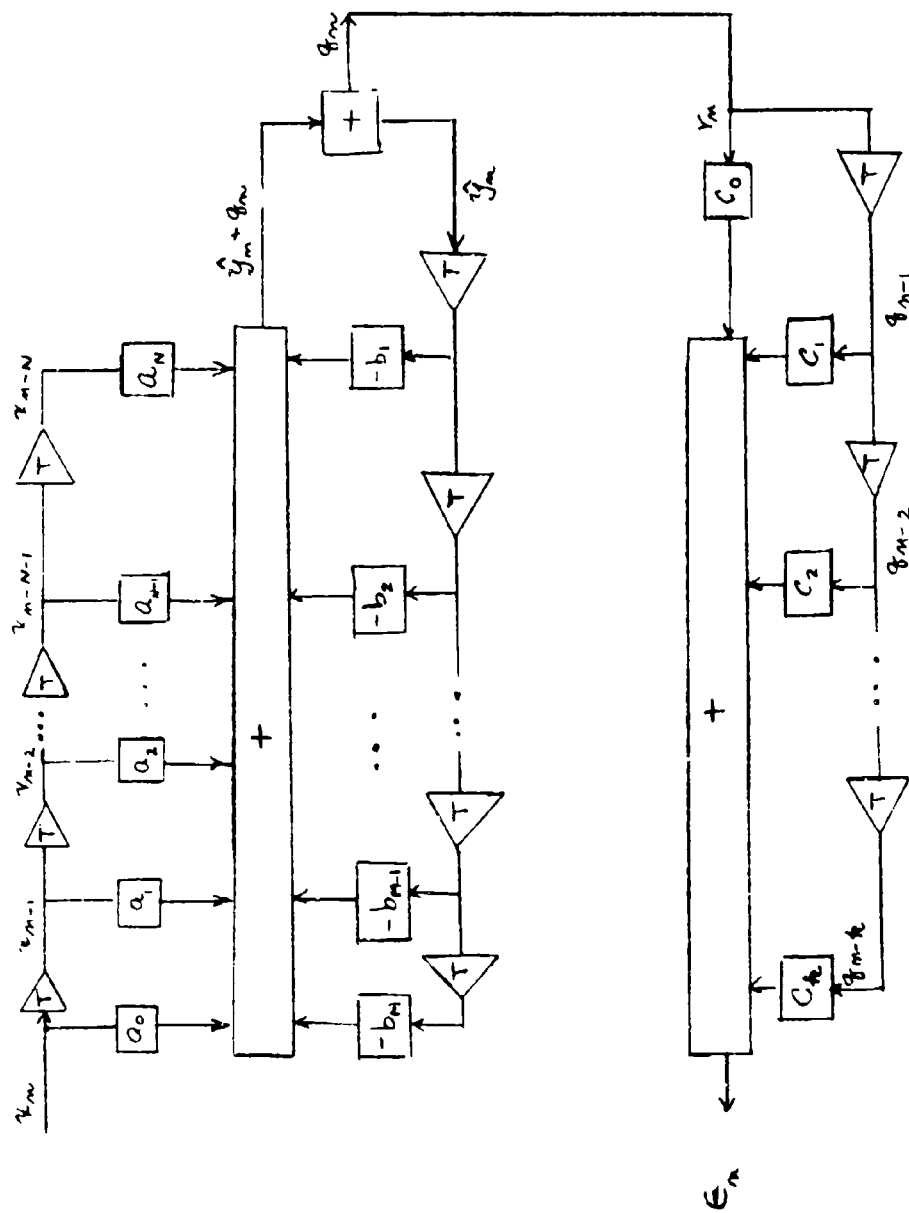


FIGURE V-7: A RECURSIVE DIGITAL FILTER WITH AN AUXILIARY STORAGE

The second use of the storage is to periodically test the error, (at a slower than input sample rate) improving the value  $\hat{y}_n$  with the weighted overflow whenever the error value overflows. Overflow is defined as that part of the error equal to or greater than the gross quantization of the running arithmetic. The residue of the overflow would be reinserted as the new round-off for the  $n^{\text{th}}$  value and the whole process repeated.

The third possible application is dependent on the nature of the overflow. If the bandwidth of the overflow samples is small relative to the input samples, then it is conceivable that a refinement of  $\hat{y}_n$  can be made periodically but at a rate slower than the input sampling rate.

#### An Illustrative Example

An example is next presented for an arbitrary filter where the sum never overflows. However, a correction is made at the 8<sup>th</sup> sample time using a truncated (approximate) and non-truncated (exact) technique.

#### Example

Assume the filter is given by

$$y_n = a_0 x_n - b_1 y_{n-1} - b_2 y_{n-2}$$

where:

$$a_0 = 1$$

$$b_1 = 1/2$$

$$b_2 = 1/4$$

$$x_n = 1 \quad n \geq 0$$

$$x_n = 0 \quad n < 0$$

Table VI lists exact values of the output,  $y_n$ , approximate values of the output,  $\hat{y}_n$ , assuming a quantization of 1/8 and the resulting round-off.



TABLE VI  
EXACT AND APPROXIMATE OUTPUTS VALUES

$n$	$Q_0 x_n$	$b_1 y_{n-1}$	$b_2 y_{n-2}$	$y_n$	$\hat{y}_n$	$b_1 \hat{y}_{n-1}$	$b_2 \hat{y}_{n-2}$	$q_n$
0	1	0	0	1	1	0	0	0
1	1	1/2	0	1/2	1/2	1/2	0	0
2	1	1/4	1/4	1/2	1/2	1/4	1/4	0
3	1	1/4	1/8	5/8	5/8	1/4	1/8	0
4	1	5/16	1/8	9/16	1/2	5/16	1/8	1/16
5	1	9/32	5/32	9/16	1/2	1/4	5/32	3/32
6	1	9/32	9/64	37/64	5/8	1/4	1/8	0
7	1	37/128	9/64	73/128	1/2	5/16	1/8	1/16
8	1	73/256	37/256	73/128	1/2	1/4	5/32	3/32
9	1	73/512	73/512	293/512	5/8	1/4	1/8	0

Assume a quantization of 1/8  
and record (i.e., store) the  
round-off  $q_n$ .

By using the algorithm for obtaining  $C_g$ , the following coefficients are developed.

$$C_0 = 1, C_1 = 1/2, C_2 = 0, C_3 = -1/8, C_4 = -1/16, C_5 = 0, C_6 = 1/64, C_7 = 1/128, \dots$$

Using these coefficients, the error for the 8<sup>th</sup> output will be computed.

$$E_8 = 1 \times 3/32 - 1/2 \times 1/16 + 0 \times 0 + 1/8 \times 3/32 - 1/16 \times 1/16 + 0 \times 0 + 1/64 \times 0 \dots$$

$$E_8 = 24/256 - 8/256 + 3/256 - 1/256 = 18/256 = 9/128$$

$$\hat{y}_8 = 1/2 = 64/128$$

since

$$y_8 = \hat{y}_8 + E_8$$

$$\therefore y_8 = 73/128$$

The above numerical example illustrates that the exact result is obtained if all of the round-off values are used.

If only the current and next to last round-off values are stored, an approximate correction to  $\hat{y}_n$  is obtained as  $\tilde{y}_n$

$$\text{where } \tilde{y}_n = \hat{y}_n + \tilde{E}_n$$

$$\tilde{E}_8 = 1 \times 3/2 - 1/2 \times 1/16 = 2/32 = 8/128$$

$$\therefore \tilde{y}_8 = 72/128.$$

The error, after refinement, using the approximate correction is one part in 128 while the error between  $\hat{y}_8$  and  $y_8$  is nine parts in 128.

If the round-off error is pessimistically assumed to be always equal to the least significant bit (LSB) then the max error  $E_n \text{ max}$  is defined as

$$E_n(\text{max}) = \lim_{k \rightarrow \infty} S(\text{LSB})$$

where

$$\lim_{k \rightarrow \infty} S = \sum_{g=0}^{\infty} C_g$$

For the example above  $\lim_{k \rightarrow \infty} S = 4/7$  and  $\text{LSB} = 1/8$ .

$\therefore E_n \text{ max } 4/7 \times 1/8 = 1/14$ . If the storage values are not utilized at all, the max error for the conditions assumed would be less than  $1/14$ .

If the stored round-off error itself were quantized (which is generally the case) then the error (conservative) due to this approximation would be  $\lim_{k \rightarrow \infty} S_k \approx (\text{LSB})$ . Where (LSB) is the least significant bit of stored round-off value. Thus, this auxiliary storage technique offers the possibility of reducing errors.

Two sources of errors in digital filtering have been discussed. The errors resulting from a truncation of the filter coefficients were related to such critical filter parameters as the order of the filter and the ratio of sampling rate to critical frequencies using the tabular approach. This approach allowed for an interpretation of the filter degradation, the onset of instability and the bit truncation of the filter coefficients. The conditions under which the cascade synthesis approach is preferred is also discussed. The errors due to computational quantization and the effect of both the direct and canonical implementation forms on these errors are then discussed. Curves are obtained showing the regions in which one implementation is superior to the other. Lastly, an error reduction technique utilizing an auxiliary storage approach is presented. This technique offers the possibility for reducing computational quantization errors.

## VI. RECOMMENDATIONS

As is often the case with analytical studies, the various techniques investigated suggest areas where further efforts would be desirable. In addition, some of the results themselves may show sufficient promise to warrant experimental justification or breadboarding. Summarized below are the areas which, as a result of this investigation, fall into the above categories.

1. The results of Section II (B and C) and Section III, concerning the various techniques and constraints which are associated with the design of bandpass filters, point out the interplay between the sampling rate, carrier frequency, and filter bandwidth. The foregoing, in addition to the results of Appendix A, clearly shows the need to develop sampling and processing techniques which will enable one to operate digital filters at sampling rates at or near the information bandwidth.
2. The results of Section V (A and C) concerning stability and coefficient representation illustrate the difficulties encountered when filters are to be designed under the constraints of small  $K_{\omega_u}$  factors and high order filters. Since truncation invites stability problems and the foregoing constraints require an inordinate amount of processing, techniques should be investigated which overcome these difficulties and will thus allow for the processing or extraction of narrow band information from broadband signals.
3. The error considerations discussed in Section III indicate that the development of techniques which provide for approximate filter shapes through coefficient modification should be investigated. These modifications should be directed towards an overall reduction in the time required to perform the arithmetic processing.
4. The results of Section II (B and C) and those of Section III (C and E) suggest that a more detailed study be made of the relative advantages of the two specific bandpass filter design techniques discussed. The shifting technique offers a possibility for developing the bandpass coefficients from those of the lowpass filter directly on line. It also appears more desirable for tracking filter applications. The LP-BP transformation offers other advantages in terms of control over bandwidth and carrier frequency.
5. The results of Section IV indicate that a further investigation be directed toward the relationship between the process of zero-removal and relocation and the class of allowable frequency response characteristics achievable for nonrecursive filters.

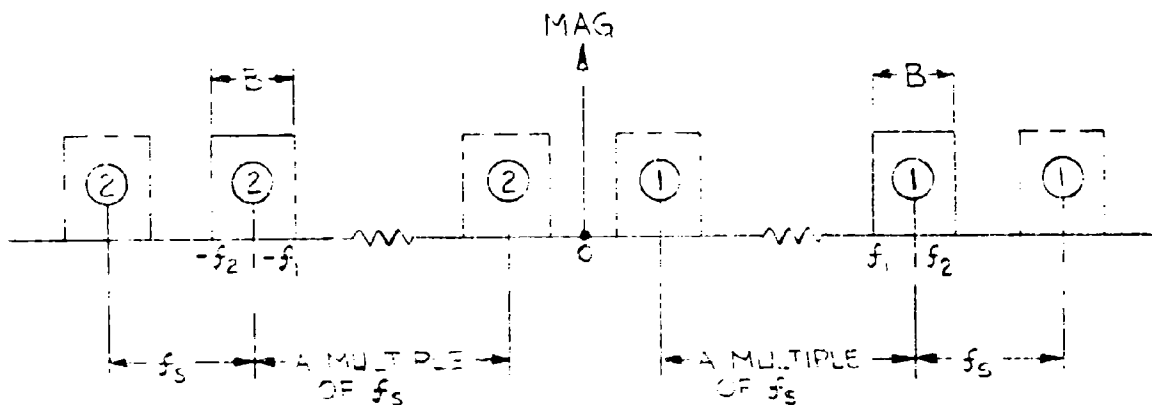
6. An extension of the results of Section V-C concerning computational quantization is desirable. This extension to higher order filters as well as arbitrary bandpass filters would allow the designer to properly choose the best implementation for the particular critical parameters of the filter.
7. The error reduction technique discussed in Section V-D has shown sufficient merit to warrant an experimental breadboarding. This auxiliary storage technique area requires some additional study with regard to the optimum number of coefficients to be used in the storage "bank" as well as a determination of which of the three modes it should operate.
8. An experimental investigation should be initiated concerning the digital oscillator implementation technique discussed in Appendix B. This technique has applications to such areas as frequency translators, bandpass processing and tracking filters.
9. Besides the discussion of the shifting technique for bandpass digital filters and the nonrecursive design from tabulated data, the majority of the synthesis techniques discussed have utilized a transformation procedure which converts an analog filter to an equivalent digital filter. These approaches might be generally termed digital equivalence procedures. An alternate approach is to synthesize digital filters without reference to an equivalent analog filter. This approach, which might be termed direct digital synthesis, warrants detailed investigation in that it will allow for more flexibility in the designs that can be achieved. Two approaches to this problem of direct design which have been investigated to a limited extent under very specific conditions have utilized polynomial approximation procedures and pole-zero shifting procedures in the  $Z$  plane. Both of these procedures as well as several other approaches should be expanded for use in the direct synthesis of digital filters.

## APPENDIX A

### A BANDPASS SAMPLING TECHNIQUE

The sampling and reconstruction of a lowpass signal with a (positive) bandwidth of  $B/2$  (Hz) and no spectral energy beyond this frequency can be accomplished (theoretically) by sampling at a rate of  $B$  samples per second.  $B$  also represents twice the highest frequency component present in the signal. If this procedure were carried over directly to bandpass signals, unreasonably high sampling rates would result. Moreover, since it is well known that the information content in a signal is dependent upon its bandwidth and not its center frequency, one would expect that it is possible to recover the bandpass waveform with a sampling procedure at rates in the order of the bandwidth of the bandpass signal. Direct application by the sampling theory for bandpass signals shows this to be the case.

The periodic nature of digital filters suggests the following sampling procedure. Assume a bandpass signal as shown below.



The process of sampling produces spectral repeats or aliased spectra at multiples of the sampling frequency. The repeats are shown as the dotted spectra. It is desired to choose a sampling rate,  $f_s$ , such that there are no spectral overlaps. With this objective the following constraints can be placed upon  $f_s$ ,  $B$ ,  $f_1$  and  $f_2$ . Let  $k$  be the index representing the  $k^{\text{th}}$  repeat or shifted spectrum. Then for no overlap at bandpass one requires

$$-f_2 + k f_s > f_2 ; \quad -f_1 + (k-1) f_s < f_1 \quad \text{A-1}$$

Simplifying equation A-1 yields

$$f_s > \frac{2}{k} f_2 \quad \text{A-2}$$

$$f_s < \frac{2}{k-1} f_2 - \frac{2B}{k-1}$$

or

$$\frac{f_s}{B} > \frac{2}{k} \frac{f_2}{B} \quad \text{A-3}$$

$$\frac{f_s}{B} > \frac{2}{k-1} \frac{f_2}{B} - \frac{2}{k-1}$$

From these equations one obtains

$$f_s > 2B \quad \text{A-4}$$

$$1 \leq k \leq \frac{f_2}{B}$$

Thus, the absolute minimum allowable sampling rate is  $2B$ . The allowable normalized sampling rates relative to  $f_2/B$ , the ratio of the upper frequency to the bandwidth, are shown in figure A-1. This diagram shows that care must be exercised in choosing a sampling rate. It is of interest to note that the sampling rate of  $2B$  is allowed only when  $f_2$  and  $B$  are integrally related. It is also of interest to note that if two sampling rates  $f_{s1}/B$  and

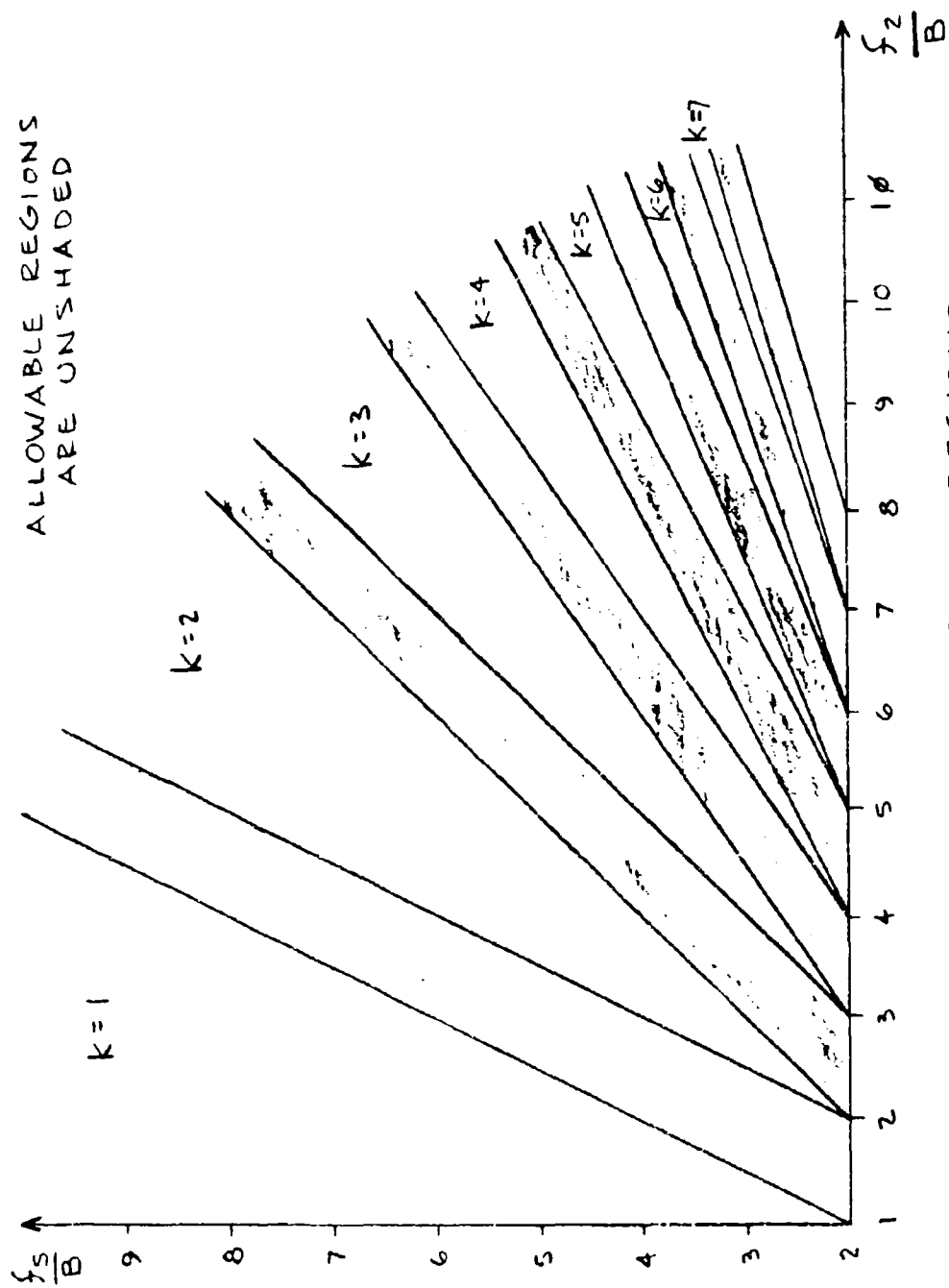


FIGURE A-1: ALLOWABLE SAMPLING REGIONS



$f_{s2}/B$  are chosen ( $f_2 > f_1$ ), then the allowable sampling region or area can be shown to be

$$A = \frac{f_{s2} - f_{s1}}{B} \left[ \frac{f_{s1} + f_{s2}}{2B} - 2 \right] \quad A-5$$

which is independent of  $k$ . Furthermore, the extend of validity on the  $f_2/B$  axis is

$$\Delta \left[ \frac{f_2}{B} \right] = \frac{k}{2} \left[ \frac{f_{s2} - f_{s1}}{B} \right] + \frac{f_{s1}}{2B} - 1 \quad A-6$$

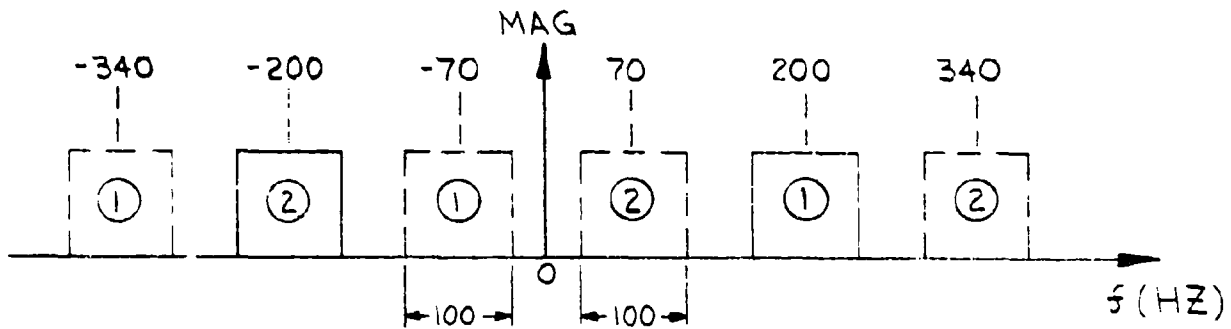
which is an increasing function of  $k$ .

The foregoing considered the required sampling rate for no bandpass overlap. Additional constraints should be placed on the sampling rate in order to filter this signal digitally at a reasonably low frequency. One such constraint is to require that there be no spectral interchange. That is, if the  $r^{\text{th}}$  repeat is the last negative repeat from the negative spectral lobe (moving to the right) the  $(r+1)^{\text{th}}$  repeat is the last positive repeat from the positive spectral lobe (moving to the left); then for no spectral interchange one requires that

$$(r+1) f_s - f_2 > f_2 - r f_s \quad A-7$$

$$\frac{f_s}{B} > \frac{2}{2r+1} \frac{f_2}{B}$$

As an example of the case where the sampling rate is sufficient for no spectral overlap but spectral interchange does occur, consider the following. A band-pass signal has  $f_2 = 250$  Hz,  $f_1 = 150$  Hz,  $B = 100$  as shown below



$f_s$  is chosen as 270 Hz. As shown in the figure, no spectral overlap occurs, but spectral interchange occurs since

$$\frac{f_s}{B} = 2.70 \quad \frac{f_u}{B} = 2.50 \quad r = 0 \quad \text{A-8}$$

Thus from A-7, 2.7 must be greater than  $2 \times 2.5 = 5$  which is not the case.

## APPENDIX B

### DIGITAL OSCILLATORS

Digital oscillators play an integral part in such areas as frequency translators, heterodyning techniques and tracking and frequency hopping filters as well as other applications. Thus several configurations for the digital generation of sine and cosine oscillators will be discussed.

A starting point in the development of these generators is their Z transforms which can be shown to be

$$\frac{\cos \omega_o t}{Z \left\{ \cos \omega_o t \right\}} = \frac{1 - (\cos a) Z^{-1}}{1 - 2(\cos a) Z^{-1} + Z^{-2}} \quad \text{B-1}$$

$$\frac{\sin \omega_o t}{Z \left\{ \sin \omega_o t \right\}} = \frac{(\sin a) Z^{-1}}{1 - 2(\cos a) Z^{-1} + Z^{-2}} \quad \text{B-2}$$

where  $a$  is  $2\pi$  divided by the ratio of sampling frequency to center frequency. That is the sinusoidal values are obtained at increments of  $a$  (radians).

In equations B-1 and B-2 the Z transforms are in the form of a ratio. Therefore, they can be interpreted as transfer functions of a recursive digital filter. Inverse transforming these equations leads, respectively, to

$$\frac{\cos \omega_o t}{y_k = x_k - (\cos a) x_{k-1} + (2 \cos a) y_{k-1} - y_{k-2}} \quad \text{B-3}$$

$$\frac{\sin \omega_o t}{y_k = (\sin a) x_{k-1} + (2 \cos a) y_{k-1} - y_{k-2}} \quad \text{B-4}$$

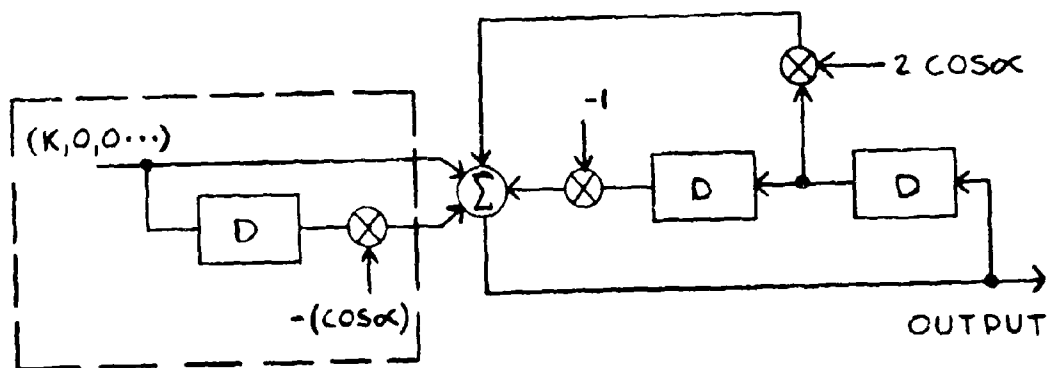
Thus, these generators have been modeled as recursive digital filters whose impulse responses provide the samples of sine and cosine at any desired increment. That is, if 20 samples per cycle were desired, then  $\alpha = (2\pi/20) = 18^\circ$  and the outputs would correspond to the values of these sinusoids at  $18^\circ$  increments. It should also be noted that these digital filters have poles on the unit circle and thus if allowed to run indefinitely an "infinite" amount of noise would result due to computational quantization. This problem can be circumvented by periodically re-starting the oscillators. The implementation of these generators is shown in figure B-1. The dotted region of the figure is shown merely for illustrative purposes and represents the first two initial conditions to be loaded into the delay elements. That is, the cosine generator requires  $K$  and  $K \cos \alpha$  and the sine generator  $0$  and  $K \sin \alpha$ . Thus B-3 and B-4 can both be written as

$$\frac{\cos \omega_0 t \quad (\text{and } \sin \omega_0 t)}{y_k = (2 \cos \alpha) y_{k-1} - y_{k-2}} \quad \text{B-5}$$

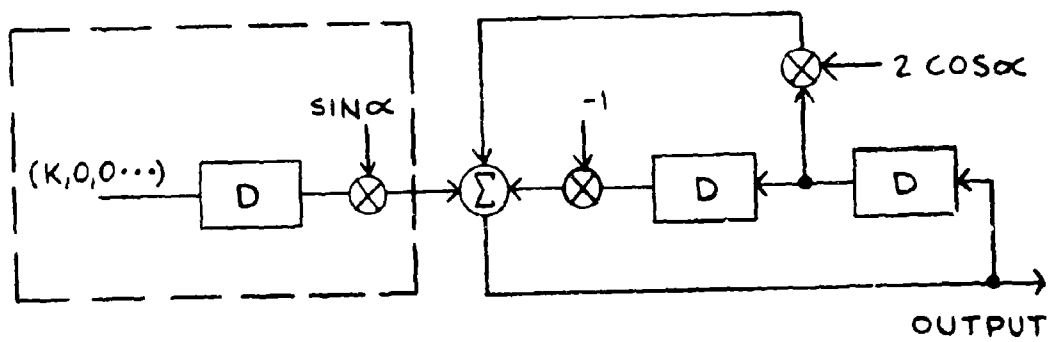
where the cosine terms are obtained by setting  $(y_{-1}, y_{-2})$  to be  $(K, K \cos \alpha)$  and the sine terms by setting the initial outputs to be  $(0, K \sin \alpha)$ .

The configuration shown in figure B-1 is instrumented in direct form and, therefore, has some of the error problems discussed in section VI with regard to computational quantization. An alternate configuration is based on the identities

$$\begin{aligned} \cos (A + B) &= \cos A \cos B - \sin A \sin B \\ \sin (A + B) &= \sin A \cos B + \cos A \sin B \end{aligned} \quad \text{B-6}$$



(a) COSINE GENERATOR



(b) SINE GENERATOR

FIGURE B-1

These identities lead to the recursion equations

$$y_n = (\cos \alpha) y_{n-1} + (\sin \alpha) x_{n-1}$$

B-7

$$x_n = (\cos \alpha) x_{n-1} - (\sin \alpha) y_{n-1}$$

where the  $y$ 's represent the sine output and the  $x$ 's the cosine output. This configuration is shown in figure B-2. For sampling rates that are in the order of 10-30:1 and resetting the system every cycle, these two configurations produced very similar results. Without resetting, the configuration of figure B-2 was superior. A considerable simplification occurs in both of these configurations when these generators yield 4 samples per cycle. In this case,  $\alpha = \pi/2 = 90^\circ$ ,  $\cos \alpha = 0$  and  $\sin \alpha = 1$  and the outputs can be shown to yield the sequence 1, 0, -1, 0, 1, 0, -1, .... This of course merely corresponds to a sampled square wave and there are no computational quantization problems. For this case, the oscillators have been reduced to a rather trivial configuration. This result is expected in that it is common practice to build heterodyners which square wave modulate a signal in order to shift the signal by an amount (in the frequency domain) equal to the fundamental frequency of the square wave. Energy centered at the higher harmonics is then filtered out.

A third configuration yielding improved performance with less hardware is shown in figure B-3. This configuration is based on expressing B-1 and B-2 in canonical form. The resulting equations are

$$f_n = x_n + (2 \cos \alpha) f_{n-1} - f_{n-2}$$

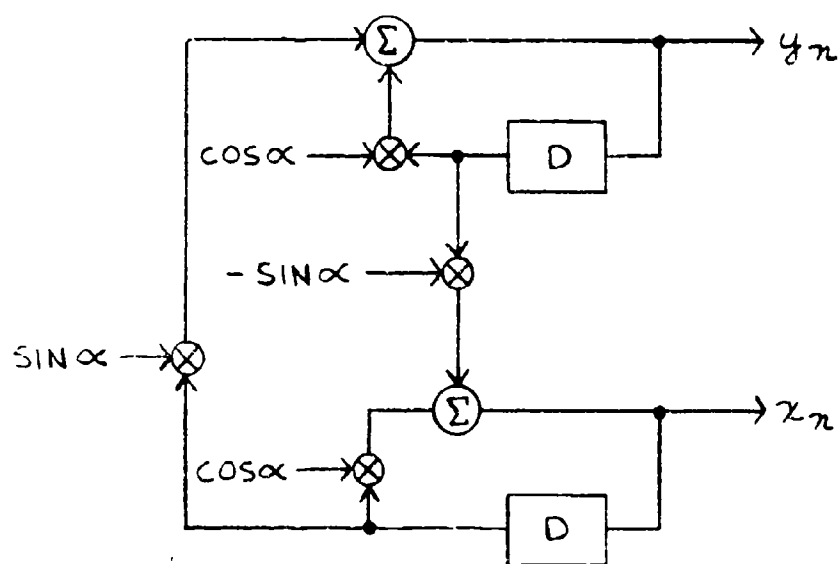
B-5

$$s_n = (\sin \alpha) f_{n-1}$$

$$f'_n = x'_n + (2 \cos \alpha) f'_{n-1} - f'_{n-2}$$

B-6

$$c_n = f'_n - (\cos \alpha) f_{n-1}$$



$$y_n = \cos \alpha y_{n-1} + \sin \alpha x_{n-1}$$

$$x_n = \cos \alpha x_{n-1} - \sin \alpha y_{n-1}$$

FIGURE B-2: SINE-COSINE GENERATOR

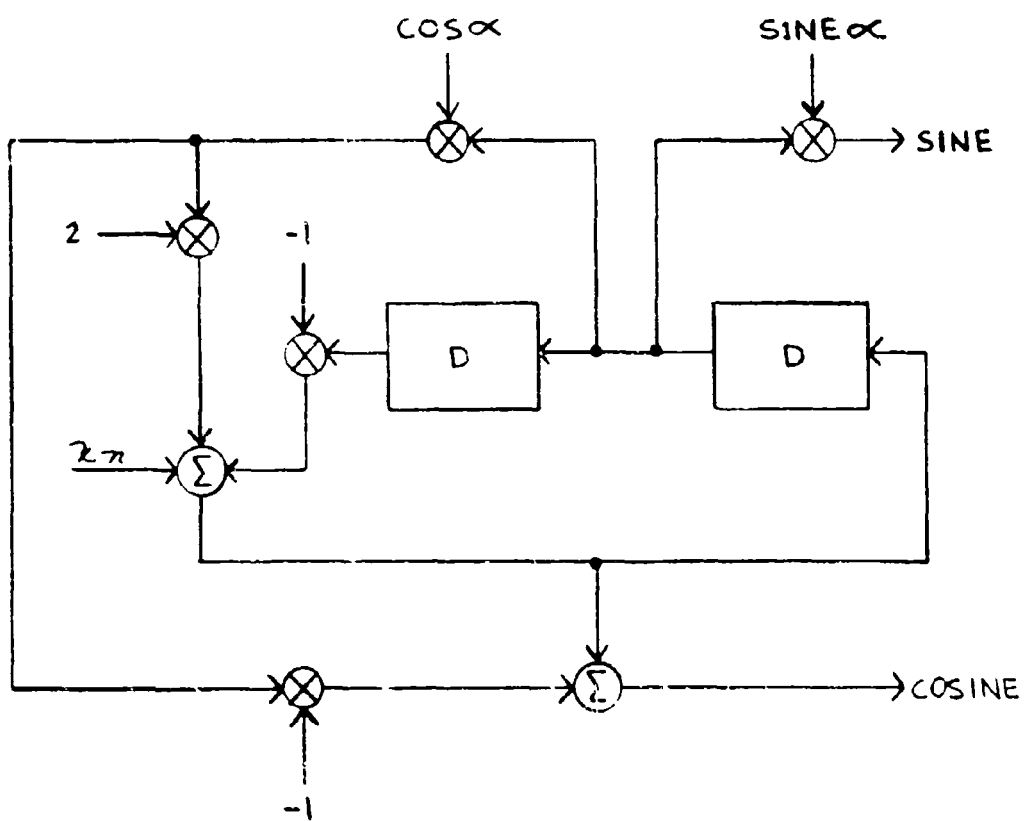


FIGURE B-3: CANONICAL SINE-COSINE GENERATOR



From the above it can be seen that since  $x'_n = x_n$ ,  $f'_n = f_n$  that the sine and cosine generators share the same auxiliary variable but are not interlocked as in figure B-2. It is also to be noted that there is a reduction in the required number of multipliers using sine  $\alpha$  and cos  $\alpha$ . Furthermore, the errors in the sine  $\alpha$  multiplication do not affect the alternate or cosine output.

Using the techniques discussed in section V, it was shown that the error performance of this configuration is superior to that of the previous configurations. Simulation of the recursion equations with 10 bit and 14 bit quantization bears this out as shown in tables I and II.

TABLE I  
10 Bit Quantization

<u>Angle (degrees)</u>	<u>Generated (sine)</u>		<u>Ideal (rounded)</u>
	(Figure B-2)	(Figure B-3)	
0	0	0	0
10	.174	.174	.174
20	.343	.342	.342
30	.501	.501	.500
40	.644	.644	.643
50	.768	.767	.766
60	.869	.867	.866
70	.948	.942	.940
80	.989	.987	.985
90	1.006	1.003	1.000

TABLE II  
14 Bit Quantization

<u>Angle (degrees)</u>	<u>Generated (cosine)</u>	<u>Ideal (rounded)</u>
0	1.000	1.0000
10	.9848	.9848
20	.9401	.9397
30	.8671	.8660
40	.7679	.7660
50	.6458	.6428
60	.5043	.5000
70	.3478	.3420
80	.1807	.1737
90	.0083	.0000

The results shown in this table are for output generated at  $10^\circ$  increments. For smaller increment, the improvement shown in the performance of the configuration of figure B-3 over that of the previous figures increases. This is once again due to the fact that the canonical form is best when the sampling rate is high. The outputs shown in these tables result from quantizing the appropriate equations to the specified number of bits.

Digital oscillators not only are important devices as frequency synthesizers but also play an integral part in such important communication devices as translators, tracking filters and bandpass processing among many others. The configuration of figure B-3 can therefore be combined with the results concerning digital bandpass filters to yield a completely digital device.

## APPENDIX C

### REFERENCES

1. Steiglitz, K., "The General Theory of Digital Filters with Applications to Spectral Analysis", AFOSR Report 64-1664, New York University, New York, May 1963.
2. Tustin, A., "A Method Analyzing the Behavior of Linear Systems in Terms of Time Series", J. I. E. E. (Proceedings of the Convention on Automatic Regulators and Servomechanism) Vol. 94, Part II-A, May 1947.
3. J.F. Kaiser, (ed.) "Systems Analysis by Digital Computer", New York: Wiley, 1966, Chapter 7.
4. Broome, P.W., "Discrete Orthonormal Sequences", J. AC M, Vol. 12, No. 2, April 1965, pp. 151-168.
5. Calahan, D.A., "Modern Network Synthesis", Hayden Publishing Company, Inc., New York, 1964.
6. Campbell, T.B.; Chang, S.H.; Ferment, D.W.; Tsao-Wu, N.T., "Pulse Shaping by Manipulating Transform Zeros", Scientific Report, No. 1 (Dec. 1964) Northeastern University.
7. Levin, B.J., "Distribution of Zeros of Entire Functions", Translation of Mathematical Monographs, Vol. 5, American Mathematical Society, 1964.
8. Blackman, R.D., "Linear Data-Smoothing and Prediction in Theory and Practice", Addison-Wesley, Reading, Mass., 1965.
9. J.F. Kaiser, (ed.) "Systems Analysis by Digital Computer", New York: Wiley, 1966, pp. 260-271.
10. Radar, C.M. and Gold, B., "Digital Filter Design Techniques", Lincoln Laboratory Report, M.I.T., Preprint JA 2612, September 1965.
11. J.F. Kaiser, (ed.) "Systems Analysis by Digital Computer", New York: Wiley, 1966, p. 265.
12. Knowles, J.B. and Olcayto, E.M., "Coefficient Accuracy and Digital Filter Response", IEEE Trans. on Circuit Theory, Vol. CT-15, No. 1, March 1968, pp. 31-41.

## APPENDIX D

### BIBLIOGRAPHY

1. Greaves, C.J., "Digital Filter Synthesis", Cornell Aeronautical Labs., Inc., RADC-TR-67-123.
2. Kaiser, J.F., "Design Methods for Sampled-Data Filters", Proceedings First Allerton Conference on Circuit and System Theory, November 1963, pp. 221-236.
3. Cheney, E.W. and Loeb, H.L., "Generalized Rational Approximation", J. SIAM, Numerical Analysis, B. Vol. 1, 1964, pp. 11-25.
4. Boxer, R. and Thaler, S., "A Simplified Method of Solving Linear and Nonlinear Systems", Proc. IRE, Vol. 44, January 1956, pp. 89-101.
5. Golden, R.M. and Kaiser, J.F., "Design of Wideband Sampled-Data Filters", BSTJ, Vol. 43, Part 2, July 1964, pp. 1533-1546.
6. Ormsby, J.F.A., "Design of Numerical Filters with Applications to Missile Data Processing", J. AC M, Vol. 8, No. 3, July 1961, pp. 440-466.
7. Blum, M., "Recursion Formulas for Growing Memory Digital Filters", IRE Trans. Info. Theory, March 1958.
8. Knowles, J.B. and Edwards, R., "Effect of a Finite-Word-Length Computer in a Sampled-Data Feedback System", Proc. IEE, Vol. 112, No. 6, June 1965, pp. 1197-1207.
9. Wilkinson, J.H., "Rounding Errors in Algebraic Processes", Prentice Hall, Englewood Cliffs, New Jersey, 1963.
10. Kuo, B.C., "Analysis and Synthesis of Sampled-Data Systems", Prentice-Hall, 1963, pp. 397-404.
11. Ragazzini, J.R., and Franklin, G.F., "Sampled-Data Control Systems", McGraw-Hill, 1958, pp. 267-272.
12. Bordner, G.W., Greaves, C.J., and Wierwille, W.W., "Research Studies of Random Process Theory and Physical Applications", NASA Contractor Report CR-61081, August 4, 1965.

UNCLASSIFIED

Security Classification

DOCUMENT CONTROL DATA - R & D		
(Security classification of title, body of abstract and indexing annotation must be entered when the overall report is classified)		
1. ORIGINATING ACTIVITY (Corporate author) The Marquardt Corporation 16555 Saticoy Street Van Nuys CA 91409		2a. REPORT SECURITY CLASSIFICATION UNCLASSIFIED
		2b. GROUP N/A
3. REPORT TITLE  DIGITAL FILTERING TECHNIQUES		
4. DESCRIPTIVE NOTES (Type of report and inclusive dates) Final Report		
5. AUTHOR(S) (First name, middle initial, last name)  Langenthal, Ira M.		
6. REPORT DATE March 1969	7a. TOTAL NO. OF PAGES 130	7b. NO. OF REFS 12
8a. CONTRACT OR GRANT NO. F30602-67-C-0160	9a. ORIGINATOR'S REPORT NUMBER(S)	
b. PROJECT NO. 4519		
c. Task No. 451902	9b. OTHER REPORT NO(S) (Any other numbers that may be assigned this report)	
d.	RADC-TR-69-27	
10. DISTRIBUTION STATEMENT This document is subject to special export controls and each transmittal to foreign governments, foreign nationals or representatives thereto may be made only with prior approval of RADC (EMCRS), GAFB, N.Y. 13440		
11. SUPPLEMENTARY NOTES	12. SPONSORING MILITARY ACTIVITY Rome Air Development Center (EMCRS) Griffiss Air Force Base, New York 13440	
13. ABSTRACT  This investigation was concerned with various digital filtering techniques and associated constraints. The synthesis procedures discussed in this report emphasize the interplay of the various critical design parameters. Generalized design procedures for lowpass, bandpass and band stop filters are developed using a tabular procedure which enables one to obtain the digital filter coefficients by inspection. This approach allows for a simpler evaluation and interpretation of such problems as coefficient truncation, stability and error constraints as well as illustrating the importance and significance of the concept of normalization in digital filters. The inter-relations among the foregoing are discussed in detail leading to performance curves for various implementations. A bandpass and band stop synthesis technique which is accomplished through a simple conversion of the lowpass coefficients is also developed. Bandpass filters having arithmetic symmetry are then synthesized using a frequency shift technique as well as a lowpass to bandpass transformation. The validation of these approaches for various ratios of sampling rate to carrier frequency is discussed. An analysis of synthesis errors is then accomplished. Under the assumption that tabular data is available, design procedures which minimize the sum-squared error are developed for design of non-recursive digital filters. A second approach to the design of these filters was accomplished under the assumption that a satisfactory recursive digital filter design using the bilinear transform was available.		

DD FORM 1473  
1 NOV 65

UNCLASSIFIED

Security Classification

UNCLASSIFIED

Security Classification

14. KEY WORDS	LINK A		LINK B		LINK C	
	ROLE	WT	ROLE	WT	ROLE	WT
Communication Systems Communication Theory Digital Filters Digital Signal Processing Digital Communications						

UNCLASSIFIED

Security Classification